UNIVERSITY OF OKLAHOMA

GRADUATE COLLEGE

PHYSICAL CHARACTERIZATION OF THE ECDYSTEROID AND RETINOID X RECEPTOR (UPECR AND UPRXR) IN THE FIDDLER CRAB UCA PUGILATOR

A Dissertation

SUBMITTED TO THE GRADUATE FACULTY

In partial fulfillment of the requirements for the

degree of

Doctor of Philosophy

By

XIAOHUI WU
Norman, Oklahoma
2003

PHYSICAL CHARACTERIZATION OF THE ECDYSTEROID AND RETINOID X RECEPTOR (UPECR AND UPRXR) IN THE FIDDLER CRAB UCA PUGILATOR

A Dissertation APPROVED FOR THE
DEPARTMENT OF ZOOLOGY

By

David S. Durica

Penny M. Hopkins

James N. Thompson, Jr.

Rosemary Knapp

William Ortiz

ACKNOWLEDGMENTS

It would be impossible to express here my deep gratitude to all those people for their support and encouragement during my time in graduate school here in Norman. First, I want thank Dr. David S. Durica, my major professor, for providing me the opportunity to come to America and be a graduate student in his laboratory. In one hand, Dr. Durica provides me with meticulous supervision and guidance in my research, on the other hand, he also gives me the freedom to work independently. I always admire his enthusiasm for science and nature.

I would like to give special thanks to Dr. Penny M. Hopkins, Dr. Durica's close collaborator, with whom I have been fortunate to work with since the first day of my research on the little cute fiddler crab. Her knowledge in biological science greatly broadens my view of science, and enables me to see the "big picture" of many biological problems.

Thanks are also due to Dr. Alyce DeMarais, Dr. Rosemary Knapp, Dr. David McCarthy, Dr. James N. Thompson, Jr., and Dr. William Ortiz for serving on my graduate committee and providing constructive criticism and encouragement during these years.

I would like to thank my family for their love and support. I thank my parents for their vision on what education can mean to a person. I thank my sister for her first hand introduction of the western culture to me. Her full support without any reservation throughout my whole life will always be remembered. I also want thank my brother for taking the responsibility to be the man in our family, and taking care of my aging parents.

TABLE OF CONTENTS

Abstract

Ecdysteroid hormones regulate growth, metamorphic differentiation, vitellogenesis, and oogenesis in insects. In crustaceans, molt, limb regeneration, and reproduction are closely related to ecdysteroid titers. In the fiddler crab, *Uca pugilator*, limb regeneration is coordinated with the molt cycle. Both limb regeneration and molting correlate with the fluctuation of circulating ecdysteroid titers. The actions of ecdysteroids are mediated through a nuclear receptor (NR), the ecdysteroid receptor (EcR). EcR needs to dimerize with another nuclear receptor, the insect ultraspiracle (USP) protein, or its vertebrate homolog, retinoid X receptor (RXR), to form a functional receptor dimer. A functional EcR/USP(RXR) heterodimer regulates gene expression by binding to a specific DNA sequence in the promoter region, the ecdysteroid hormone responsive element (HRE), or EcRE. Both EcR and USP/RXR can exist as multiple forms with variant amino acid (aa) sequences, or isoforms. Most characterized insect EcRs and USPs have amino-terminal (N-terminal) variant isoforms. Studies in insects and vertebrates show that specific NR isoforms exhibit tissue and cell type specific expression, suggesting receptor isoform-specific physiological function.

EcR and RXR gene homologs in *U. pugilator* (*UpEcR* and *UpRXR*) have been previously cloned. Library screenings recovered cDNA clones containing a unique amino terminal open-reading frame (A/B domain) for each gene, most similar to insect EcR-B1 and USP1/RXR isoforms. Several *UpRXR* cDNA splicing variants, however, are found in coding regions that could potentially

influence function. A five-aa insertion/deletion is located in the "T" box in the hinge region. Another 33-aa insertion/deletion is found inside the ligand-binding domain (LBD), between helix 1 and helix 3. All these UpRXR mRNA variants are expressed in regenerating limb buds, and the predominant mRNA isoform represents the UpRXR(-5+33) isoform.

Initial physical characterization of *E. coli* and *in vitro* synthesized UpEcR and UpRXR(-5+33) suggest that these crab receptors, just like insect EcR and USP/RXR, are able to heterodimerize. Dimerization is obligatory for the UpEcR/UpRXR to bind to an ecdysteroid HRE. The receptor-DNA interaction is independent of the presence of 20-hydroxyecdysone. Using A/B domain-specific and common domain probes, experiments were conducted to study the expression of UpEcR and UpRXR transcripts during limb regeneration and oogenesis. RNase protection assays were conducted to study the relative amount of A/B domain-specific and common domain UpEcR and UpRXR in regenerating limb buds and ovaries at several stages. Both transcripts are present in limb bud tissues, and they are seen at all the stages examined. These transcripts also are expressed in ovaries at early, mid, and late stages of oocyte maturation. For several of the limb bud and ovarian stages examined, the relative level of A/B domain sequence protected was less than common domain, suggesting alternative amino terminal isoforms other than those isolated through cloning.

Using electrophoretic mobility shift assay (EMSA) and GST-pull down experiments, the DNA-binding and receptor protein-protein binding characteristics of UpEcR and variant UpRXR were further studied. EMSA results showed that UpEcR/UpRXR(-5+33) heterocomplexes bound with a series of hormone response elements including *eip28/29*, IRper-1, DR-4, and IRhsp-1 with appreciable affinity. Competition EMSA also showed that the affinity decreased as sequence composition deviated from a perfect consensus element. Binding to IRper-1 HREs occurred only if the heterodimer partner UpRXR contained the 33-aa LBD insertion. Additionally, UpRXR lacking both the five-aa and 33-aa insertion bound to a DR-1G HRE in the absence of UpEcR. The results of GST-pull down experiments showed that UpEcR interacted only with UpRXR variants containing the 33-aa insertion, and not with those lacking the 33-aa insertion. These *in vitro* receptor protein-DNA and receptor protein-protein interactions occurred in the absence of hormone (20-hydroxyecdysone and 9-cis retinoid acid). Transactivation studies using a hybrid UpEcR ligand-binding domain construct and UpRXR (±33) ligand-binding domain constructs also showed that the 33-aa insertion was indispensable in mediating ecdysteroid-stimulated transactivation.

The expression of UpEcR and UpRXR protein in regenerating limb buds was also examined by immunohistochemical studies. The immunohistochemical staining results showed that throughout the regeneration process, UpEcR and UpRXR were often found in the same tissues and cell types. The occasional

discrepancy from an equivalent staining pattern suggests that UpRXR or UpEcR may have other dimerization partners. When the immunoreactive patterns were compared to the circulating ecdysteroid titers, receptor immunoreactivity was observed regardless of the level of ecdysteroid. Expression of UpEcR and UpRXR was observed when either low or high titers of ecdysteroid were present in the circulating hemolymph, indicating that any change in receptor distribution pattern could not be explained by a simple change of circulating ecdysteroid titer alone.

Chapter I

General introduction to the arthropod ecdysteroid signaling pathway

Introduction

Molting, limb regeneration, and ecdysteroid fluctuation in the fiddler crab, *Uca pugilator*

With the increase in size due to growth, crustaceans have to replace their old exoskeletons with new bigger ones. Unlike most holometabolous insects, the fiddler crab, *Uca pugilator*, continues to grow as an adult and must coordinate growth with reproductive activity. The crustacean molt cycle is operationally described as five stages: A, B, C, D, and E (Drach, 1939). Stages A and B, called metecdysis, follow the last cycle's stage E, which is the stage where ecdysis or molting occurs. Metecdysis is the time for expansion and hardening of the new exoskeleton. Stage C is called anecdysis, which is the time for feeding and reproduction. Stage D is proecdysis, which is the period of preparation for shedding of the old exoskeleton and synthesis of a new one. Crustaceans usually maintain a very low ecdysteroid hormone titer until proecdysis (Chang et al., 1976), which implies the increase of ecdysteroid titer plays an important role in the physiological changes occurring during this premolt period.

In addition to this periodic intermolt (the period between successive molting) growth cycle, *Uca pugilator* has another kind of growth-the regeneration of lost limbs. When injured, *Uca pugilator* can reflexively cast off (called autotomy) the damaged limbs at a predetermined site proximal to the injury and replace them with new functional limbs (Skinner, 1985; Hopkins, 1993). The process of

regeneration is coordinated with the molt cycle and is, in part, under the control of circulating ecdysteroids (Hopkins, 1988, 1989, 1993). Regenerating limb bud growth can be monitored by the R-value (Bliss, 1956; the length of the right third walking leg limb bud divided by the width of the carapace, $R_{3,}$) and ER (arctangent of the ratio of R-value difference/days between the two R-value samplings). Regeneration following autotomy is divided into two stages: basal growth and proecdysial growth (Bliss, 1956). Basal growth results in the formation of a "minilimb", which involves cellular processes such as cell migration, pattern formation, proliferation, and differentiation. Proecdysial growth is primarily an increase in limb size due to protein synthesis and water uptake (Adiyodi, 1972). The minilimb will undergo hypertrophy during proecdysis and molt into a functional limb at the end of the molting cycle (Hopkins 1993). There are also two plateau periods after both basal growth and proecdysial growth, called basal plateau and terminal plateau, when the R-value stops increasing. Depending on physiological conditions, the duration of the basal plateau and terminal plateau varies. Basal growth and basal plateau fall in the C_4 substage of the molt cycle; whereas proecdysial growth falls in the D_0 substage, and terminal plateau corresponds to the $D_{1\text{-}4}$ substages prior to ecdysis (Hopkins, 1986). Apolysis, the separation of the exoskeleton from the underlying epidermal cells, occurs at the beginning of the $D_{1\text{-}4}$ substages, followed by synthesis of the new cuticle in both the body and the bud. After ecdysis, the folded limb will extend and fill with blood and become functional.

In *Uca pugilator*, there are at least four kinds of ecdysteroids in circulation, 25-deoxyecdysone, ecdysone, ponasterone A and 20-hydroxyecdysone (20E) (Lachaise et al., 1986, Hopkins, 1986, 1989). All four ecdysteroids can be detected by RIA (radioimmunoassay), though the affinity differs with specific antibody (Hopkins, 1992). Both the total circulating ecdysteroid and the relative concentrations of these four ecdysteroids vary during the molt cycle (Hopkins, 2001), upon which regeneration is superimposed (Hopkins, 1992). The total ecdysteroid levels are low when basal growth is initiated. At the end of basal growth, there is a small peak of RIA-active ecdysteroids, which is necessary for the switch from basal growth to proecdysial growth (Hopkins, 1989, 2001). Proecdysial growth is the fastest growth period for regenerating limb buds. This is primarily due to muscle protein synthesis in the limb bud and water uptake (Hopkins, 1989), however, cell proliferation may also play a part in this process (see Chapter III, Figure 10). At the end of stage D, a series of larger ecdysteroid peaks appear before the terminal plateau begins (Hopkins, 1989). Major physiological events at this time include apolysis, withdrawal and storage of calcium salt from old cuticle, and synthesis of new cuticle in the body and limb bud (Chang, 1989).

The role of nuclear receptors in mediating ecdysteroid signaling

In arthropods, the ecdysteroid hormones regulate growth, differentiation and reproduction by influencing gene expression (Segraves, 1994; Thummel, 1996).

A natural active ecdysteroid in most insects appears to be 20-hydroxyecdysone (20E), often abbreviated to "ecdysone" in the insect literature (Riddiford 1993, 2001). Based on examination of the giant salivary polytene chromosome puffing patterns during the last larval instar in the midge *Chironomus tentans* and fruit fly *Drosophila melanogaster* (Clever, 1964; Ashburner et al., 1974), it was hypothesized that ecdysone works like a master signal to trigger a cascade of gene activation. These studies, following chromosome puffing activity upon hormone treatment and inhibition of RNA and protein synthesis, suggest that early genes are turned on by ecdysone bursts and the products of early genes in turn activate late genes. This idea was later supported by combining *Drosophila* cytogenetic analysis with the use of molecular cloning techniques. Some of the genes corresponding to the early puff and late puff sites have been cloned, and the expression pattern of these genes seems to indeed match with the oft-said "Ashburner model". Some early genes are found to be transcription factors that can activate late gene expression (Burtis et al., 1990; Segraves and Hogness, 1990; Urness and Thummel, 1990; Cherbas et al., 1991; Brodu al., 1999; Martin et al., 2001).

Ecdysone exerts its function by binding to its cognate receptor, the ecdysteroid receptor (EcR). EcR together with the ultraspiracle protein (USP, a homologue of the vertebrate retinoid X receptor, RXR) forms a functional heterodimer, which binds to DNA (Koelle et al., 1991; Koelle at al., 1992; Yao et al., 1992; Thomas et al., 1993; Yao et al., 1993; Swevers et al., 1996; Hall and

Thummel, 1998). Both EcR and RXR are members of the nuclear receptor (NR) superfamily (Mangelsdorf et al., 1995). Nuclear receptors can be classified into different groups by functional criteria, such as modes of DNA binding and dimerization (see below). NRs act as transcription factors to influence gene expression. They have important roles in metazoan growth, differentiation, development, metabolism, reproduction, and metamorphosis (Aranda and Pascual 2001).

All nuclear receptors share a great similarity in gene structure and mechanism of gene regulation. All nuclear receptors have an N-terminal A/B domain; a C domain, the DNA binding domain (DBD); a D domain, the hinge region; and an E domain, the ligand binding domain (LBD). Some NRs, like the *Drosophila* EcR, also contain a carboxyl terminal F domain of indeterminate function (Koelle et al., 1991; Talbot et al., 1993; Riddiford et al., 2001, for review). In some vertebrate NRs, this domain may mediate ligand affinity, dimerization, and co-regulator interactions (Ruse et al., 2002; Schwartz et al., 2002). Among subfamilies within the nuclear receptor superfamily, the DNA binding domain is the most conserved domain, followed by the ligand binding domain, whereas the N-terminal A/B domain is often variable. Originating from alternative splicing and/or transcription from a different promoter, nuclear receptors can be represented by several isoforms with different amino acid sequences. The most common isoforms arise when variant N-terminal A/B domains are linked to an invariant

DBD and LBD (Koelle et al., 1991; Talbot et al., 1993; Riddiford et al., 2001; Aranda and Pascual, 2001).

As discussed above, nuclear receptors were among the first hypothesized transcription factors. They influence gene expression by binding to specific DNA sequences, known as hormone responsive elements, or HREs, in target genes. HREs are located at regulatory regions of the controlled target genes (Evans, 1988; Beato, 1989; Tsai and O'Malley, 1994; Mangelsdorf and Evans, 1995; Mangelsdorf et al., 1995). Detailed analysis of natural and synthetic HREs has revealed that two conserved 6 base pair motifs constitute the core recognition sequence for DNA binding, AG[G/T]TCA and AGAACA, existing either singly or as half sites within inverted, direct, or everted repeats (Tsai and O'Malley, 1994). Nuclear receptors can bind to HREs as a homodimer, a heterodimer or as a monomer (Aranda and Pascual, 2001). Vertebrate steroid hormone receptors usually recognize an inverted repeat AGAACA motif, and bind HREs as a homodimer (Beato et al., 1995; Beato and Klug, 2000), whereas vertebrate non-steroid receptors bind direct repeat AG[G/T]TCA motifs as a heterodimer. Both the DBD and the LBD contribute to dimerization (Aranda and Pascual, 2001). Many nuclear receptors repress transcription in the absence of ligand, due to a repression function in the LBD, which recruits one or more corepressor proteins (N-CoR, SMRT) interacting with other multi-protein complexes with histone deacetylase (HDAC) activity (Aranda and Pascual, 2001). Deacetylating histones, by compacting nucleosomes into a tight and inaccessible structure,

presumably will shut down gene expression. Interaction of the LBD with ligand abolishes repression and activates transcription via a C-terminal activation domain (activation function 2, or AF2), with the recruitment of p160 coactivators such as SRC1 (steroid receptor coactivator 1) with histone acetylase activity. In some receptors, AF2 works in synergy with an additional activation domain (AF1) in the N-terminal, or A/B region (Bevan et al., 1999). Like AF2, AF1 may also interact with p160 coactivators to activate transcription (Darimont et al., 1998; Chen et al., 1999; Xu et al., 1999). However, the AF1 mediated transactivation mechanism is not as well understood as that of AF2. As described in more detail later, tissue-specific A/B isoforms of nuclear receptors have been identified in several organisms (Talbot et al., 1993; Truman et al., 1994; Mouillet et al., 1997).

As mentioned above, the functional insect ecdysteroid receptor is a heterodimer of EcR and USP. Neither EcR nor USP (synthesized *in vitro*) binds ecdysteroids alone (Yao et al., 1993). However, there are experiments suggesting that it is EcR that binds ecdysteroids, while USP is an obligatory allosteric effector for ligand binding by EcR (Hu, 1998). Like other NRs, EcR also influences its target genes' expression by binding to DNA: an "ecdysteroid response element", EcRE (Cherbas et al., 1991; Dobens et al., 1991; Brodu et al., 1999; Tsai et al., 1999; Thormeyer et al., 1999). In a study of the mechanism of control of gene expression during differentiation and development in *Drosophila melanogaster*, the first EcRE was found by analyzing the upstream regulatory

sequence of the ecdysteroid responsive *hsp27* gene (Riddihough and Pelham 1986, 1987). EcREs usually contain the imperfect AGGTCA sequence as inverted repeats (Riddibough and Pelham, 1987; Cherbas et al., 1991; Antoniewski et al., 1993, 1995; Lehmann and Korge, 1995; Lehmann et al., 1997; Lan et al., 1999). However, in *Drosophila melanogaster*, functional EcR/USP also can bind to direct repeats with various spacers as EcREs (Horner et al., 1995; Antoniewski et al., 1996; Vögtli et al., 1998), and even composite (containing both DR and IR sequences) EcREs such as the response element of the *Drosophila eip28/29* gene (Cherbas et al., 1991). Many of these EcREs were first discovered by testing if the crude nuclear extracts from ecdysteroid responsive tissues were able to bind DNA sequences isolated from 20E responsive gene promoters. The ability of an EcRE to activate gene expression in transient transfection assays was also used to define these elements. The ecdysone receptor gene (*EcR*), however, was not cloned until several years later. Using the DBD region sequence of the earlier characterized *Drosophila E75* NR gene as a probe, *EcR* was identified in a screening for additional members of the steroid receptor gene superfamily (Koelle et al., 1991). Characterization of the *Drosophila* S2 cell line expressing EcR showed that EcR can bind ecdysteroids, specific hormone response elements, and confer hormone responsiveness to ecdysone-resistant cells (Koelle et al., 1991). The *Drosophila usp* gene was cloned independently by several labs in 1990 (Henrich et al., 1990; Shea et al., 1990; Oro et al., 1990), but it took several years to establish that USP was the heterodimeric partner of EcR (Yao et al., 1992, 1993; Thomas et al., 1993).

Since then, EcR and USP genes have been cloned in several orders of insects and from several other arthropods, and receptor isoforms that are products of alternative splicing and/or transcription from alternative promoters of the same gene have also been discovered (Riddiford et al., 2001). In *Drosophila melanogaster*, three isoforms (EcR-A, EcR-B1, and EcR-B2) of ecdysteroid receptor have been discovered (Talbot et al, 1993). These isoforms share common DNA- and hormone-binding domains but have different N-terminal A/B regions. The expression and distribution of these EcR isoforms is different in different target tissues during the larval-to-adult process of metamorphosis. Two EcR isoforms have been discovered in the lepidopterans *Manduca sexta* (Fujiwara et al, 1995; Jindra et al, 1996), *Bombyx mori* (Swevers et al, 1995; Kamimura et al, 1996, 1997), and *Choristoneura fumiferana* (Perera et al, 1999), as well as in the coleopteran *Tenebrio molitor* (Mouillet et al, 1997). In addition to these insects, three different isoforms of EcR from the ixodid tick *Amblyomma americanum* have been cloned (Guo et al, 1997), as well as two subtypes (different genes) of tick USP (Guo et al., 1998). In the mosquito *Aedes aegypti* (Kapitskaya et al, 1996), and tobacco hornworm *Manduca sexta* (Jindra et al., 1997), two isoforms of USP have been cloned and characterized. Several studies with insects show receptor expression is stage- and tissue-specific, with different isoforms showing different expression patterns. In *D. melanogaster*, EcR-A and EcR-B1 have different expression combinations as evidenced by northern, western and immunohistochemical studies (Talbot et al., 1993); genetic mutant

analysis also indicates that receptor isoforms have different roles both in embryonic development and during metamorphosis (Bender et al., 1997). Both northern blot and immunohistochemical studies show differential expression for the two ecdysone receptor isoforms in different tissues (epidermis and wing) of *Manduca sexta* (Jindra et al., 1996). Though the expression pattern is different from that of *Drosophila*, in the silkworm, *Bombyx mori*, northern hybridization studies also showed differential isoform expression patterns at different developmental stages and in different tissues (Kamimura et al., 1997). In the mosquito *Aedes aegypti,* both mRNA and protein expression patterns are different between two USP receptor isoforms during vitellogenesis in response to an ecdysone signal. *In vitro* transactivation studies also suggest that the two USP isoforms may have different roles (Wang et al., 2000b). In *Drosophila*, female flies that carry a temperature-sensitive EcR mutation exhibit severe reductions in fecundity at the restrictive temperature. These females are also defective in oogenesis, suggesting that EcR is needed in normal oogenesis (Carney and Bender 2000). Studies on *Drosophila* and *Manduca* neuronal development also show isoform-specific expression patterns that correlate to stage-specific responses to ecdysteroids (Robinow et al., 1993; Truman et al., 1994). Finally, studies on *Drosophila* neuron remodeling indicate that specific EcR isoform (EcR-B) expression is required for cell-autonomous pruning of the larval-specific dendrites and axons during metamorphosis (Schubiger et al., 1998; Lee et al., 2000). Nevertheless, the notion that specific receptor isoforms are obligatory for tissue specific ecdysteroid responses still requires further investigation, and

several recent experiments suggest EcR isoforms can be redundant in function (D'Avino and Thummel, 2000; Cherbas et al., 2003).

Hypotheses and experimental design

Ecdysteroid hormones mediate a variety of physiological activities during the crustacean molt cycle through ecdysteroid receptors. The genes recovered by this laboratory through cDNA cloning represent the crustacean ecdysteroid receptor. Different combinatorial arrays of both ligand and receptor may be important in mediating gene expression that controls growth and molting, limb regeneration and reproduction in crustaceans.

To understand how ecdysteroids are involved in the regulation of limb regeneration and molting-related events such as apolysis and cuticle synthesis during the molt cycle in *Uca pugilator*, further characterization of the UpEcR and UpRXR receptors is needed. My first hypothesis is that the structural similarity of UpEcR to the insect receptor represents an ability to activate target gene expression in response to hormone. To support this hypothesis, it needs to be demonstrated that the cloned ecdysteroid receptor is able to interact with typical hormone response elements, and transactivate target gene expression in *in vivo* or *in vitro* model systems. It is also necessary to verify if UpEcR, like other insect EcRs, requires UpRXR to bind to EcREs and transactivate gene expression, i.e. functions as a heterodimer. These studies require the construction of expression

vectors that will produce sufficient receptor proteins for biochemical studies. Using *E.coli* and *in vitro* expressed crab receptors, an array of synthetic standard or natural EcREs, and electrophoretic mobility shift assay (EMSA) and GST-pull down experiments, the DNA-binding and protein-protein interaction properties of the UpEcR and UpRXR protein were investigated.

My second hypothesis is that there exist UpEcR and UpRXR isoforms with unique physical properties. Cloning experiments did recover hinge and ligand binding domain isoforms for UpRXR. These receptor isoforms may have distinct DNA-binding and protein-protein interaction properties. By EMSA and GST-pull down experiments, the physical characteristics of DNA-binding and receptor protein-protein interactions of receptor isoforms could be studied, and differences between isoforms in DNA- and protein-binding identified. Similarly, by transfection assays, these receptor isoforms' transactivation properties in response to a hormone signal could also be examined.

The next portion of my research examined through immunocytochemistry and radioimmunoassay (RIA) the temporal and spatial profile of receptor proteins and their relationship to levels of circulating ecdysteroids. Antibodies aginst the UpExR and UpRXR A/B domain and common domain proteins have been obtained from recombinant epitopes generated from expression vectors. My third hypothesis is that UpEcR and UpRXR protein expression and distribution will reveal potential ecdysteroid target cell populations in different tissues of the limb

bud, and may accompany changes in physiological functions. Immunohistochemistry and RIA will be used to help test this hypothesis. The expression and distribution of these receptor proteins will be measured against the hemolymph levels of circulating ecdysteroids. Whereas the nuclear co-localization of both UpEcR and UpRXR would imply that they function as heterodimers, lack of co-localization might suggest that other pairing partners exist for these receptors. Evidence for this latter situation has been seen in other insects (Sutherland et al., 1995; Kozlova et al., 1998; Zhu et al., 2000; Baker et al., 2003).

Organization of the dissertation

This dissertation is organized into three chapters and an appendix. Chapter II is a reprint from a published paper in Molecular and Cellular Endocrinology (Durica et al., 2002). Chapter III is a manuscript just accepted to Molecular and Cellular Endocrinology. Chapter IV is a manuscript in preparation. The appendix contains data on the autotomy response and regeneration that will be submitted for publication for an invited conference presentation.

I am the second author on the manuscript presented in Chapter II and my contributions include the development of the probes (RNA probes and antibody probes, used in these and subsequent experiments), the protein-protein interaction characterization studies, and some of the EMSA analysis. I am first author on the manuscript presented in Chapter III. I performed all of the GST-pull down

experiments, and many of the EMSA analyses. The transfection studies were done in collaboration with the laboratory of Dr. Subba R. Palli, University of Kentucky. I performed the experiments in Chapter IV and the appendix.

Chapter II

Characterization of crab EcR and RXR homologs and expression during limb regeneration and oocyte maturation

Characterization of crab EcR and RXR homologs and expression during limb regeneration and oocyte maturation

David S. Durica[a,*], Xiaohui Wu[a], Gopinathan Anilkumar[a,b], Penny M. Hopkins[a], Arthur C.-K. Chung[a,1]

[a] Department of Zoology, University of Oklahoma, 730 Van Vleet Oval, Norman, OK 73019, USA
[b] Post Graduate Department of Zoology, Sree Narayana College, Kannur, India

* Corresponding author. Tel.: +1-405-325-1528; fax: +1-405-325-7560.
E-mail address : ddurica@ou.edu (D.S. Durica).
[1] Present address: Department of Molecular and Cellular Biology, Baylor College of Medicine, 1 Baylor Plaza, Houston, TX 77030, USA.

Keywords : Ecdysteroid receptor; Retinoid X receptor; Ultraspiracle; *Uca pugilator*

Abstract

We report here complete coding sequences for the *Uca pugilator* homologs of the ecdysteroid (UpEcR) and retinoid X receptors (UpRXR). Library screenings recovered cDNA clones containing a unique amino terminal open-reading frame (A/B domain) for each gene, most similar to insect B1 EcR and USP1/RXR isoforms. Splicing variants in the UpRXR ligand-binding domain were also identified, in a region critical for folding of *Drosophila* and lepidopteran USP. UpEcR and UpRXR proteins were able to associate, and both are required for binding to an ecdysteroid HRE; these interactions were not hormone-dependent. Ribonuclease protection assays (RPA) were conducted using A/B domain and 'common' (C or E) domain probes on RNA isolated from various stages of regenerating limb buds and ovaries. For several of the limb bud and ovarian stages examined, the relative level of A/B domain sequence protected was significantly less than common domain suggesting alternative amino terminal isoforms other than those isolated through cloning. This is the first report of *UpEcR* and *UpRXR* transcription during ovarian maturation, implicating the ovary as a potential target for hormonal control in crustacea.

1. Introduction

Among arthropods, ecdysteroid hormones are involved in the regulation of a wide variety of physiological events such as growth, reproduction and metamorphosis (for reviews, see Chang, 1989; Riddiford, 1993; Koslova and Thummel, 2000). The actions of ecdysteroids in arthropods are mediated through a ligand-dependent transcription factor, composed of two members of the nuclear receptor (NR) superfamily (for reviews, see Thummel, 1995; Riddiford et al., 2001). The NRs contain an array of protein domains characteristic for this class of receptors (for reviews, see Mangelsdorf et al., 1995; Renaud and Moras, 2000). The amino terminal A/B domain is variable even among closely related orthologs and is associated with transcriptional activation. The highly conserved C region primarily serves as the DNA binding domain (DBD), while the variable D domain represents a flexible hinge region, linking the DNA binding domain to the E, or ligand-binding domain (LBD). The LBD, in addition to containing a hydrophobic pocket for ligands, is also involved in receptor dimerization and interactions with other proteins that can serve as co-activators or co-repressors of transcription. A carboxyterminal F domain is another highly variable region that may also be reduced or absent, even among closely related members of the superfamily.

The insect ecdysteroid receptor has been characterized most extensively in *Drosophila*; it is a heterodimer composed of the ecdysteroid receptor (EcR) protein (Koelle et al., 1991) and the ultraspiracle (USP) protein (Shea et al., 1990; Henrich et al., 1990; Oro et al.,1990), a homolog of the vertebrate retinoid X

receptor (RXR). This heterodimer model has been supported through transfection studies monitoring ecdysteroid mediated reporter gene activation (Yao et al., 1992; Thomas et al., 1993), DNA and ligand-binding properties of *in vitro* synthesized receptor proteins (Yao et al., 1992, 1993; Thomas et al., 1993) and genetic analysis of EcR and USP mutants (Bender et al., 1997; Hall and Thummel, 1998).

The function of ecdysteroids in the regulation of gene transcription during insect metamorphosis has been the object of intense study (for review, see Riddiford et al., 2001). Variations in 20-hydroxyecdysone (20E) titers have long been associated with molting and metamorphosis in insects (reviewed in Karlson, 1996), and a hierarchy of transcription factor gene expression mediated by ecdysteroid exposure has been characterized in *Drosophila* (see Thummel, 1996, 1997; Riddiford et al., 1999 for reviews). Correlated with the responses observed during the larval-to-adult transition in *Drosophila* is the tissue-specific synthesis of distinct EcR receptor isoforms through alternative promoter usage and differential splicing (Talbot et al., 1993; Robinow et al., 1993; Truman et al., 1994; Schubiger et al., 1998). Three isoforms, classified as A, B1 and B2, contain variant N-terminal (A/B) domains associated with the same DBD and LBD (i.e. 'common' domains for all isoforms). A/B domain EcR isoforms have also been identified in other insects (Fujiwara et al. 1995; Kamimura et al., 1997; Mouillet et al., 1997) and in ticks (Guo et al., 1997). As in *Drosophila*, stage- and tissue-specific profiles of isoform expression have been observed (Jindra et al., 1996;

Hegstrom et al., 1998), as well as differences in transcriptional responses to hormonal exposure (Robinow et al., 1993; Hiruma et al., 1997).

Although only a single form of the USP protein has been found in *Drosophila*, two A/B domain isoforms of USP have been identified in other insects (Kapitskaya et al. 1996; Jindra et al., 1997) while at least two USP/RXR homolog genes have been identified in ticks (Guo, et al., 1998). Similar to EcR, USP isoform expression patterns show tissue and stage specificity (Jindra et al., 1997; Hiruma et al., 1999; Lan et al., 1999; Wang et al., 2000b).

This heterogeneity in isoform distribution has led to the hypothesis that a common hormonal signal could provoke dissimilar transcriptional responses through cell-specific production of combinatorial arrays of pairing partners with distinct affinities for ligand, response elements and/or co-regulatory molecules (Talbot et al., 1993). Moreover, other members of the nuclear receptor superfamily, by mediating EcR/RXR interactions or competing for DNA binding sites, may influence steroid responsiveness by forming additional pairing partners with either the RXR homolog or possibly EcR (Zelhof et al., 1995a,b; Sutherland et al., 1995; White et al., 1997; Zhu, et al., 2000).

In crustaceans, as in insects, ecdysteroid signaling appears to be critical to the timing of growth and reproduction. In the fiddler crab, *Uca pugilator*, and other crustaceans, several major ecdysteroids circulate in the hemolymph (Lachaise and

Lafont, 1984; Snyder and Chang, 1991; Hopkins, 1992). Changes in these ecdysteroid titers and ratios during the molt cycle are temporally correlated with major physiological events involved in the molting and subsequent replacement of old exoskeleton (for reviews, see Chang, 1989; Hopkins, 1992). Superimposed on the incremental growth via molting is a specialized form of growth, the epimorphic growth associated with regeneration of limbs. In response to limb damage, the crab can reflexively discard an injured limb (autotomy). In the fiddler crab, limbs that are lost to injury or predation as a result of the reflexive autotomy response can be regenerated completely during a single molt cycle (see Skinner, 1985; Hopkins, 2001 for reviews). Regeneration of limbs occurs in two phases. The first phase immediately follows the loss of the limb and is called basal growth. This phase can occur at any time during the life cycle of the crab but usually occurs prior to the initiation of molting. During basal growth, a blastema forms under the wound site and differentiates into a fully segmented miniature limb. Although the specification of a new limb primordium following limb loss assumes as yet uncharacterized signaling pathways, the deposition of a flexible cuticle during basal growth suggests a role for ecdysteroid signaling. The second phase of regeneration, called proecdysial growth, is restricted to the brief period that preceeds molting and is completed as the crab molts. Proecdysial growth is primarily hypertrophic; the small limb bud that developed during basal growth increases in size as much as 3-fold. The increase in size is due to protein synthesis and water uptake; it is not due to increase in cell numbers. Rates of protein synthesis increase during proecdysial growth in response to ecdysteroids

(Hopkins, 1993). Furthermore, crustaceans continue to grow as adults, and the molt cycle must, therefore, be coordinated with cycles of reproductive activity. In many crustaceans, ecdysteroids have been shown to accumulate in the ovaries and have been postulated to play a role in vitellogenesis, the resumption of meiosis, and subsequent embryogenesis (for review, see Subramoniam, 2000).

To aid in an examination of the roles of ecdysteroids in these processes, we isolated *U. pugilator* cDNA clones (*UpEcR* and *UpRXR*) that were structural homologs of the ecdysteroid and retinoid X classes of NR (Durica and Hopkins, 1996; Chung et al., 1998a). Monitoring the expression of these genes has identified putative ecdysteroid targets in a number of non-regenerating crab somatic tissues, in regenerating limb bud tissue, and provided structural information on the DBD, hinge, and LBD regions of these molecules (Durica and Hopkins, 1996; Chung et al., 1998a,b). Original screenings of oligo-dT primed libraries produced from late proecdysial limb bud mRNA, however, produced clones lacking complete A/B domains, precluding a search for differences in stage- or tissue-specific A/B isoform distribution. We, therefore, conducted additional screens to determine if variant forms of the receptor could be identified. Since reproduction, growth and regeneration occur in concert in adult crabs, we also initiated a study of receptor gene expression in ovarian tissues. We report here the results of a random-primed library screening, which have led to the recovery of a unique, invariant A/B domain for both UpEcR and UpRXR. LBD variants have also been identified in UpRXR, within the H1–H3 loop region

important in insect USP LBD folding. As expected from the high degree of sequence similarity to other arthropod receptors, we report that these proteins are able to interact, and that a UpEcR/UpRXR heterodimer is capable of binding to hormone response elements. We have also used ribonuclease protection assays (RPA) to determine whether additional A/B isoforms might be present during limb bud regeneration or during the process of oogenesis. These studies provide evidence for the existence of additional amino-terminal variants, distinct from those recovered from library screenings, which differ in their relative distributions during limb regeneration and the oocyte maturation cycle. This is the first report of ecdysteroid- and retinoid X receptor gene expression in reproductive tissues during the crustacean reproductive cycle. Consistent with recent findings in other systems, these results implicate the developing ovaries as a target for hormonal control.

2. Materials and Methods

2. 1. Animals and RNA extractions

U. pugilator were purchased from Gulf Specimen, Panacea, FL. The animals were acclimated to the laboratory as previously described (Hopkins, 1982; Hopkins and Durica, 1995). Seven limbs including the large cheliped were pinched with a forceps distal to the coxa, causing autotomy (the reflexive dropping of a damaged limb). For limb bud regeneration experiments, stagings were performed by calculating *R* values (Bliss, 1956) and the growth rate of the limbs (Bliss and Hopkins, 1974). Limb blastemal tissue was isolated 4 days (A+4) and 8 days after autotomy (A+8) during basal growth. Proecdysial limb buds were removed at the D0 and D1–4 stages (after Drach, 1939), marked by rapid tissue hypertrophy and growth (Do), with a slowing of growth just prior to molt (D1–4). For ovarian tissue isolations, ovaries were staged according to size and morphological criteria (Anilkumar, unpublished). Ovaries were dissected by cutting open the carapace from the dorsal side; the dissection was performed in *Uca* saline (46 mM $MgCl_2$, 42 mM Na_2SO_4, 286 mM NaCl, 11 mM KCl, 16 mM $CaCl_2$, 76 mM Tris, pH 7.8). Care was taken to prevent contamination by non-varian tissues in the sample. The ovarian samples were pooled into three ('early', 'mid' and 'late') stages, based on the oocyte width (OW, measured through an ocular micrometer to the nearest μm) and color of the ovary. Ovaries in the 'early' stage (OvE) were purple and the OW was 90–180 μm. The 'mid' stage

ovaries (OvM) were purple–brown in color and 181–320 μm in OW, while the ovaries at 'late' stage (OvL) appeared brownish with an OW~320 μm. Soon after dissection, the tissue was rinsed in *Uca* saline. Total RNA from limb buds and ovaries was isolated using Trizol reagent (Invitrogen corporation, Carlsbad, CA) according to the manufacturer's instructions. Following ethanol precipitation and washing, pellets were resuspended in diethylpyrocarbonate-treated water and RNA concentrations determined by UV absorbance at 260 nm. Poly(A)+ mRNA was isolated either by oligo-dT cellulose chromatography (library construction) or oligotex (Qiagen, Valencia, CA) spin chromatography (Northern blot analysis).

2. 2. Library screenings and plasmid subcloning for probe and antibody production

A random-primed cDNA library was constructed from late proecdysial limb bud mRNA and screened as previously described (Chung et al., 1998b), with the exception that priming was accomplished using random 9-mers (Amersham, Piscataway, NJ), methyl-dCTP was not used for first strand synthesis and the double-stranded cDNA was non-directionally introduced into *Eco*RI-cut lambda ZapII vectors (Stratagene, La Jolla, CA). Hybridization probes complementary to the DBDs of *UpEcR* and *UpRXR* were used for screenings and following plaque purification of positive clones, phagemids were recovered by *in vivo* excision. Clones were then analyzed for sequence heterogeneity by restriction digestion, hybridization analysis, and PCR amplifications using A/B domain primers and DNA sequencing. DNA sequencing (ABI model 3700) and oligonucleotide

synthesis were performed at the Recombinant DNA/Protein Resource Facility at Oklahoma State University. DNA similarity searches were performed using the BLAST 2.0 search engine at the National Center for Biotechnology Information (Madden et al., 1996). Multiple sequence alignments were generated by ClustalW 1.8 (Thompson et al., 1994) at the Baylor College of Medicine Search Launcher, and output was formatted using the BOXSHADE server (http://www.ch.embnet.org/software/BOX–form.html). Predictions of protein structure were performed using the PredictProtein server (Rost, 1996) at the Columbia University BioInformatics Center (http://cubic.bioc.columbia.edu/predictprotein/).

To construct a complete in-frame coding sequence for UpEcR, a oligo-dT primed UpEcR cDNA clone (p11Ab) containing the LBD, hinge, part of the DBD and 3' non-coding region was digested with *Apa*I, and the larger fragment containing the coding region and vector (pBSIISK) religated and recovered as a plasmid (p11Ab4). This plasmid was then digested with *Not*I and *Sph*I, which cut within the vector sequence and the DBD, respectively. This fragment and a *Not*I/*Sph*I fragment containing the amino-terminal UpEcR sequence from a clone (p3-1) isolated from the randomprimed library were gel-purified (Qiagen), ligated and transformed (Statagene Epicurian cells). This construct (pBSEcR) contains 262 nt upstream of the first methionine codon, the UpEcR coding sequence, and 193 nt downstream of the stop codon. To construct a complete in-frame coding sequence for UpRXR, an oligo-dT primed cDNA clone (3B) was cut with *Not*I

and *Bst*EII, which produced a fragment containing vector sequences and the LBD, hinge and a portion of DBD from UpRXR. Primers (5'-ATGCGGCCGCATGA-TTATGATTAAAAAGGAGAAGCCGGTG-3'; 5'-TGAGGCGCGGTCACCAC-A-3') were then designed to incorporate a *Not*I and *Bst*EII site flanking the amino terminal coding region of UpRXR, and the A/B domain was PCR amplified using a random primed UpRXR clone (17C) as template. The recovered fragments were purified, cut with the appropriate restriction enzymes, ligated and transformed into bacteria to yield the construct pBSRXR. To construct the GST–RXR fusion vector, primers specific to the amino- and carboxyl terminal ends of the RXR coding region (5'-ACGAATTCCCATGATTATGAT TAAAAAGGAGAAGC-3'; 5'-ACCTCGAGCTAGCTGGTGGGGGGAGTG-3'), with incorporated *Eco*RI and *Xho*I sites, respectively, were used to PCR amplify the UpRXR coding region from pBSRXR, which was then introduced into the pGEX4T2 vector (Promega, Madison, WI) which had been linearized with the same enzymes.

For production of single-stranded RNAs for *in vitro* protein synthesis and RPA analysis, subclones were introduced into the BlueScriptII (pBSII) KS vector (Stratagene). For full-length *UpRXR* sequences, the pGEX-RXR vector was digested with *Xho*I and *Eco*RI and the coding-region-containing fragment was ligated into *Xho*I–*Eco*RI digested pBSIIKS. For *UpEcR*, the complete coding sequence that had been subcloned into the pBlueBacHis2-C vector (Invitrogen) was removed by digestion with *Eco*RI and *Kpn*I and introduced into the

appropriate sites of pBSIIKS. These full-length coding subclones were sequenced to verify the integrity of the reading frame. An A/B domain subclone of *UpEcR* was constructed by PCR amplification of plasmid DNA (18-2F) using a universal reverse primer and a primer complementary to a region of the *UpEcR* DBD (5'-CTTCAGGTCGCCG-TAGGA-3'). The amplification product was digested with *Eco*RI and *Xho*II, gel purified, and cloned to the *Eco*RI and *Bam*HI sites of the pBSIIKS vector. This clone contained 210 nt of 5'non-coding DNA upstream of the putative start codon. A *UpRXR* A/B domain subclone was constructed using a reverse primer containing an *Xho*I site (5'-ATCTCGAGAGGTGCTTGGAG-CCAGACAGT-3') and a forward primer containing a *Not*I site (5'-ATGCG-GCCGCATGATTATGATTAAAAAGGAGAAG-3'); amplification of UpRXR cDNA (17C) produced a fragment containing only coding region DNA plus the indicated restriction sites. Following amplification, restriction digestion and purification, the fragment was introduced into the appropriate sites of the pBSIIKS vector. The construction of the *UpRXR* and *UpEcR* vectors containing distinct common domain (DBD and LBD, respectively) sequences has been described previously (Chung et al., 1998a).

To construct a subclone that would express the *UpRXR* E domain in bacterial cells, a phagemid (3B) containing the hinge and LBDs of *UpRXR* was digested with *Bam*HI and *Kpn*I and introduced into the corresponding sites of the QE-31 vector (Qiagen). This clone encodes the carboxy-terminal 250 amino acids of the UpRXR protein that has been fused in frame to a 6xHis tag. For the UpRXR A/B

domain, primers were designed to incorporate a *Bam*HI and a *Hin*dIII site to either side of the A/B domain sequence (5'-GAAAGCTTGCTGG-GTGGGTACTGGC-3'; 5'-GAAAGCTTGCTGGGTGGGTACTGGC-3'). The appropriate fragment was amplified using the 17C clone as template and then introduced into the corresponding sites of the QE-31 vector. For the UpEcR A/B domain, the primers incorporated *Bam*HI and *Kpn*I sites to either side of the coding region (5'-ACGGATCCGTATGGCCAAGGTGCTG-3'; 5'-CAGGTA-CCTGATAACGAAGAGGTGTC-3'); the amplified fragment was then introduced into the QE-32 vector.

Following induction with IPTG, UpEcR and UpRXR immunogens produced from the vectors described above were purified from bacterial cell (M15; Qiagen) extracts using nickel chelate chromatography, solubilized in standard SDS-PAGE sample buffer and run on a 10% polyacrylamide gel. The proteins were excised from the gel following visualization of the band by precipitating the protein in situ with 0.1 M KCl. Polyclonal rabbit antisera against the recombinant proteins were then generated by a commercial supplier (Cocalico Biologicals, Philadelphia, PA).

2. 3. Probe synthesis

Synthetic mRNA encoding full-length UpEcR, UpRXR or GST-UpRXR and A/B and common domain antisense probes for RPA were produced using

Riboprobe T3 and T7 polymerase *in vitro* transcription systems (Promega). Where 3' overhang restriction sites were needed to linearize plasmid DNA, the ends were repaired using T4 DNA polymerase (Promega) according to the manufacturer's protocol. For full-length transcripts used for *in vitro* translation or RPA titrations, following synthesis and removal of DNA template by RQ1 DNAse (Promega) digestion, the reactions were phenol-extracted, precipitated by ethanol precipitation, and resuspended in DEPC-treated water. An aliquot was denatured and run on an agarose gel; the size and amount of transcript synthesized was determined by comparison to an RNA standard (Century RNA markers, Ambion, Austin, TX) using Kodak 1D Image Analysis Software. For probe radiolabelings with [α-^{32}P]UTP (Amersham, 800 Ci/mmol), following probe synthesis and removal of the DNA template, an equal volume of Gel Loading Buffer II (Ambion) was added to the reactions, the reactions were heated for 3 min at 95°C, and run for 1.5 h at 250 V on an 8 M urea 5% acrylamide gel. The radioactive bands were cut from the gel and placed in 350 µl Probe Elution Buffer (Ambion) for overnight elution at 37 °C.

In vitro protein synthesis was performed using the Flexi Rabbit Reticulocyte Lysate System (Promega). For optimal synthesis from the *UpRXR* template, the standard reaction was supplemented with 1 µl 25 mM magnesium acetate. For synthesis of radiolabeled protein, 1 µl of 1 mM amino acid mix without methionine and 1 µl of [^{35}S]methionine (Amersham, 1000 Ci/mmol) was added to the standard reaction; for unlabeled reactions, 0.5 µl each of amino acid mixes

without methionine or leucine were used. The amount of protein synthesized was calculated from percent incorporation into TCA-precipitated counts, relative to the methionine content of UpEcR and UpRXR. Calculations ranged from 30 to 80 fmoles per synthesis.

For electromobility shift assays (EMSA), 2 pmol of forward and reverse complement deoxyoligonucleotides containing a DR-4 element (ttggacaAGGTCAcaggAGGTCActtgtctt) were end-labeled with [γ-^{32}P]ATP (Amersham, 3000 Ci/mmol) and polynucleotide kinase prior to annealing. For blot hybridizations, DNA probes were radiolabeled by random priming (Megaprime system, Amersham) as described previously (Chung et al. 1998a).

2. 4. GST-pulldown experiments and electromobility shift assays

For use in pull-down experiments, bacterially expressed GST-UpRXR fusion protein was bound to glutathione-sepharose beads (Amersham-Pharmacia) using a modification of the protocol of Smith and Corcoran (1994). Following induction and harvesting, bacterial cells were resuspended in ice-cold PBS containing protease inhibitors (0.5 mM PMSF, 1 μg/ml pepstatin and leupeptin). Lysozyme was added to 1mg/ml and the incubation continued for 30 min. The cells were then briefly sonicated on ice and the cell debris removed by centrifugation at 11000×*g* for 30 min at 4 °C. Beads were then added to the supernatant and the mixture was gently spun on a rotator for 1 h at 4 °C. The beads were washed

twice in 20 vol. of PBS containing 1% Triton X-100 and collected by centrifugation. Binding of [^{35}S]methionine labeled-UpRXR and -UpEcR was conducted essentially as described by Melcher and Johnson (1995). Two hundred microliters of *E. coli* extract (DH5α) was incubated as competitor with 15 µl of reticulocyte lysate containing *in vitro* synthesized receptor (~10 fmol) for 15 min on ice. Ten microliters of bait GST-RXR (~1 pmol) bound to beads, in 200 µl of *E. coli* competitor extract, was then combined with the above and the incubation continued for 1 h at 4 °C with gentle spinning on a rotator. The beads were taken through three consecutive washings in 50 mM KCl pH 7.5, 150 mM NaCl, 10% glycerol, 1% Triton X-100, followed by centrifugation. The beads were suspended in SDS sample buffer, boiled and the released proteins displayed through SDS-PAGE. Gels were stained in Coomassie Blue, dried, and receptor bound to the bait protein assessed by conventional or electronic autoradiography (Packard InstantImager, Meriden, CT). Control experiments were conducted as above, with the exception that 10 µl of bait GST protein was used in lieu of GST-UpRXR.

For EMSA analysis, radiolabeled complementary oligonucleotides were mixed, brought to 20 mM $MgCl_2$ in 1× kinase buffer (70 mM Tris–HCl, pH 7.6, 10 mM $MgCl_2$, 5 mM DTT) heated to 60 °C and allowed to anneal while cooling to room temperature. Also 5× loading dye (10 mM Tris–HCl, 1 mM EDTA, 20% glycerol, 0.25% bromphenol blue) was added and the annealed probe was run in 1× TBE on a non-denaturing 10% polyacrylamide gel, excised, and eluted from

the gel slice into 10 mM Tris–HCl, pH 7.6, 50 mM NaCl, 1 mM EDTA, at 4 °C overnight on a rotator. For binding reactions, varying amounts of each reticulocyte lysate containing *in vitro* synthesized protein (see below) was added to 4 µl of 5× buffer R (50 mM Tris–HCl, pH 7.5, 250 mM NaCl, 5 mM $MgCl_2$, 2.5 mM DTT, 2.5 mM EDTA, 20% glycerol), 1 µl of 1 mg/ml poly (dI-dC), 1 µl of 15 µM 20E (Sigma, St Louis, MO), and non-specific single-stranded DNA (29–34 oligomers, 0.3 mg/ml). Reactions contained either none (1 µl control lysate without added template), 0.5 µl (1/2×), 1 µl (1×) or 2 µl (2×) of lysate containing UpEcR or UpRXR. For supershift and competition experiments, antisera to receptor protein (1:4 dilution) or unlabeled HRE (2–50× competitor) were added to the reactions, the volume was taken to 18 µl, and the reactions incubated at 25 °C for 30 min. After a 30 min incubation, 2 µl of probe (~20 fmol) was added and the incubation continued for an additional 30 min. Retardation complexes were identified using 6% non-denaturing PAGE run at 150 V at room temperature until the dye marker was approximately 2/3 through the gel. The gel was dried and the location of the bound radiolabeled oligomer quantified using electronic autoradiography.

2. 5. Northern hybridizations and ribonuclease protection assays

Northern blotting and hybridization analysis were performed as previously described (Chung et al. 1998a). Ribonuclease protection assays were done using RPA III reagents (Ambion), essentially according to the supplier's instructions,

using 50 000 cpm of antisense probe for hybridizations to 10 µg total RNA. Optimal removal of unbound probe was observed when the RNAse cocktail was used at a 1:30 dilution. Fragments were resolved by 5% denaturing PAGE as described under probe preparation. Quantification of protected RNA was performed essentially as described in Chung et al. (1998b) using Packard InstantImager software. Total RNA in the samples was calculated from ultraviolet spectrophotometry while protection of standardized amounts of *in vitro* synthesized *UpEcR* and *UpRXR* sense strand templates were used to normalize results within and between gels. The EcR A/B domain probe contains 5' non-translated sequence upstream of the initiation codon, producing a larger protected fragment for native mRNA than for cRNA, which contains only coding sequence. Positive and negative control experiments were run in parallel with sample RNAs and either treated with RNAse (tRNA+) or mock digested (tRNA-). Error bars on data represent standard errors of the mean (S.E.M.) that were calculated from at least three separate assays. Graphs and statistical analysis using Student's *t* test were performed using the SigmaStat and SigmaPlot software package (SPSS Science, Chicago, IL).

3. Results

3. 1. DNA sequence analysis of UpEcR and UpRXR cDNA clones isolated from random-primed libraries

We have constructed oligo-dT and random-primed cDNA libraries from late proecdysial regenerating limb bud mRNA. As previously reported, screening of the oligo-dT-primed library has led to the recovery of the DNA-binding (C), hinge (D) and ligand-binding (E/F) domains for both the *UpEcR* and *UpRXR* gene homologs (Chung et al., 1998a,b; Durica et al. 1999). The *UpEcR* and *UpRXR* genes encode large transcripts and full-length cDNA clones were not recovered from the oligo-dT-primed library. The random-primed library was subsequently screened, and clones representing the amino terminal A/B regions of the *UpEcR* and *UpRXR* genes were recovered and characterized. Detailed analyses of the *UpEcR* and *UpRXR* clones indicated a single A/B domain open-reading frame for each gene. Although clones containing alternative sequences were identified in the library, none contained a complete open reading frame upstream of the C domain, and presumably represent incorrectly processed splicing intermediates. A similar situation has been described for EcR processing variants in ticks (Guo et al., 1998). We have also failed to recover A/B isoforms using anchored PCR techniques for late proecdysial mRNA, with the majority of recovered clones again representing presumed splicing intermediates.

Fig. 1 depicts the deduced sequence of the recovered A/B domain of the UpEcR (1A) and UpRXR (1B) proteins, relative to the sequences of the most closely related receptors. BLAST searches and ClustalW alignments indicate that the UpEcR A/B domain (156 amino acids) shows greatest similarity to the 'B1-like' EcR proteins from a variety of insect orders. Following alignment, for

residues that show conservation among at least 50% of arthropod EcRs at any given position, UpEcR shows 29% identity with *Drosophila* EcR-B1, and 12% identity to *Drosophila* EcR-A (the A/B domain of the *Drosophila* EcR-B2 isoform is only 17 amino acids in length). The UpEcR A/B domain sequence shares the greatest sequence relatedness to *Tenebrio* EcR, where amino acid identities are approximately 42% in the A/B domains, compared with 97 and 68% for the DBD and LBD, respectively. The UpRXR A/B domain (Fig. 1B; 105 amino acids) has greatest similarity to the USP-1/USP-A homologs identified in several insects; the alternative USP-2/USP-B isoforms are considerably shorter without a string of charged residues at the amino terminus. Within the amino terminal domain, the UpRXR sequences show the highest degree of relatedness to *Apis* USP(~47% identity) and *Aedes* USP-A (~36% identity), relative to 91% identity in the DBD and 65–43% identity in the respective LBD domains. In sequencing the random-primed clones, a nucleotide difference from that previously reported for the UpEcR coding region was detected; this represents an M→L change at position 160, immediately preceeding the C domain (Chung et al., 1998b). Since this sequence was seen in three separate cDNA isolates and is highly conserved, this correction was entered into the database.

Although A/B domain variant clones were not isolated, we have previously reported three distinct hinge region variants for the UpEcR protein (Chung et al., 1998b). Alternative splicing at the D–E boundary leading to variant hinge region domains has also been observed in insect EcRs (Fujiwara et al., 1995). Screening

of the random primed-library also led to the recovery of D–E domain variants for the UpRxR protein in two different regions (Fig. 2). We have isolated a variant that contains an insertion of five amino acids within the 'T' box, a highly conserved domain adjacent to the DBD implicated in hormone response element (HRE) recognition. Among characterized receptors, only the zebrafish RXR-ε contains an insertion in this region (Jones et al., 1995). A second variant region involves an insertion/deletion of a 33 amino acid segment located between the flexible loop region and helix 3 of the LBD (Fig. 2). The variant lacking this insert shares greater similarity to characterized USP/RXR proteins; we have previously reported a splicing variant from the oligo-dT primed library which lacks a complete LBD and apparently represents an unprocessed intermediate of this splice junction (Chung et al., 1998b). Recently solved crystal structures of insect USPs (Billas et al., 2001; Clayton et al., 2001) indicate this region is important in promoting distinct LBD folding differences relative to the vertebrate RXRs.

3. 2. GST-pulldown and EMSA analysis on in vitro synthesized UpEcR and UpRXR

We have cloned the entire coding regions for *UpEcR* (Genbank AF034086) and *UpRXR* (GenBank AF32983; contiguous sequence in Fig. 2) into vectors containing T3 and T7 promoters and have produced synthetic mRNAs for translation in reticulocyte lysates. The coding region for *UpRXR* was also

introduced into the pGEX-4T-2 vector (GST fusion, Amersham Pharmacia). We tested to see if the *in vitro* synthesized UpEcR or UpRXR proteins are capable of interacting with GST-UpRXR in GST-pull down experiments (Fig. 3). Under the conditions of these experiments, any protein that interacts with GST–RXR can be captured with the affinity-tagged fusion protein using glutathione-linked Sepharose beads. Reticulocyte lysates containing [^{35}S]methionine-labeled UpRXR or UpEcR were individually mixed with beads containing a GST-UpRXR fusion protein in the presence of competitor proteins. The recovered proteins were resolved by SDS-PAGE (Fig. 3A) and the radiolabeled proteins bound to GST-UpRXR were displayed by autoradiography (Fig. 3B). As shown in Fig. 3B, [^{35}S]-labeled *in vitro* synthesized UpRXR (Fig. 3B, lane 1) is not recovered in this assay, whereas [^{35}S]-UpEcR (arrow, Fig. 3B, lane 2; predicted molecular weight 57.4 kDa) is capable of binding to GST-UpRXR. This interaction requires UpRXR and is not a function of binding to the GST affinity tag. Fig. 3C and D represent an experiment where reticulocyte lysates containing labeled UpEcR are mixed with beads containing the GST protein alone (arrow, Fig. 3C, lane 1) or GST-UpRXR (arrow, Fig. 3C, lane 2). As indicated in the autoradiograph in Fig. 3D, binding of UpEcR is observed (arrow, Fig. 3D, lane 2) only with GST-UpRXR. These experiments indicate that UpEcR and UpRXR are capable of protein/protein interactions, presumably heterodimer formation, but UpRXR does not complex with GST-UpRXR under these experimental conditions.

Electrophoretic mobility shift assays (EMSA) using *in vitro* synthesized UpEcR and UpRXR proteins indicate both receptors are required for binding to an EcR hormone response element (HRE) and this binding is not hormone-dependent. This has been observed for both direct repeat (Fig. 4) and inverted repeat (not shown) HREs. In the representative experiment shown in Fig. 4, the radiolabeled oligonucleotide probe contains a direct repeat hormone response element separated by a 4-nucleotide spacer (DR-4 HRE) plus flanking sequences derived from an ecdysteroid responsive *Drosophila* gene (*hsp*27, Riddibough and Pelham, 1987; Wang et al., 1998). When complexed with receptor, bound DNA (bold arrow) is retarded relative to free DNA (open arrow). HRE incubated with reticulocyte lysate containing no added receptor mRNA (Fig. 4; lane 1), *in vitro* synthesized UpEcR alone (Fig. 4; lane 2), or *in vitro* synthesized UpRXR alone (Fig. 4; lane 3) showed no retardation. Both UpEcR and UpRXR are required for probe binding to this HRE (Fig. 4; lane 4). Binding is dependent on the amount of lysate that is added to the reaction (Fig. 4; lanes 4–6), and can occur in absence of 0.75 μM 20E (Fig. 4; lane 7). Binding of a polyclonal antibody (directed against the UpRXR LBD) to the receptor complex leads to a supershift in retardation (lane 8, thin arrow). Polyclonal antibodies directed against the A/B domains of UpEcR or UpRXR are also capable of inducing a supershift (data not shown). Binding can also be reduced with increasing amounts of unlabeled competitor HRE (Fig. 4; lanes 9–13).

3. 3. Northern blot analysis during limb regeneration using A/B domain-specific probes

We conducted Northern blot experiments using mRNA isolated from regenerating limb buds to assess whether transcript size heterogeneity correlated with heterogeneity in A/B domain hybridization patterns (Fig. 5). Using *UpRXR* common domain (DBD) probes, previous experiments had identified two *UpRXR* transcript sizes of approximately 5 kb in all tissues examined (Chung et al., 1998a). Recent experiments using a slightly modified RNA isolation protocol (Trizol, Life Technologies) have also recovered a larger transcript of approximately 9.6 kb. In parallel experiments using a *UpRXR* A/B domain probe (Fig. 5A), transcript size distributions are similar to those observed with the DBD domain probe. All the transcript sizes hybridize to the recovered A/B domain probe (i.e. none can be classified as A/B domain-specific). Similar experiments with *UpEcR* A/B and DBD-specific probes also show no differences in hybridization to the 7 kb *UpEcR* transcript (Fig. 5B). Thus, a specific mRNA amino terminal domain is not represented in a distinct transcript size.

3. 4. Ribonuclease protection assays (RPA) on regenerating limb buds and ovary tissue

Using RPA analysis, we measured the steady-state concentrations of transcripts containing the *UpEcR* and *UpRXR* A/B domain coding regions relative

to mRNAs representing conserved coding regions of the DBD or LBD domains of the receptor (Figs. 6 and 7). Since conserved regions of the DBD or LBD domains should be present in all receptor mRNA, significant variations in the A/B:'common' domain ratio would suggest the possibility of other receptor isoforms and indicate tissues potentially enriched for these variants. Limb bud (Fig. 6) or ovarian (Fig. 7) RNAs were hybridized to both A/B domain and common (DBD or LBD) domain probes, and the level of protection titrated against known amounts of sense cRNAs, containing the complete coding sequences of *UpRXR* and *UpEcR*. For *UpRXR* (Fig. 6A and Fig. 7A), the A/B domain and DBD probes were of similar size (~300 nt) and experiments were set up in parallel. For *UpEcR*, the A/B and LBD probes differed in size by ~150 nt, and quantification of A/B and LBD domains could be determined within the same RNA sample (Fig. 6B) or on parallel samples (Fig. 7B); both protocols yielded similar results.

For regenerating limb buds, Fig. 6A and B represent typical autoradiographs for *UpRXR* and *UpEcR*, respectively; data from at least three separate assays, quantified using electronic autoradiography, is summarized in the histograms in Fig. 6C and D. For both *UpRXR* and *UpEcR* at the A+8 and D_0 regeneration stages, the relative levels of protected A/B domain mRNA sequence is significantly less ($P \leq 0.05$) than common domain. *UpRXR* A/B domain mRNA sequences are also significantly under-represented in D_{1-4} limb buds and *UpEcR* A/B domain mRNA sequences under-represented in A+4 limb buds. Additional

bands of lower molecular weight resulting from hybridization to the A/B domain probe are also observed (asterisks on autoradiographs). These results suggest that in some transcripts only a portion of the A/B domain is protected, and that exon shuffling and/or alternate promoter usage could give rise to additional isoforms.

Similar results were obtained using ovarian tissue samples (Fig. 7). In these experiments, there was more heterogeneity in both *UpEcR* and *UpRXR* transcript measurements within the same stages than in limb buds, which may relate to some lack of synchronicity during oogenesis as the animals were leaving the reproductive cycle. Nevertheless, for *UpRxR*, A/B domain mRNA sequences are significantly under-represented relative to DBD domain in early and mid oogenesis (Fig. 7A and C). Due to the large amount of variance in transcript abundance between stagings, no significant differences were observed for *UpEcR* (Fig. 7B and D). For any given RPA experiment, however, A/B domain sequences consistently appear in lower abundance than those protected with LBD domain probes (panel 7B).

4. Discussion

4. 1. Sequence analysis of UpEcR and UpRXR cDNA clones from random-primed library

Sequence analyses of the crustacean clones recovered from late proecdysial regenerating limb bud cDNA libraries indicate a unique amino-terminal A/B domain open-reading frame for both *UpEcR* and *UpRXR*. A/B domain isoforms for both the EcR and RXR/USP proteins have been identified in several insects (see Riddiford et al., 2001 for review). As is characteristic of NRs, the A/B domains of these genes show considerably more sequence variability among orthologs than other regions of the receptor. Relative to the characterized insect isoforms, the crustacean A/B domain sequences share greatest similarity to the EcR 'B1-like' isoform, and the 'USP-A' and 'USP1-like' isoforms.

Expression studies and mutant analysis strongly suggest that isoform specificity in insects may be linked to their ability to perform a discrete developmental function (Bender et al., 1997; Schubiger et al., 1998; Schubinger and Truman, 2000; Lee et al., 2000), although situations where isoforms may be functionally redundant have also been described (D'Avino and Thummel, 2000). Although homologs to proteins that interact with the AF-2 region of the vertebrate NR LBD domains have been isolated in *Drosophila* (Tsai et al., 1999; Bai et al., 2000; Beckstead et al., 2001), how amino-terminal activation domain specificity might mediate distinct tissue-specific transcriptional responses remains largely unexplored in arthropods.

Although only single A/B domains for UpEcR and UpRXR were recovered from library screenings, clones lacking an open reading frame were recovered,

presumably representing splicing intermediates. We also failed to recover A/B isoforms using anchored PCR techniques (not shown), which produced clones containing unprocessed splicing variants and sequence rearrangements. The inability to recover alternative A/B isoforms by either of these technologies could reflect lower amounts of a particular isoform in the RNA population used for library construction (see below), and/or a problem in reverse-transcribing mRNAs with unfavorable secondary structure.

The LBDs of NRs are responsible for ligand-binding specificity and ligand-dependent transactivation. We have previously reported that sequence relatedness in the UpRXR LBD is significantly greater to vertebrate RXRs than to dipteran USPs (Chung et al., 1998b); this has also been observed for other arthropod RXR homologs (Guo et al., 1998; Hayward et al., 1999). The divergence of the lepidopteran and dipteran ultraspiracle proteins from vertebrate RXRs (which bind 9-*cis* retinoic acid) has led to the speculation that USP may have no cognate ligand or a different ligand-binding specificity (Kapitskaya, et al., 1996; Guo et al. 1998; Chung et al., 1998b; Hayward et al., 1999). Ligand binding and transcriptional activation studies have tested a variety of ecdysteroid, retinoid and juvenile hormone (JH) analogues for activity with negative results (Oro et al., 1990; Yao et al., 1992, 1993; Harmon et al., 1995), although low-affinity binding of *Drosophila* USP to JH esters and acids has been reported (Jones and Sharp, 1997). The crystal structures of the lepidopteran *Heiliothis virescens* and the dipteran *Drosophila melanogaster* USPs have recently been reported (Billas et al.,

2001; Clayton et al., 2001). The bacterially-synthesized proteins used in these studies contained bound lipids in their ligand-binding cavities that were not displaced by competition with JH ester or methoprene (Billas et al., 2001). Additionally, when compared with the conformations of the previously characterized free (apo) and ligand-bound vertebrate RXR receptors, the insect USP LBD adopts an 'antagonist' conformation, rather than the 'agonist' conformation associated with transactivation and coactivator binding (for review, see Egea et al., 2000). A structural element important in promoting the antagonist conformation is the connecting loop (L1-3) between helices H1 and H3, which sterically hinders the transactivation domain in H12 from adopting an agonist conformation. Notably, the LBD variants that were isolated for the crustacean RXR ortholog fall within this region. The crustacean cDNA variants differ by 33 residues in the region separating the canonical helices H1 and H3, with the shorter variant closer to that observed in other NRs. The L1-3 loop in the lepidopteran sequence appears to be less flexible than that of vertebrate RXRs, due to interactions with several secondary structural elements in the LBD (Billas et al., 2001). Secondary structural predictions (Rost, 1996) estimate a longer loop region for the larger L1-3 crustacean LBD variant. Sequence variation in this region could influence transactivation properties or ligand affinities, i.e. contribute to an LBD isoform specificity. In crustaceans, the sesquiterpenoid methyl farnesoate (MF) has been implicated in both stimulation of ecdysteroid synthesis (Borst et al., 1987; Tamone and Chang, 1993) and, in some species, stimulation of ovarian maturation (Laufer et al., 1993). Additionally, biosynthetic

pathways leading to retinoid synthesis have recently been demonstrated in *Uca* limb bud blastemal tissue (Hopkins, 2001). Exposure to exogenous retinoids during early limb regeneration can adversely affect limb bud development (Hopkins and Durica, 1995) and increase steady-state levels of *UpRXR* transcripts as well as levels of circulating ecdysteroids (Chung et al., 1998b). These observations support the hypothesis that UpRXR may bind a retinoid-like or MF-like ligand, which could be influencing gene expression during blastemal development in limb regeneration. We have also recovered a cDNA variant that contains a five amino acid insert in the 'T' box, another conserved region of RXR NRs adjacent to the DBD. This region is important in mediating HRE binding interactions with RXR homodimers or RXR/RAR heterodimers (Zhao et al., 2000; Rastinejad et al., 2000). RXR-ε, a novel zebrafish RXR, also carries an 8 amino acid insert in this region, along with a 14 amino acid insert corresponding to H7 of the LBD. This variant does not bind 9-*cis* RA and shows no activity on RXR response elements in transfection assays, presumably due to the insertion seen in the LBD (Jones et al., 1995). This receptor is expressed during zebrafish development, but shows no elevation in expression during caudal fin regeneration (Beckett and Petkovich, 1999). It can bind DNA as a heterodimer with RAR and TR, and since it is active in TR transfection assays, may be involved *in vivo* in mediating a balance in homodimer/heterodimer concentrations for selective response elements (Jones et al., 1995). To summarize, although the biological significance of the crustacean RXR receptor variants requires further characterization, heterogeneity has been identified in regions of the molecule

important for DNA binding, dimer formation, ligand affinity and transactivation. These structural differences could reflect conformational flexibility and the potential for distinct allosteric interactions between different NRs and/or HREs, coactivators/corepressors, and ligands.

4. 2. Functional studies on in vitro synthesized UpEcR and UpRXR

GST pull-down experiments indicate that an *E. coli* expressed GST–RXR fusion protein can bind to *in vitro* synthesized UpEcR protein and this interaction can occur in the absence of ligand. Under these experimental conditions, we were unable to detect the ability of UpRXR to self-associate. In vertebrates, RXRs are able to form homodimers in the presence of 9-*cis* retinoic acid, the RXR ligand (Mangelsdorf et al. 1992; Zhang et al. 1992; Zhao et al. 2000). It is possible that homodimer formation of the crustacean RXR might occur under different experimental contexts, i.e. DNA binding to specific response elements or presence of specific ligands (D'Avino et al., 1995; Wang et al., 1998). Gel shift experiments also indicated that both UpEcR and UpRXR are required for binding to a DR-4 HRE used in the characterization of dipteran EcR/USP. Antibody supershift experiments confirm that RXR is a component of this hetero-complex; experiments using antibodies directed against UpEcR also result in a supershift (not shown). In these experiments, a band shift could be observed with the HRE in the absence of 20E, and addition of hormone had no effect on binding. Thus, hetero-complexes involved in protein–protein binding and protein–DNA binding

can occur in the absence of hormone under these experimental conditions. We observe similar results using an imperfect inverted repeat (IR) element derived from a *Drosophila* ecdysone-responsive gene (*hsp*27; Riddibough and Pelham, 1987; not shown). HRE binding in the absence of hormone *in vitro* is a general characteristic of type II NRs and has been observed with several insect receptors (Wang et al., 1998; Perera et al., 1998). For some insect receptors, addition of 20E has been shown to enhance binding to certain response elements during EMSA analysis (D'Avino et al., 1995; Wang et al., 2000a). Using differential salt extractions, distinct EcR/USP complexes have been isolated from nuclear extracts during mosquito vitellogenesis. These complexes differ both in their developmental profiles and in their responsiveness to 20E in DNA-binding assays (Miura et al., 1999), suggesting that they represent unliganded and liganded subpopulations. Sequences within the dipteran EcR LBD that confer differential sensitivity to ligand-independent DNA binding, as well as ecdysone (as opposed to 20E) stimulated transactivation in cultured cells, have recently been mapped using chimeric constructs (Wang et al., 2000b). *In vivo* studies have indicated that differing ecdysteroid titers may initiate distinct developmental programs (Champlin and Truman, 1998), while mutant analysis suggests that unliganded EcR/USP may also serve as a silencer for specific response elements (Schubinger and Truman, 2000). Thus, in insects, evidence suggests that transcriptional regulation may be effected via changes in ecdysteroid type, concentration, or both. At least four major ecdysteroids are subject to molt-cycle variations in crustaceans; 25-deoxyecdysone, ponasterone A, ecdysone and

20-hydroxyecdysone. The specificity of the crustacean receptor for these ligands requires further characterization, as does the relationship between receptor distribution *in vivo* to titers of circulating ligand (see below).

4. 3. Expression studies of UpRXR and UpEcR during limb regeneration and oogenesis

We conducted several experiments designed to detect alternate *UpRXR* and *UpEcR* A/B isoform transcription in *Uca*. We had previously identified heterogeneity in *UpRXR* transcript sizes using Northern blots probed with DBD domain probes (Chung et al., 1998a), suggesting the possibility of isoform transcription. Northern blot experiments using A/B domain probes indicated this heterogeneity is not A/B isoform-specific, however, since all transcript classes hybridize to the recovered *UpRXR* A/B domain. Hybridizations to the A/B domain *UpEcR* probe likewise produced results indistinguishable from hybridizations using common domain probes.

We employed RPAs, which are more readily quantifiable than filter-bound hybridizations for low abundance transcripts, to assess whether *UpEcR* and *UpRXR* mRNAs are equivalently protected by A/B domain-specific probes, relative to DBD or LBD domain-specific probes. As in our previous studies, we observed distinct patterns of transcript abundance during limb regeneration, indicating developmental regulation of expression. These experiments also

indicated that levels of the A/B domains recovered through cloning were less abundant than total 'common' domain transcript levels only at specific times of regeneration and, for *UpRXR*, for different stages of ovarian maturation. This is clearly not a definitive argument for the presence of alternative A/B isoforms; there could be, for example, stage-specific differences in processing intermediates containing varying amounts of common versus A/B domain sequences. Processing intermediates exist within the RNA populations screened and, as discussed above, were detected in the cDNA clones analyzed. The data, however, are consistent with the hypothesis that alternate A/B isoforms may not have been recovered in screenings of late proecdysial cDNA libraries, and identify candidate mRNA populations for further screening. Evidence for tissue-specific differences in A/B isoform distribution may also be addressed with immunohistochemical localization using common and A/B domain-specific antibodies.

What role a functional ecdysteroid receptor may be playing during early blastemal development remains unclear. Ecdysteroid titers in the hemolymph remain very low during early blastemal formation, correlating with lower levels of *UpEcR* transcripts. As discussed earlier, enzymatic pathways for retinoid synthesis and retinoid-like molecules have recently been detected in early blastemal tissues (Hopkins, 2001), and limb development is perturbed by treatment with exogenous retinoic acid, which also alters levels of UpRXR transcription and transiently affects ecdysteroid titer (Hopkins and Durica, 1995; Chung et al., 1998b). Immunohistochemical studies (Hopkins et al., 1999; Wu et

al., unpublished) have localized UpRXR to nuclei of epithelial cells bordering areas of cuticle secretion, an early cytological marker of limb differentiation. It remains to be determined whether UpEcR co-localizes in these cells, or whether another potential heterodimer partner for UpRXR may be present.

On the other hand, 20E and ecdysone are both able to stimulate protein synthesis in explants of proecdysial limb buds, and levels of *UpEcR* and *UpRXR* transcripts are high during proecdysial growth *in vivo*. This effect occurs when hemolymph titers of ecdysteroids are low, but follows an obligatory pulse of ecdysteroid prior to proecdysial growth (Hopkins, 1989). Proecdysial growth ceases and limb bud *UpEcR* mRNA concentration slightly decreases at the end of proecdysis, when circulating levels of ecdysteroid are highest, prior to apolysis and the subsequent molt (Chung et al., 1998b).

This is the first study where crustacean *EcR* and *RXR* transcripts have been identified in ovarian tissues, and RPA analysis suggests the possibility of differential isoform expression for UpRXR. The role of ecdysteroids in insect reproduction is well documented (Pierceall et al., 1999; Carney and Bender, 2000; Martin et al., 2001). Although the role of ecdysteroids in crustacean reproduction is still unclear, ecdysteroids are sequestered in ovarian tissues in several species, and have been implicated in the regulation of secondary vitellogenesis, release from meiotic prophase I, and may serve as a potential morphogenetic agent during embryogenesis (Subramoniam, 2000). Recent observations also suggest that

retinoids could influence reproduction in vertebrates (van Pelt and deRooij, 1991; Kastner et al., 1996; Morita and Tilly, 1999; Livera et al., 2000; Minegishi et al., 2000). The presence of *UpRXR* mRNA in crustacean ovaries raises the hypothesis that these organs may also be targets for retinoids or structurally related ligands. As discussed above, enzymatic capability for retinoid synthesis and evidence for retinoid signaling has been observed during early limb bud regeneration (Hopkins, 2001). JH has been implicated in vitellogenin synthesis in insects, and the crustacean terpenoid MF may be involved in ovarian maturation (Laufer et al., 1998; Jo et al., 1999). What potential ovarian cell populations may be targets for hormonal signaling, and the physiological consequences of that regulation, should now be open for analysis using nucleic acid and antibody probes directed against the UpEcR and UpRXR receptor proteins.

Acknowledgements

This research was supported by NSF grant IBN-9816709 to David S. Durica and Penny M. Hopkins and an Overseas Associateship granted to Gopinathan Anilkumar by the Department of Biotechnology, Government of India.

Figure legends

Figure 1.

Analysis of amino-terminal regions for UpEcR (1A) and UpRXR (1B). A BLAST search of the GenBank database was performed using the crab receptor A/B domain and a portion of the C (DBD) domain as the query sequence. Sequences showing the highest degree of similarity to *Uca* sequences, representative of ten different insect genera (and five different orders), were recovered and aligned using Clustal W. Dark-shaded residues represent identities in greater than half of the aligned residues; light-shaded residues represent conservative substitutions. GenBank accession numbers and references for (A) EcR: *Uca*, (F034086, this paper); *Tenebrio* (coleoptera; Y11533, Mouillet et al., 1997); *Ceratitis* (diptera; AJ224341, Verras, et al., 1999); *Locusta* (orthoptera; AF049136, Saleh et al., 1998); *Lucilia* (diptera; U75355, Hannan and Hill, 1997); *Bombyx* (lepidoptera; L35266, Swevers, et al., 1995); *Choristoneura* (lepidoptera; U29531, Kothapalli, et al., 1995); *Drosophila* (diptera; M74078, Koelle et al., 1991); (B) USP/RXR: *Uca*, (AF032983, this paper); *Manduca* (lepidoptera; U44837; Jindra et al., 1997); *Choristoneura* (lepidoptera; AF016368, Perera et al., 1998); *Aedes* (diptera; AF305213; Kapitskaya et al., 1996); *Apis* (hymenoptera; AF263459, Maleszka, et al., submitted); *Locusta* (orthoptera; AF136372, Hayward et al., 1999); *Tenebrio* (coleoptera; AJ251542, Nicolai et al., 2000).

Figure 2.

Sequence variants observed among *UpRXR* random-primed clones. The contiguous sequence (including 33-amino acid insert; see text) represents the coding region from clone 3B introduced into the full-length expression vectors described in Section 2 and used for physical characterizations of protein–protein interaction and DNA binding. The shaded sequences represent variant cDNA coding sequences identified among clones recovered from the random-primed library; clone R13b contains a five-amino acid insertion; clones R8a and R13b contain a 33-amino acid deletion.

Figure 3.

GST-pulldown experiment using *in vitro* synthesized UpEcR and UpRXR. Reticulocyte lysates containing radiolabeled UpEcR (predicted 57.5 kDa protein) and UpRXR (predicted 50.9 kDa protein) were incubated with glutathione-sepharose bound GST-UpRXR (predicted 77 kDa protein; Panel 3A, lanes 1 and 2, Panel 3C lane 2) or GST alone (predicted 26 kDa protein; Panel 3C, lane 1) as indicated in Section 2.4. Proteins released from glutathione-sepharose beads were resolved using SDS-PAGE. Panels 3A and C represent stained gels monitoring recovery of GST–RXR fusion protein. Panels 3B and D represent autoradiographs of the stained gels displaying the labeled proteins that bound to the GST–RXR fusion. Radiolabeled proteins running below full-length UpEcR in 3B and D are synthesized only if *UpEcR* mRNA is added to lysate and presumably result from internal initiations on this template. Tick marks represent relative positions of protein size standards, resolved in lane 3 of Panels 3A and B.

Figure 4.

Representative EMSA using a DR-4 HRE. Complementary oligonucleotides representing an HRE (5'-ttggacaAGGTCAcaggAGGTCActtgtctt-3') that had been shown to bind to the mosquito ecdysteroid receptor (Wang et al., 1998) were radiolabeled, annealed and used in EMSAs with reticulocyte lysate-synthesized UpEcR, UpRXR, and 20E as indicated in Section 2.4. Omissions to the standard reaction (e.g. reticulocyte lysates lacking receptor mRNA; 20-hydroxyecdysone) or additions (inclusion of unlabeled competitor HRE) are indicated above the lanes. Free probe is indicated by an open arrow; retarded probe is indicated by a bold arrow; supershifted probe is indicated by a small arrow.

Figure 5.

Northern blot analysis of Poly(A)+ mRNA isolated from various stages of limb regeneration. Poly(A)+ mRNA from each stage was isolated from 10 μg of total RNA, separated by electrophoresis on glyoxal gels, transferred to nitrocellulose and hybridized to radiolabeled probes specific for the DNA-binding domains (DBD) and amino-terminal domains (A/B) of the *UpRXR* (5A) and *UpEcR* (5B) genes. In 5A, the three panels represent autoradiographs of hybridizations to *UpRXR* DBD (top) and A/B domain (middle, bottom) probes, respectively. The bottom panel in 5A represents a longer exposure of the panel directly above it. In 5B, the two panels represent autoradiographs of hybridizations to *UpEcR* DBD (top) and A/B domain (bottom) probes, respectively. The lane markers above the panels indicate the source of mRNA

samples, from 4 days (A+4) and 8 days (A+8) following autotomy through premolt (D_0 and D_{1-4}). Characterization of limb bud stages is described in Section 2.1. The sizes (in kb) of transcripts complementary to the respective probes are given at the right of the panels.

Figure 6.

Representative ribonuclease protection assays (RPA) of RNAs isolated from regenerating limb buds. Ten micrograms of total RNA for each of the indicated limb bud stages (as indicated in legend to Figure 5) was hybridized to A/B and DBD *UpRXR* antisense probes (6A) or A/B and LBD *UpEcR* antisense probes (6B). The unhybridized material was removed by ribonuclease digestion, and the protected fragments resolved by denaturing PAGE and autoradiography. For 6A, the protected fragments for the *UpRXR* A/B domain (312 nt) and DBD domain (307 nt) probes are approximately the same size so the assays were set up independently on parallel RNA samples. For 6B, the protected fragments for the *UpEcR* A/B domain (~310 nt) and LBD domain (162 nt) differ in size and a single assay was conducted on the same RNA sample. The gel in 6B shows duplicate assays run for each limb bud stage. Lanes marked 'tRNA+' represent control digests in which probe was hybridized to 10 µg of yeast tRNA. Lanes marked 'tRNA-' represent similar hybridizations which were followed by mock digests lacking ribonuclease; these lanes contain undigested probes. Lanes marked 'cRNA' represent hybridizations to 5 or 10 pg of full-length sense template RNA and were included as standards for quantification. The *UpEcR*

A/B domain probe is expected to protect 242 nt of coding sequence in the cRNA standard, which begins at the start codon. The larger size fragment protected in the *Uca* tissue samples represents protection of 5' non-coding sequence in mRNA by the antisense probe. For 6A and 6B, the double asterisks represent fragments that are consistently observed in *Uca* tissue samples, but not cRNA standards, using the A/B domain probes. The single asterisk represents a fragment that is observed in *Uca* tissue samples, but not cRNA standards, using the *UpEcR* LBD domain probe. Panels 6C (*UpRXR*) and 6D (*UpEcR*) represent quantifications of the steady-state transcript levels calculated from multiple experiments using electronic autoradiography. Standard errors are indicated for each limb bud stage in the histogram. For 6C and 6D, asterisks represent values calculated for A/B domain probes that are significantly different ($P \leq 0.05$) from those obtained using common domain probes for any given stage.

Figure 7.

Representative RPA of RNAs isolated from developing ovaries. Ten micrograms of total RNA for each of the indicated stages (as described in Section 2.1) were hybridized to A/B and DBD *UpRXR* antisense probes (7A) or A/B and LBD *UpEcR* antisense probes (alternating lanes, respectively, 7B) as described in the legend to Figure 6. The expected protected fragments are indicated by bold arrows; some undigested full-length probe is observed in the *UpEcR* positive control lane (light arrow; 7B). Panels 7C (*UpRXR*) and 7D (*UpEcR*) represent

histograms indicating quantification and comparisons of steady-state transcript levels, as described in Figure 6.

1A

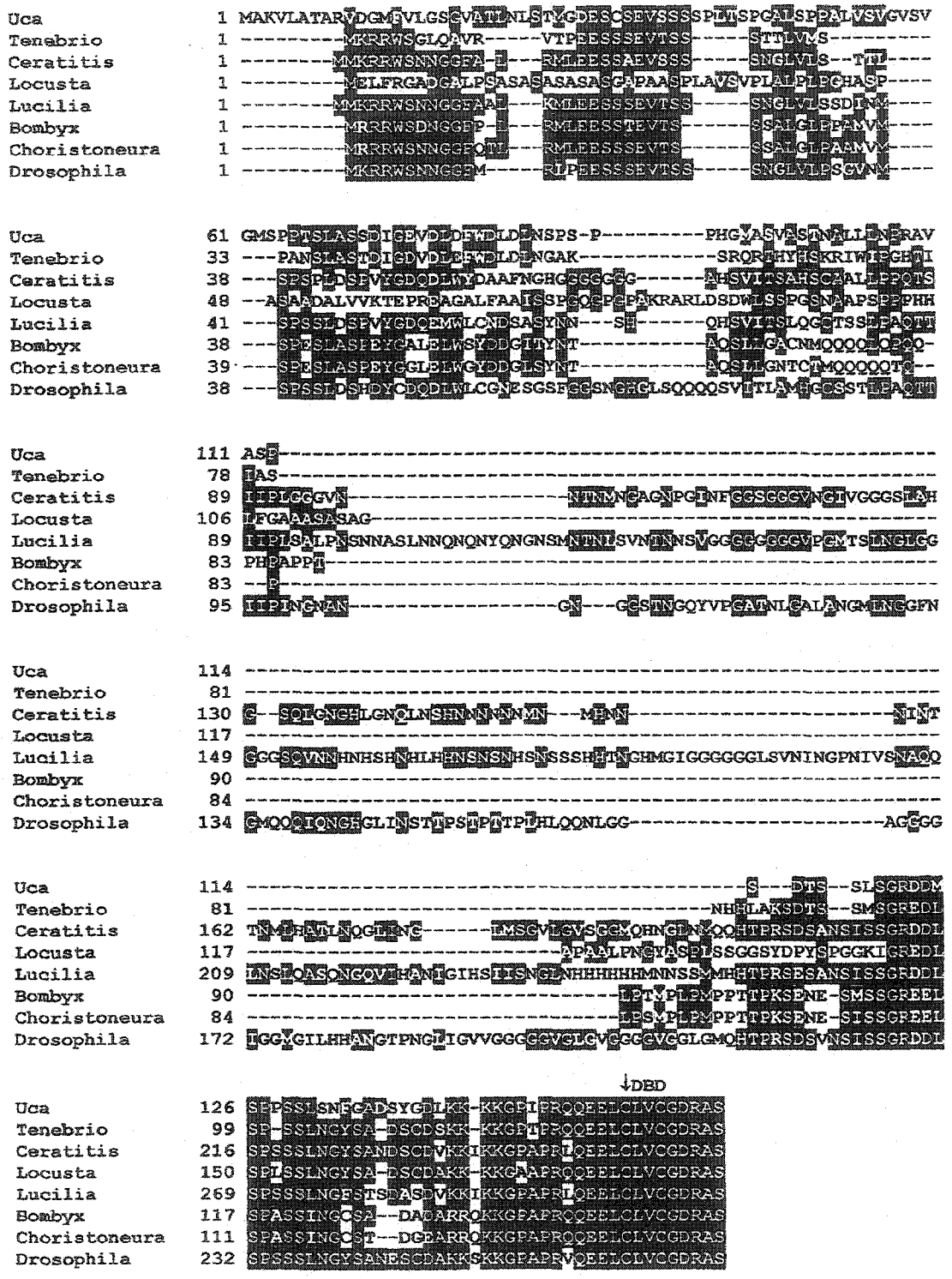
Uca
Tenebrio
Ceratitis
Locusta
Lucilia
Bombyx
Choristoneura
Drosophila
DBD

Figure 1

1B

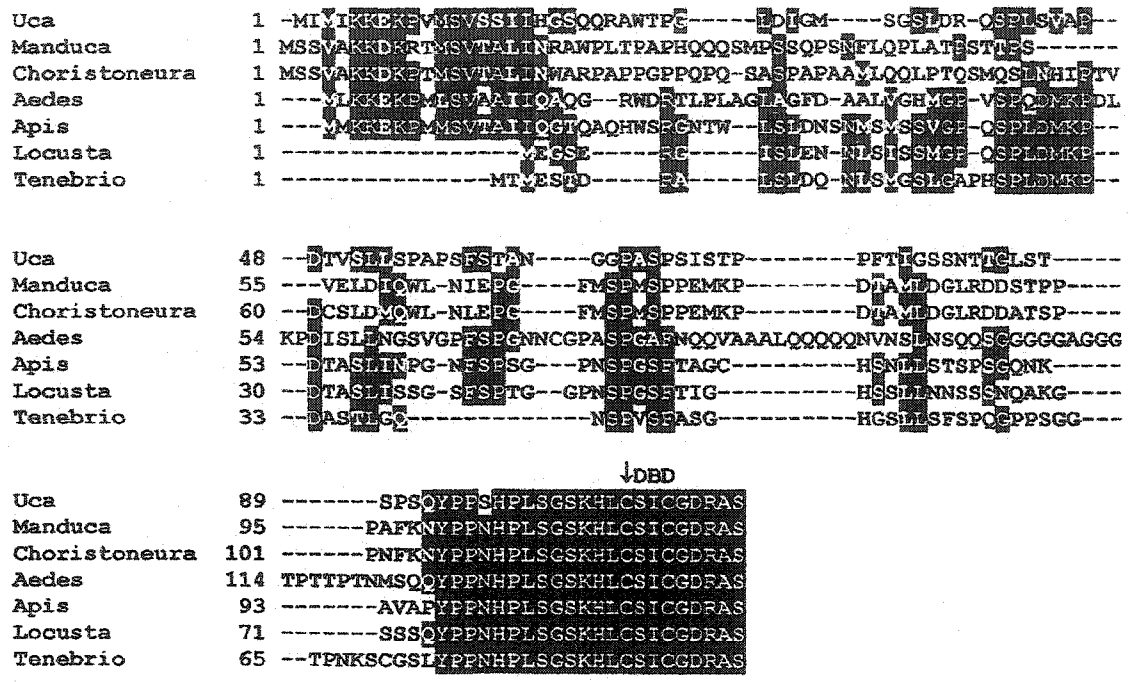
Uca 1 -MIYIKKEKEVMSVSSITHGSQQRAWTPG-----LDIGM----SGSLDR-QSPLSYAP--
Manduca 1 MSSVAKNDKRTMSVTALINRAWPLTPAPHQQQSMPSSQPSNFLQPLATSSTLES------
Choristoneura 1 MSSVAKNDKPTMSVTALINWARPAPPGPPQPQ-SASPAPAAYLQQLPTQSMQSLNHIPTV
Aedes 1 ---MLKKEKPMLSVAAIIQAQG--RWDRTLPLAGLAGFD-AALVGHMGP-VSPQDMKPDL
Apis 1 ---MKNEKPMMSVTAIIQGTQAQHWSRGNTW--LSLDNSNMSMSSVGF-QSPLDMKP---
Locusta 1 ----------VEGSE-----RG-----ISLEN-NLSISSMGF-QSPLDMKP---
Tenebrio 1 ----------MTVESTD-----RA-----LSLDQ-NLSVGSLGAPHSPLDMKP---
Uca 48 --DTVSLLSPAPSFSTAN----GGPASPSISTP--------PFTIGSSNTTGLST-----
Manduca 55 ---VELDIQWL-NIEPG-----FMSPMSPPEMKP--------DTAVLDGLRDDSTPP----
Choristoneura 60 --DCSLDMQWL-NLEPG-----FMSPMSPPEMKP--------DTAVLDGLRDDATSP----
Aedes 54 KPDISLENGSVGPFSPGNNCGPASPGAFNQQVAAALQQQQQNVNSLNSQQSGGGGGAGGG
Apis 53 --DTASLINPG-NFSPSG---PNSPGSFTAGC---------HSNLLSTSPSGQNK-----
Locusta 30 --DTASLISSG-SFSPTG--GPNSPGSFTIG---------HSSLLNNSSSNQAKG----
Tenebrio 33 --DASTLGQ-------------NSPVSPASG---------HGSLLSFSPQGPPSGG---
↓DBD
Uca 89 -------SPSQYPPSHPLSGSKHLCSICGDRAS
Manduca 95 -------PAFKNYPPNHPLSGSKHLCSICGDRAS
Choristoneura 101 -------PNFKNYPPNHPLSGSKHLCSICGDRAS
Aedes 114 TPTTPTNMSQQYPPNHPLSGSKHLCSICGDRAS
Apis 93 -------AVAPYPPNHPLSGSKHLCSICGDRAS
Locusta 71 -------SSSQYPPNHPLSGSKHLCSICGDRAS
Tenebrio 65 --TPNKSCGSLYPPNHPLSGSKHLCSICGDRAS

Figure 1

MIMIKKEKPVMSVSSIIHGSQQRAWTPGLDIGNSGSLDRQSPLSVAPDTV
SLLSPAPSFSTANGGPASPSISTPPFTIGSSNTTGLSTSPSQYPPSEPLS
GSKHLCSICGDRASGKHYGVYSCEGCKGFFKRTVRXDLTYACREERSCTI

VGAVE

DKRQRNRCQYCRYQKCLTMGMKREAVQ↓EERQRTKGDKGDGDTESSCGAIS
DMPIASIREAELSVDPIDEQPLDQG[redacted]
[redacted]QDVVSNICQAADRHLVQLVEWAKHIPHFTDLPIEDQVVLLKA
GWNELLIASFSHRSMGVEDGIVLATGLVIHRSSAHQAGVGAIFDRVLSEL
VAKMKEMKIDKTELGCLRSIVLFNPDAKGLNCVNDVEILREKVYAALEEY
TRTTYPDEPGRFAKLLLRLPALRSIGLKCLEYLFLFKLIGDTPLDSYLMK
MLVDNPNTSVTPPTS

Sequence added in clone R13b

[redacted]Sequence deleted in clones R8a and R13b

Figure 2

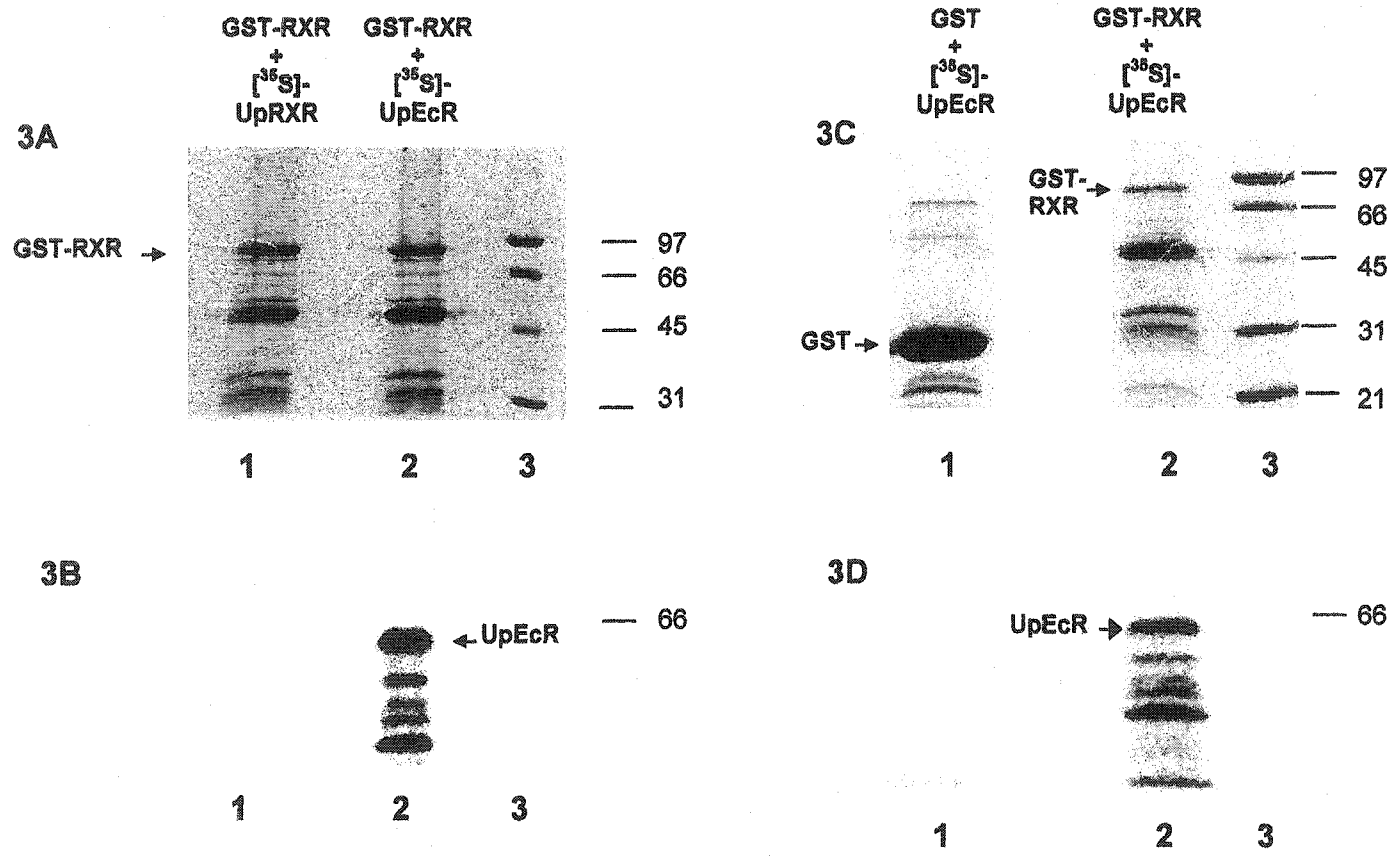
3A
GST-RXR + [35S]-UpRXR
GST-RXR + [35S]-UpEcR
GST-RXR
97
66
45
31
1
2
3
3B
UpEcR
66
1
2
3
3C
GST + [35S]-UpEcR
GST-RXR + [35S]-UpEcR
GST-RXR
GST
97
66
45
31
21
1
2
3
3D
UpEcR
66
1
2
3

Figure 3

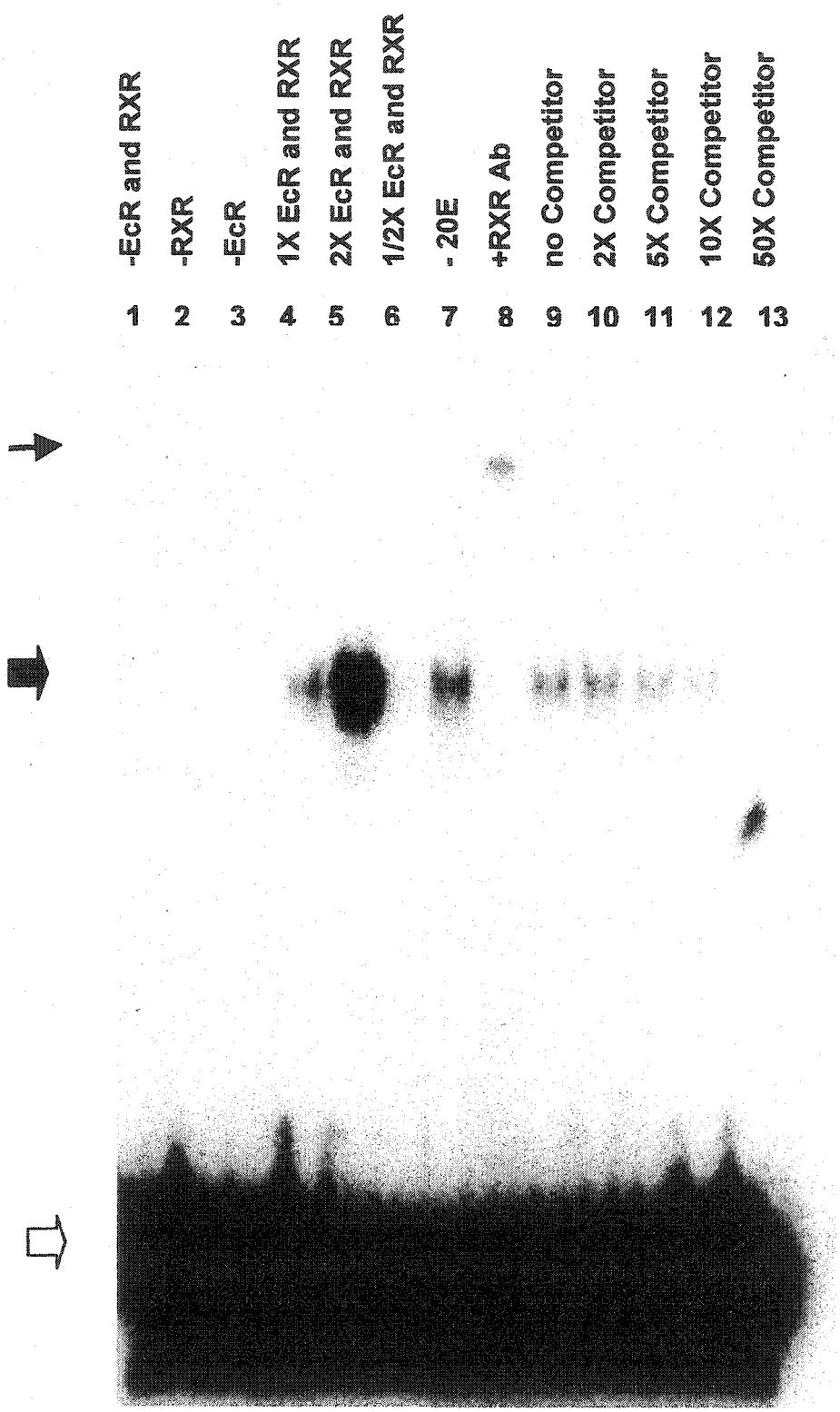
-EcR and RXR
-RXR
-EcR
1X EcR and RXR
2X EcR and RXR
1/2X EcR and RXR
- 20E
+RXR Ab
no Competitor
2X Competitor
5X Competitor
10X Competitor
50X Competitor
1 2 3 4 5 6 7 8 9 10 11 12 13

Figure 4

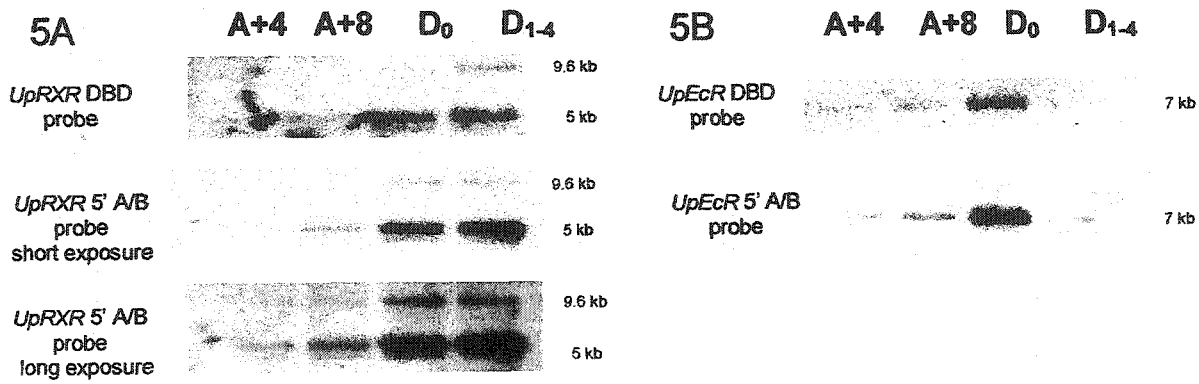
5A
A+4
A+8
D0
D1-4
UpRXR DBD probe
9.6 kb
5 kb
UpRXR 5' A/B probe short exposure
9.6 kb
5 kb
UpRXR 5' A/B probe long exposure
9.6 kb
5 kb
5B
A+4
A+8
D0
D1-4
UpEcR DBD probe
7 kb
UpEcR 5' A/B probe
7 kb

Figure 5

6A

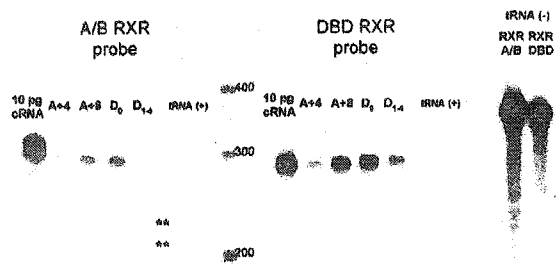

6B

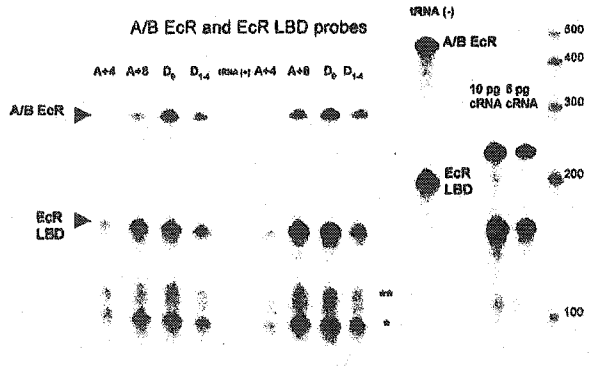

6C

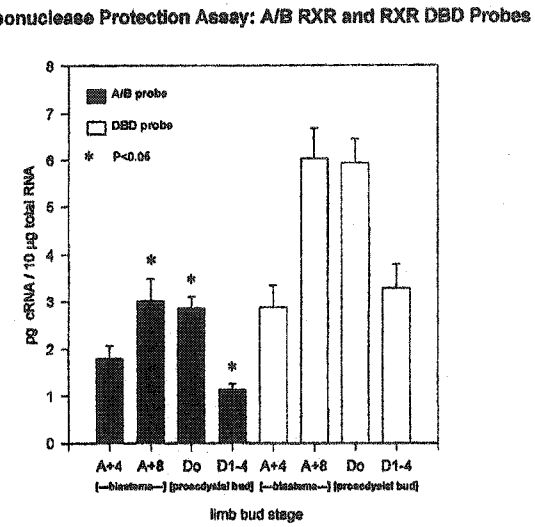

6D

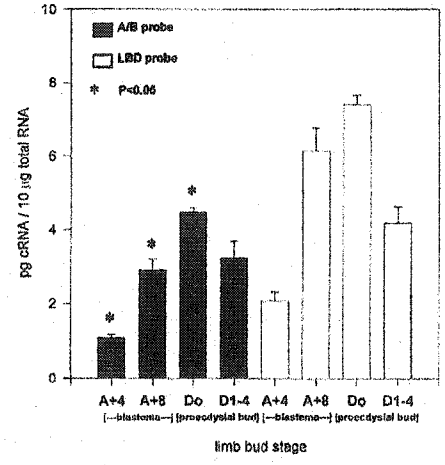

Figure 6

7A

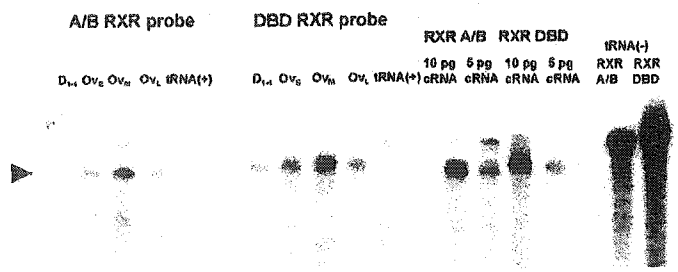

7B

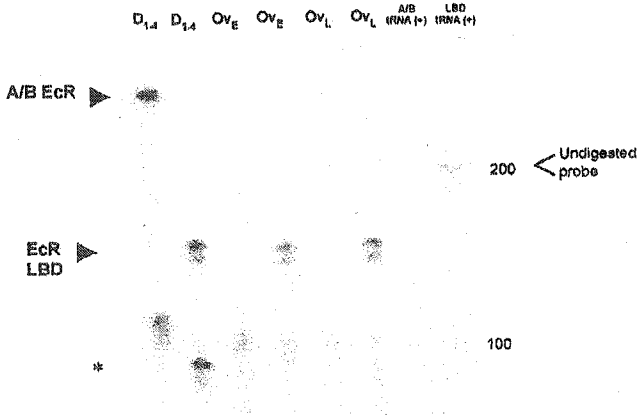

7C Ribonuclease Protection Assay: A/B RXR and RXR DBD probes

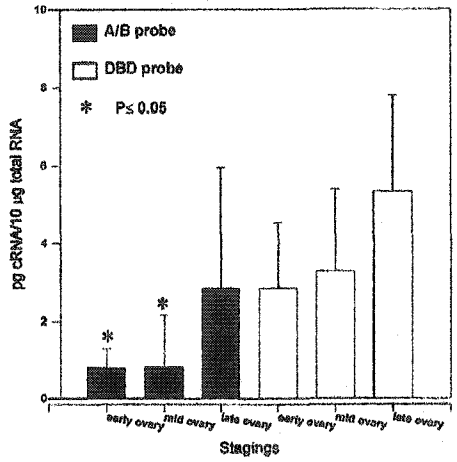

7D Ribonuclease Protection Assay: A/B EcR and EcR LBD Probes

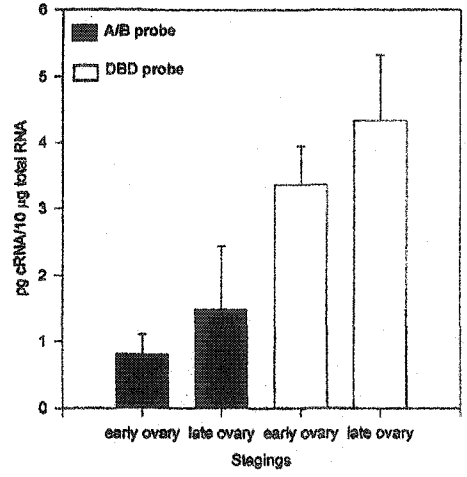

Figure 7

Chapter III

Crustacean retinoid X receptor isoforms: Distinctive DNA binding and receptor-receptor interaction with a cognate ecdysteroid receptor

Crustacean retinoid X receptor isoforms: Distinctive DNA binding and receptor-receptor interaction with a cognate ecdysteroid receptor

Xiaohui Wu, David S. Durica*, Subba R. Palli[§], Penny M. Hopkins

Department of Zoology, University of Oklahoma, 730 Van Vleet Oval., Norman, OK 73019, USA

§ Department of Entomology, College of Agriculture, University of Kentucky, KY, USA

* Corresponding author. Tel.: + 1-405-325-1528; fax: + 1-405-325-7560; Email address: ddurica@ou.edu (D.S. Durica)

Keywords: retinoid X receptor; ecdysteroid receptor; Ultraspiracle; *Uca pugilator*; nuclear receptor

Abstract

We have identified cDNA clones that encode homologs of the ecdysteroid receptor and retinoid X receptor/USP classes of nuclear receptors from the fiddler crab *Uca pugilator* (*UpEcR* and *UpRXR*). Several *UpRXR* cDNA splicing variants were found in coding regions that could potentially influence function. A five-amino acid (aa) insertion/deletion is located in the "T" box in the hinge region. Another 33-aa insertion/deletion is found inside the ligand-binding domain (LBD), between helix 1 and helix 3. Ribonuclease protection assays (RPA) showed that four *UpRXR* transcripts [*UpRXR(+5+33), UpRXR(-5+33), UpRXR(+5-33) and UpRXR(-5-33)*] were present in regenerating limb buds. *UpRXR(-5+33)* was the most abundant transcript present in regenerating limb buds in both early blastema and late premolt growth stages. Expression vectors for these UpRXR variants and UpEcR were constructed, and the proteins expressed in *E. coli* and *in vitro* expression systems. The expressed crab nuclear receptors were then characterized by electrophoretic mobility shift assay (EMSA) and glutathione S-transferase (GST) pull down experiments. EMSA results showed that UpEcR/UpRXR(-5+33) heterocomplexes bound with a series of hormone response elements (HREs) including *eip28/29*, IRper-1, DR-4, and IRhsp-1 with appreciable affinity. Competition EMSA also showed that the

affinity decreased as sequence composition deviated from a perfect consensus element. Binding to IRper-1 HREs occurred only if the heterodimer partner UpRXR contained the 33-aa LBD insertion. UpRXR lacking both the five-aa and 33-aa insertion bound to a DR-1G HRE in the absence of UpEcR. The results of GST-pull down experiments showed that UpEcR interacted only with UpRXR variants containing the 33-aa insertion, and not with those lacking the 33-aa insertion. These *in vitro* receptor protein-DNA and receptor protein-protein interactions occurred in the absence of hormone (20-hydroxyecdysone and 9-cis retinoid acid). Transactivation studies using a hybrid UpEcR ligand-binding domain construct and UpRXR (±33) ligand-binding domain constructs also showed that the 33-aa insertion was indispensable in mediating ecdysteroid stimulated transactivation.

1. Introduction

In arthropods, the ecdysteroid hormones regulate growth, differentiation, and reproduction by influencing gene expression (Segraves, 1994; Thummel, 1996). The natural active ecdysteroid in most insects, 20-hydroxyecdysone (20E; Riddiford 1993, 2001), functions by binding to a cognate receptor, the ecdysteroid receptor (EcR). The insect EcR binds with the Ultraspiracle protein (USP, a homolog of the vertebrate retinoid X receptor, RXR), forming a functional heterodimer (Koelle et al., 1991; Yao et al., 1992; Koelle at al., 1992; Thomas et al., 1993; Yao et al., 1993; Swevers et al., 1996; Hall and Thummel, 1998). This EcR/USP heterodimer controls gene expression by binding to an array of specific regulatory DNA sequences, the ecdysone responsive elements (EcREs). This binding activates or inactivates an array of down-stream genes, a cascade of events well characterized in *Drosophila melanogaster* (Segraves and Hogness, 1990; Karim and Thummel, 1992; Thummel, 1995, for review; Fisk and Thummel, 1998).

EcR and its heterodimer partner USP belong to the nuclear receptor (NR) superfamily. NRs share similarities in domain structures and mechanisms of gene regulation (Mangelsdorf et al., 1995 for review; Aranda and Pascual., 2001 for review). A typical NR consists of a variable amino terminal A/B domain, implicated in transcriptional activation; a highly conserved C domain, which functions as a DNA-binding domain (DBD); a less conserved D domain, which

functions as a flexible linker hinge region; and a conserved E domain, or ligand-binding domain (LBD), involved in ligand binding, receptor dimerization, and interaction with other transcription co-factors. Some NRs, like the *Drosophila* EcR, also contain a carboxyl terminal F domain of indeterminate function (Koelle et al., 1991; Talbot et al., 1993; Riddiford et al., 2001, for review). In some vertebrate NRs, this domain may mediate ligand affinity, dimerization, and co-regulator interactions (Ruse et al., 2002; Schwartz et al., 2002).

NRs can be represented by several isoforms with different amino acid sequences, resulting from alternative splicing or transcription from a different promoter. Most of the characterized isoforms have different N-terminal A/B domains. Though not well investigated, hinge D region splicing variants have also been found in several NRs (Fujiwara et al., 1995; Guo et al., 1998; Gervois et al., 1999; Zennaro et al., 2001; Zhang et al., 2002). LBD isoforms have also been found in Steroid Hormone Receptor 2 (SpSHR2) of the sea urchin *S. purpuratus* (Kontrogianni-Konstantopoulos and Flytzanis, 2001), and human constitutive androstane receptor CAR (Auerbach et al., 2003). C-terminal variants of NRs have also been found in the *Xenopus* farnesoid X receptor (FXR)-like Orphan Receptor, FOR (Seo et al., 2002).

EcR and *usp* genes have been cloned in several orders of insects and from a few other arthropods, and receptor isoforms that are products of alternative splicing and/or transcription from alternative promoters have also been discovered

(Riddiford et al., 2001 for review). In *Drosophila melanogaster*, three EcR A/B domain isoforms (EcR-A, EcR-B1, and EcR-B2) have been characterized (Talbot et al., 1993), which share common DNA and hormone-binding domains but have different N-terminal A/B regions. Two EcR A/B isoforms have been discovered in the lepidopterans *Manduca sexta* (Fujiwara et al., 1995; Jindra et al., 1996), *Bombyx mori* (Swevers et al., 1995; Kamimura et al., 1996, 1997), and *Choristoneura fumiferana* (Perera et al., 1999), in the coleopteran *Tenebrio molitor* (Mouillet et al., 1997), the mediterranean fruit fly *Ceratitis capitata* (Verras et al., 2002), and rice stem borer *Chilo suppressalis* (Minakuchi et al., 2002). In addition to these insects, three A/B isoforms of EcR from the ixodid tick *Amblyomma americanum* have been cloned (Guo et al., 1997), as well as two subtypes (different genes) of tick USP (Guo et al., 1998). In the mosquito *Aedes aegypti* (Kapitskaya et al., 1996), tobacco hornworm *Manduca sexta* (Jindra et al., 1997), and midge *Chironomus tentans* (Vögtli et al., 1999), two A/B isoforms of USP have been cloned and characterized.

Receptor isoforms are hypothesized to be involved in tissue-specific and stage-specific gene expression. In *D. melanogaster*, EcR-A and EcR-B1 have tissue-specific and stage-specific expression patterns as shown by northern blot, western blot and immunohistochemistry studies (Talbot et al., 1993). Both northern blot and immunohistochemistry studies show differential expression for the two ecdysone receptor isoforms in different tissues (epidermis and wing disc) of *Manduca sexta* (Jindra et al., 1996). In the silkworm, *Bombyx mori*, northern

hybridization studies also show differential isoform expression patterns at different developmental stages and in different tissues (Kamimura et al., 1997). In mosquito *Aedes aegypti* fat bodies, both mRNA and protein expression patterns differ for two USP receptor isoforms during vitellogenesis in response to an ecdysone signal. Transactivation assays using *Aedes* USP also suggest that the two isoforms may have different roles (Wang et al., 2000). Genetic mutant analysis in *Drosophila* indicates that receptor isoforms have different roles both in embryonic development and during metamorphosis (Bender et al., 1997). In *Drosophila*, females that carry a temperature-sensitive EcR mutation (EcR^{A483T}) exhibit severe reductions in fecundity at the restrictive temperature, showing abnormal egg chambers and loss of vitellogenic egg stages, suggesting that EcR is needed in normal oogenesis (Carney and Bender, 2000). Studies on *Drosophila* and *Manduca* neuronal development also show isoform-specific expression patterns that correlate to stage-specific responses to ecdysteroids (Robinow et al., 1993; Truman et al., 1994). In addition, recent papers on *Drosophila* neuron remodeling indicate that specific EcR isoform (EcR-B) expression is required for pruning the larval neuron dendrites and axons during metamorphosis (Schubiger et al., 1998; Lee et al., 2000), and that this pruning is cell-autonomous. Nevertheless, the notion that specific receptor isoforms are obligatory for tissue specific ecdysteroid responses still requires further investigation, and several recent experiments suggest EcR isoforms can be redundant in function (D'Avino and Thummel, 2000; Cherbas et al., 2003).

The DNA-binding properties of the functional EcR/USP complex have been intensively studied. The first ecdysteroid response element (EcRE) identified, in the regulatory region of the *hsp27* gene, is an imperfect inverted repeat with one base pair spacer between the two half sites (Riddihough and Pelham, 1987). The EcRE found in the regulatory region of the *eip28/29* gene (Cherbas et al., 1991) is a composite EcRE containing both a direct repeat and inverted repeat. Electrophoretic mobility shift assays (EMSA) using nuclear extracts or partially purified EcR, as well as transactivation studies, confirmed a preference for a consensus inverted repeat of (A/G)GGTCA by the EcR/USP complex (Antoniewski et al., 1993; Ozyhar and Pongs, 1993; Antoniewski et al., 1994). Using EMSA and reporter gene transactivation assays, it was later found that EcR/USP bound synthetic direct repeats (DR) of various spacer lengths (D'Avino et al., 1995; Horner et al., 1995; Antoniewski et al., 1996; Crispi et al., 1998). Additional DNA binding studies have since been reported with similar results (Vögtli et al., 1998; Wang et al., 1998; Elke et al., 1999; Grad et al., 2001; Grad et al., 2002). While site directed mutation studies of the USP DNA-binding domain have examined specificity of EcRE DNA binding (Grad et al., 2001; Grad et al., 2002), most DNA binding studies have focused on the DNA sequence specificity of EcREs binding to wild type receptors.

In crustaceans, as in insects, ecdysteroids appear to be critical to growth and reproduction. In the fiddler crab, *Uca pugilator*, and other crustaceans, several ecdysteroids circulate in the hemolymph (Hopkins, 1983; Lachaise and Lafont,

1984; Snyder and Chang, 1991; Hopkins, 1992). Changes in these ecdysteroid titers and ratios during the molt cycle are temporally correlated with major physiological events involved in molting and regeneration of lost limbs (for review, see Chang, 1989; Hopkins, 1992). We have cloned from the crustacean *U. pugilator* homologs of the ecdysteroid receptor (*UpEcR*) and retinoid X receptor (*UpRXR*) (Durica and Hopkins, 1996; Chung et al., 1998a; Durica et al., 2002). Using probes derived from common regions of *UpEcR* and *UpRXR*, their temporal and spatial expression patterns in various tissues have been studied. Northern blot and ribonuclease protection assays (RPA) show both *UpEcR* and *UpRXR* transcripts are present together in all the tissues examined throughout the molt cycle. Changes in the steady-state concentrations of these NR transcripts imply molt cycle-related differences in the potential of these tissues to respond to changing titers of ecdysteroid in the hemolymph (Chung et al., 1998b; Durica et al., 2002). Immunohistochemistry studies using antibodies against the A/B region and common regions of UpEcR and UpRXR also suggest widespread distribution of both nuclear receptors and their possible co-localization (Hopkins et al., 1999; Wu et al., unpublished observations).

The deduced amino acid sequence of UpEcR is more closely related to the insect EcR DBD and LBD than any other NRs. UpRXR shares greatest similarity to insect USPs in the DBD domain, while its LBD domain shares greater amino acid similarity to vertebrate RXR (Chung et al., 1998a). Unlike the situation in some insects, only a single A/B domain has been identified for these crustacean

genes. Several hinge region and LBD variants, however, have been found (Durica et al., 2002). For UpEcR, three hinge variants have been recovered at alternative splice sites. Splicing variants at hinge regions have also been observed in tobacco hornworm (*Manduca sexta*) EcRs (Fujiwara et al., 1995) and tick (*Amblyomma americanum*) EcRs (Guo et al., 1998).

For UpRXR, two alternative hinge region variants exhibit an insertion/deletion of five-aa within the "T" box (Durica et al., 2002), a highly conserved domain adjacent to the DBD implicated in hormone response element recognition (Zilliacus et al., 1995, for review). Among characterized receptors, only the zebrafish RXR-ε contains an insertion in this region (Jones et al., 1995). Splicing variants in the UpRXR LBD have also recently been identified (Durica et al., 2002). The UpRXR LBD variants differ due to the presence or absence of a 33-aa insertion located within the flexible loop region between helix one and helix three of the LBD. This region may be important in transactivation and association with coactivators or corepressors. For example, in the dipteran and lepidopteran USPs, whose crystal structures have been solved (Billas et al., 2001; Clayton et al., 2001), this region locks the receptor into an "antagonist" conformation, implying different transactivational properties from vertebrate RXRs. To investigate the possibility that these unique UpRXR isoforms might have different physical properties, we introduced genes encoding the isoforms into vectors that allow for their expression *in vitro* and permit concomitant characterizations of the resultant proteins' DNA-binding, protein-binding, and transactivation properties.

We report here that all four forms of variant *UpRXR* transcripts are present in the regenerating limbs, but the predominant form is *UpRXR(-5+33)* (lacking the five-aa insertion in the hinge region and having the 33-aa insertion in the LBD). The predominant UpRXR(-5+33) isoform can interact with UpEcR and bind to a variety of HREs. Only UpRXR variants containing the 33-aa LBD insertion, however, interact strongly with UpEcR on IRper-1 HREs, while the UpRXR(-5-33) variant can bind to a DR-1G element independently of UpEcR. GST-pull down experiments also suggest that only those UpRXR variants containing the 33-aa LBD insertion bind strongly to UpEcR. Studies using a 3T3 mammalian cell culture system further show that only UpRXR hybrids containing the 33-aa insertion can transactivate a reporter gene in concert with hybrid UpEcR and ecdysteroid. Taken together, the protein-DNA, protein-protein, and transactivation data support the hypothesis that UpRXR hinge and LBD isoforms have distinct interaction properties which may lead to different transcriptional responses *in vivo*.

2. Materials and methods

2.1. Animals and RNA isolation

U. pugilator were purchased from Gulf Specimen Marinelabs Inc., Panacea, FL. These animals were acclimated to the laboratory as previously described (Hopkins, 1982). Seven limbs including the large cheliped were induced to autotomize (the reflexive casting off of a damaged limb) by pinching the limb distal to the coxa. Three limbs were left so the animal could stay upright and feed. Regenerating limb bud growth was monitored by the R-value (Bliss, 1956; the length of limb bud divided by the width of the carapace) and the experimental growth rate (ER; Bliss and Hopkins, 1974), and molting stages were assigned to these animals according to these parameters (Drach, 1939). Limb bud blastema tissues eight days after autotomy (A+8) and the premolt limb buds undergoing rapid growth (D_0) were harvested. Total RNA from limb buds was extracted using Trizol reagent (Life Technologies, Rockville, MA) as described (Durica et al., 2002). RNA concentrations were quantified by UV absorbance at 260 nm and RiboGreen® RNA quantification kits (Molecular Probes, Eugene, OR) according to the manufacturer's instructions.

2.2. Subcloning of variant UpRXR for in vitro expression and in vivo expression in E. coli

The hinge and ligand-binding domain clone *UpRXR13b*, a pBSIISK plasmid recovered from a late premolt cDNA library screening (Durica et al., 2002), has a five-aa insertion within the hinge region and lacks a 33-aa insertion within the LBD (see Fig 1; designated as (+5-33)). To construct a full length UpRXR(+5-33) for *in vitro* expression, the 672 bp *Nco*I/*Bgl*II fragment of *UpRXR13b*, was ligated to the *Nco*I/*Bgl*II 4.1kb fragment of UpRXR(-5+33) (Durica et al., 2002), containing the plasmid and NR coding regions proximal and distal to the regions being exchanged. The ligation mixture was used to transform competent *E. coli* cells (Stratagene, La Jolla, CA), and the recovered positive *UpRXR(+5-33)* clones were verified by restriction enzyme digestion analysis and partial DNA sequencing.

To construct *UpRXR(+5+33)* and *UpRXR(-5-33)*, a *Bam*HI fragment of *UpRXR(+5-33)* and *UpRXR(-5+33)* containing A/B, C and part of the hinge region distal to the insertion site were swapped between these two clones (Figure 1). The recovered clones were verified by restriction enzyme digestion analysis and partial DNA sequencing.

The construction of GST-UpRXR(-5+33) has been previously described (Durica et al., 2002). To construct other GST-UpRXR variants for receptor fusion protein expression in *E. coli*, primers (forward 5'-ACGAATTCCCATGATTATGATTAAAAAGGAGAAGC-3', and reverse 5'-ACCTCGAGCTAGCTGGTGGGGGGAGTG-3') were designed to incorporate

an *Eco*RI and an *Xho*I site (underlined) respectively into amplification products containing the entire coding sequences of UpRXR(+5+33), UpRXR(+5-33), and UpRXR(-5-33). The PCR products were double digested with *Eco*RI and *Xho*I, and the recovered coding DNA fragments were cloned in frame into the *Eco*RI and *Xho*I sites of the pGEX4T2 vector (Amersham Biosciences, Piscataway, NJ).

2.3. Probe for ribonuclease protection assay (RPA)

Primers (forward 5'-GACTCGAGGTAGGGCTGTAAGGAGGAGG-3', and reverse 5'-AAGAATTCCAGAGGGTTAGCACAGGATACTTCA-3') were designed to amplify a DNA fragment containing the +5 and +33-aa insertion coding sequence of UpRXR(+5+33); *Xho*I and *Eco*RI restriction sites were incorporated at the 5' and 3'ends, respectively. The PCR products were double digested with *Xho*I/*Eco*RI, and the purified DNA was ligated into pBSKSII plasmids, which had been cut with *Xho*I/*Eco*RI. The ligation mixture was transformed into Epicurean cells (Stratagene). The recovered positive clones were verified by restriction enzyme digest analysis. Antisense probe was generated by using the T7 promoter and T7 RNA polymerase.

2.4. Receptor protein expression in vitro and in vivo in E. coli

In vitro protein synthesis was performed using the TNT® system (Promega, Madison, WI) according to the manufacturer's instructions. To synthesize

radiolabeled protein, 2 μl of [^{35}S]-methionine, 1000 Ci/mmol (Amersham Biosciences, Piscataway, NJ) was added to the standard reaction. The amount of protein synthesized was calculated from the percentage of incorporated [^{35}S]-methionine into TCA-precipitated counts, relative to the methionine contents of UpEcR and UpRXR. To quantify the amount of unlabeled receptor proteins used in EMSA experiments, 5 μl aliquots were taken out from the standard reaction, then one μl of [^{35}S]-methionine was added to the aliquot. After incubation, this aliquot was resolved by SDS-PAGE, and the radioactivity incorporated into protein was quantified by electronic autoradiography (Packard InstantImager™, Meriden, CT). The radioactive counts of corresponding protein bands and the methioinine contents in each receptor protein were used to estimate the relative amount of receptor protein synthesized.

To express GST-UpRXR variant fusion receptor proteins for GST-pull down experiments, a single colony from a fresh plate was inoculated into 3 ml of LB medium with appropriate antibiotics for an overnight initial culture. The initial culture was inoculated (1/500 dilution) into 500 ml pre-warmed Circlegrow® medium (Q-Biogene, Carlsbad, CA) or TB medium, and grown for about three hours, with vigorous shaking, until the OD_{600} reached 0.5-0.7. IPTG was added to the culture to a final concentration of 0.5 mM, and 0.5 mM of PMSF was also added to the culture. The culture was allowed to grow for about 2-3 hours. Cells were harvested by centrifugation at 4000 rpm at 4°C for 20 minutes on a

Beckman bench top centrifuge. Cells were quick frozen in liquid N_2 then stored at -80°C until use.

To isolate GST-UpRXR variant fusion proteins, frozen cells were thawed on ice and washed once in ice-cold PBS. Cells were resuspended in 3 ml PBS containing protease inhibitors (0.1 mM PMSF, 0.1 mM $Na_2S_2O_5$, 1 μg/ml pepstatin and leupeptin, 2 μg/ml aprotinin). Lysozyme was added at 1 mg/ml and incubation on ice continued for 30 minutes. The cells were briefly sonicated on ice and cell debris removed by centrifugation at 11,000X g for 30 minutes. A 0.5 ml 80% Glutathione-Sepharose 4B slurry (Amersham Pharmacia Biotech) was applied to the supernatant, and the mixture was rotated on a roller drum at 4°C for 1 hour. The beads were washed twice in 20 volumes of PBS containing 1% Triton X-100 and recovered by centrifugation. The amount of protein bound to the beads was visualized by SDS-PAGE, and adjustments were made by adding buffer-equilibrated unbound beads so that a similar amount of GST-fusion protein was present in each assay.

2.5. GST-pull down experiments and EMSA

The procedures for GST-pull down and EMSA experiments have been previously described (Durica et al., 2002). Sequences for the HRE oligonucleotides used in EMSA studies are given in the figure legends. Sequences for testing monomer receptor binding to single half site

oligonucleotides were RORE (tcgactcgtataactAGGTCAagcgctg, Giguere et al., 1995), NGFI-B responsive element or NBRE (tcgactcgtgcgaaaAGGTCAagcgctg, Giguere et al., 1995) and D1G (gatccgtaggataactgAGGTCActcgagatc). Some of the EMSA experiments were also run in an alternative buffer system (TNM buffer: 10 mM Tris-HCl, pH7.5, 50 mM NaCl, 1 mM $MgCl_2$, 0.5 mM DTT, 0.5 mM EDTA, 4% glycerol; HKN buffer: 20 mM HEPES, pH7.5, 2 mM DTT, 100 mMKCl, 1% NP-40, 7.5% glycerol). For the competition EMSA, various unlabeled HREs were added in 25X (IRper-1 probe), 20X(DR-4/3C probe) or 40X (DR-1G) excess to the reaction and monitored for their ability to compete with radiolabeled probe for *in vitro* synthesized receptors. For saturation binding experiments, different amounts of the radiolabeled probes (ranging from 0.05 nM to 10 nM) were added to a series of reactions, and the bound (retarded) and free probes were quantified by electronic autoradiography (Packard InstantImager™) and used to generate Scatchard plots (Scatchard 1949). K_d values represent the absolute slope of the derived linear regression of the Bound/Free vs Bound oligonucleotide plot (SigmaPlot®, SPSS Science). For all UpRXR variant binding experiments, the UpEcR11B clone was used (Chung et al., 1998a). This variant contains a nine-aa insertion at a common splice site in the hinge region. Two other UpEcR variants in this region (six-aa, 37-aa insertions respectively; Durica et al., 2002) were not examined.

2.6. Ribonuclease protection assays (RPA)

Ribonuclease protection assays were performed using RPA III reagents (Ambion, Austin, TX), as described by Durica et al. (2002). Control sense strand template used for UpRXR(-5+33) and UpRXR(+5-33) marker were synthesized using the RiboProbe® *in vitro* transcription system (Promega) as described (Durica et al., 2002).

2.7. Transfection of UpEcR and UpRXR hybrid constructs and transactivation studies in mammalian cells

GAL4:UpEcR(DEF)[G:UpE(DEF)] was constructed by cloning the DEF domains of UpEcR into the pM vector (Clontech Inc. Palo Alto, Ca). VP16:UpRXR(EF)[V:UpR(EF)] was constructed by cloning the EF domains of UpRXR into the pVP16 vector (Clontech). The pFRLuc vector (Stratagene), where the luciferase reporter gene is regulated by 5X GAL4 response elements and synthetic TATAA, was used as a reporter vector. A second reporter, pRLTK (Promega), which expresses luciferase from *Renilla reniformis* under a thymidine kinase constitutive promoter, was co-transfected into cells and was used for normalization.

3T3 cells were grown to 60% confluency in Dulbecco's modified Eagle's medium containing 4 mM L-glutamine, 1.5 g/L sodium bicarbonate, 4.5 g/L glucose and 10% bovine calf serum. 50,000 cells were plated per well in 12-well plates. The following day, the cells were transfected with 0.25 µg of receptor(s)

and 1.0 μg of reporter constructs using 4 μl of SuperFect® (Qiagen, Valencia, CA) for 3T3 cells. After transfection, the cells were grown in medium containing ligands. Ponasterone A (Pon A) was purchased from Alexis Corporation (San Diego, CA). RG-102240, also known as GS™-E [N-(1,1-dimethylethyl)-N'-(2-ethyl-3-methoxybenzoyl)-3,5-dimethylbenzohydrazide], is a synthetic stable bisacylhydrazine ecdysone agonist synthesized at Rohm and Haas Company, Philadelphia, PA. All ligands were applied in DMSO and the final concentration of DMSO was maintained at 0.1% in both controls and treatments. After 48 hours, the cells were harvested, lysed and the reporter activity was measured in an aliquot of lysate. Luciferase was measured using the Dual-luciferase™ reporter assay system from Promega.

3. Results

3.1. Detection of UpRXR mRNA variants by Ribonuclease Protection Assay

We have constructed oligo-dT and random-primed cDNA libraries from late premolt regenerating limb bud mRNA. As previously reported, screening of the oligo-dT-primed library has led to the recovery of the DNA-binding (C), hinge (D) and ligand-binding (E/F) domains for both the *UpEcR* and *UpRXR* gene homologs (Chung et al., 1998a, b). Random-primed library screening has also led to the recovery of D-E domain variants for UpRXR protein in two different regions (Durica et al., 2002). One variant contains an insertion/deletion of five-aa within the "T" box region, a highly conserved region immediately downstream of the DBD domain (Zilliacus et al., 1995). Another variant involves an insertion/deletion of a 33-aa stretch located between helix 1 and helix 3 of the LBD in the flexible loop region. We designed a probe construct that allowed us to use RPA to detect the four potential forms of *UpRXR* transcripts simultaneously. As shown in Figure 2, all four forms of *UpRXR* transcripts *UpRXR(+5+33)*, *UpRXR(-5+33)*, *UpRXR(+5-33)* and *UpRXR(-5-33)* are detected in regenerating limbs at blastema (8 days post autotomy, or A+8) and early premolt (D_0) stages, and the predominant form is *UpRXR(-5+33)*. RPA of ovarian tissues at three different stages of oogenesis (Durica et al., 2002) was also performed. Quantification of these four transcript isoforms by RPA also indicates

that the most abundant transcript in these ovarian tissues is *UpRXR(-5+33)* (data not shown).

3.2. Examination of the DNA-binding characteristics of UpEcR and UpRXR by EMSA

Using EMSA, we tested a variety of hormone response elements. These elements differed in orientation and spacer length, including perfect elements and imperfect elements found in natural insect HREs. Previous studies showed that UpEcR, together with UpRXR(-5+33), can bind a DR-4 HRE (Durica et al., 2002). We repeated these experiments using a new set of polyclonal antibodies directed against the A/B domain of UpEcR and UpRXR. Similar to previous studies, both UpEcR and UpRXR(-5+33) were required for DR-4 binding (Figure 3, lanes 1-4). Antibodies against the UpEcR and the UpRXR A/B domains resulted in supershifted bands, whereas the preimmune sera did not produce supershifts (Figure 3, lanes 5-12). As in previous studies (Durica et al., 2002), the presence or absence of 20E did not significantly affect binding (Figure 3, lanes 5-12, and data not shown).

We continued EMSA studies characterizing the DNA binding properties of the UpEcR/UpRXR(-5+33) complex, as UpRXR(-5+33) encodes the most abundant mRNA of all the UpRXR isoforms (Figure 2). We tested the IRper-1 element, a perfect inverted repeat with one spacer between the two half sites,

which produced the strongest response element binding with the *A. aegypti* EcR/USP complex (Wang et al., 1998). Similar to DR-4, IRper-1 also showed strong binding with the UpEcR/UpRXR(-5+33) complex (Figure 4, lane 4). Cold excess competitor HRE competed off the radiolabeled HRE (Figure 4, lanes 5-8), and antibody directed against the UpEcR A/B domain resulted in a supershift (Figure 4, lanes 11-12). UpEcR without UpRXR resulted in a retardation at a different location in the gel (Figure 4, lane 2); this shift appears to require a factor that is present in the reticulocyte lysate and is lot-dependent. A shift with this element using UpEcR alone did not appear on all lots of lysate we have tested (see Figure 10, lane 2).

We tested the IRhsp-1 and *eip28/29* elements, derived from natural ecdysone response elements found in *Drosophila* ecdysone responsive genes (*hsp27*, Riddibough and Pelham, 1987; Wang et al., 1998; *eip28/29*, Cherbas et al., 1991). Similar to the DR-4 and IRper-1 elements, both UpEcR and UpRXR(-5+33) were needed for binding to these HREs (Figure 5, lanes 1-4; Figure 6, lanes 1-4). Excess cold competitor HRE displaced the radiolabeled probe (Figure 5, lanes 11-15; Figure 6, lanes 5-7). Antibodies against the UpEcR A/B domain (Figure 5, lanes 9-10), UpRXR A/B domain (Figure 5, lanes 7-8), or UpRXR common domain (Figure 5, lanes 5-6) either resulted in supershifts or disrupted the formation of the HRE-receptor complex (Figure 6, lanes 13-14).

We also studied the binding affinity of UpEcR/UpRXR(-5+33) to an array of HREs by competition EMSA, where various unlabeled HREs were added in excess to the incubation and monitored for their ability to compete with either an IRper-1 or DR-4 radiolabeled probe. In this assay, the data (Figure 7) was normalized relative to the most inefficient competitor (IRhsp-3); the most efficient competitor resulted in the lowest binding of radiolabel in a retarded complex. The UpEcR and UpRXR(-5+33) proteins interacted with a broad array of HREs, with the most efficient competition seen with IRper-1, IRhsp-1, IRper-0, and DR-4 elements. A variation in spacer length or variation in sequence composition from a perfect consensus element decreased competition (Figure 7). In Figure 8, a representative saturation binding assay using a DR-4 element was performed. The dissociation constant (K_d value) of 2.18 nM was very similar to that observed in other insect EcRs (Wang et al., 1998).

Since UpRXR coding variants were recovered in cloning studies (Chung et al., 1998b; Durica et al., 2002) and were represented during various stages of limb bud regeneration (Figure 2, and data not shown), we also investigated the HRE binding activity of these variant UpRXRs. The UpRXR constructs lacking a 33-aa LBD insertion showed markedly different HRE binding characteristics from UpRXR(±5+33) variants. Using the IRper-1 element, a significant shifted complex was only observed when UpRXR proteins containing the 33-aa LBD insertion were present in the binding reactions (Figure 9, lanes 4-11; Figure 10, lanes 6-10). Two different buffer conditions had no effect on the specificity of

HRE binding, although HKN buffer consistently resulted in more bound complex on gel analysis (Figure 9, lanes 4-11).

Since UpEcR/UpRXR(±5-33) complexes bound poorly to IRper-1 elements, we tested whether addition of reticulocyte lysate containing UpRXR(±5-33) receptors might compete with UpEcR for binding with UpRXR(±5+33) (Figure 10, lanes 14-18). Addition of lysate containing UpRXR(±5-33) had no effect, suggesting that UpRXR(±5-33) is not capable of interfering with UpEcR/UpRXR(±5+33) complex formation. Addition of each UpRXR variant by itself (Figure 10, lanes 3-5) or in all combinations (not shown) did not result in a shifted complex with IRper-1 elements. On prolonged exposure, very low binding was observed in some experiments using the UpRXR(-5-33) construct with UpEcR (data not shown). As in the previous experiments, addition or removal of 20E had no effect on binding to IRper-1 elements (Figure 10, lanes 8 and lane 10).

After normalization for protein input, UpEcR/UpRXR(+5+33) binding to IRper-1 appeared consistently higher than UpEcR/UpRXR(-5+33) (Figures 9-10). We also monitored the effect of the five-aa insertion on IRper-1 interactions by saturation binding. These saturation binding studies and Scatchard analysis suggest a slightly lower K_d for the UpEcR/UpRXR(+5+33) complex (K_d = 1.37 ± 0.26 nM, n = 3) than the UpEcR/UpRXR(-5+33) complex (K_d = 2.44 ± 0.25 nM, n = 3)(P = 0.04, representative experiment, Figure 11).

EMSA analysis was performed using DR-1G, an HRE that interacts with vertebrate RXR homodimers (Yang et al., 1995; Castelein et al., 1996). In contrast to the other UpRXR variants, reticulocyte lysates containing the UpRXR(-5-33) receptor were able to bind DR-1G in the absence of UpEcR (Figure 12, lanes 3-6). A supershift (bold arrow) was observed only with UpRXR A/B domain antibodies, not UpEcR A/B domain antibodies, indicating that UpRXR(-5-33) was binding independently of UpEcR (Figure 12, lanes 11-14). Competition experiments using a series of cold competitor HREs (Figure 13) suggested an HRE binding profile for UpRXR(-5-33) complexes quite distinct from UpEcR/UpRXR(-5+33) heterocomplexes. DR-1G and IRper-0 competed best against the DR-1G element, while IRper-1, which competed best for UpEcR/UpRXR(-5+33) heterocomplexes, competed poorly for UpRXR(-5-33) complexes. When run in parallel with UpEcR/UpRXR(-5+33) heterodimers bound to an IRper-1 element, the retarded UpRXR(-5-33)/DR-1G complex had a similar mobility as the UpEcR/UpRXR(-5+33) heterodimer complexes, suggesting binding to both half sites (data not shown). EMSA experiments testing the binding of UpRXR(-5-33) to single half-site HREs (RORE, NGFI-BE, and D1G, see Material and Methods section for sequences) did not result in retardation (data not shown).

3.3. Examination of UpEcR and UpRXR protein-protein interactions by GST-pull down

We have previously shown that UpEcR can interact with UpRXR(-5+33) in GST-pull down experiments (Durica et al., 2002). We tested for protein-protein interactions between UpEcR and other UpRXR variants, as well as interactions among UpRXR variants themselves using GST-pull down of radiolabeled receptors (Figure 14, panel E). We also tested whether these interactions were affected by potential ligands for these receptors, 20-hydroxyecdsyone (20E) or 9-cis retinoic acid (9-cis RA). Both GST-UpRXR(-5+33) and GST-UpRXR(+5+33) were capable of binding to [^{35}S]-UpEcR (Figure 14, panel A and B, lanes 1-6) under our experimental conditions, and GST alone did not bind [^{35}S]-UpEcR (Figure 14, panel C and D, lanes 5-7). This receptor protein-protein interaction occurred regardless of 20E and 9-cis RA addition, since the amount of [^{35}S]-UpEcR trapped on GST-UpRXR fusion proteins did not change in intensity with or without hormone. However, neither GST-UpRXR(+5-33) nor GST-UpRXR(-5-33) were capable of binding to [^{35}S]-UpEcR (Figure 14, panel C and D, lanes 2 and 4). They also were not able to interact as homo-complexes (Figure 14, panel C and D, lanes 1 and 3; Figure 15, panel A and B, lanes 1-8) and the presence of 20E or 9-cis RA did not lead to recovery of a UpEcR/GST-UpRXR(±5-33) complex (data not shown).

Since the DR-1G responsive element was shown to interact with UpRXR(-5-33) in the absence of UpEcR in EMSA experiments (Figure 12), we also included DR-1G in a GST-pull down experiment to test its effect on UpRXR

homocomplex formation (Figure 15, panel A and B, lanes 1 and 5). DR-1G had no apparent influence in these pull down assays. Weak UpRXR protein-protein interactions, however, were observed between GST-UpRXR(-5+33) and [^{35}S]-UpRXR(-5-33) and [^{35}S]-UpRXR(+5-33) (Figure 15, panel C and D, lanes 2 and 3). To summarize, these GST-pull down results indicated that GST-UpRXR constructs containing the 33-aa insertion sequence in the UpRXR LBD interact strongly with UpEcR. Under our experimental conditions, GST-UpRXR(-5+33) constructs did not form homocomplexes with UpRXR(+5+33) receptor and interacted weakly with UpRXR protein lacking the 33-aa insertion.

3.4. The transactivation activity of UpEcR/UpRXR(+33) and UpEcR/UpRXR(-33) hybrid complexes

To assess the differences in the ligand-induced transactivation response of the two UpRXR LBD variants, UpRXR(+33) and UpRXR(-33), we transfected DNA for G:UpE(DEF), V:UpR(EF)±33, pFRLuc, and pTKRL constructs into 3T3 cells. The transfected cells were exposed to 0.0016-25 μM of the ecdysteroid analogs RG-102240 or Ponasterone A (Pon A), or carrier DMSO. The cells were harvested at 48 hr after addition of ligands and reporter activity was measured. As shown in Figure 16, the G:UpE(DEF) and V:UpR(EF)+33 combination induced reporter activity in the presence of RG-102240 and PonA. On the other hand, the G:UpE(DEF) and V:UpR(EF)–33 combination did not induce reporter activity either in the presence of RG-102240 or PonA. These results suggest that

UpRXR(+33) is capable of mediating transactivation after heterodimerization with UpEcR, and the 33-aa insertion is critical for this transactivation.

4. Discussion

Screening of fiddler crab premolt regenerating limb bud cDNA libraries recovered *UpRXR* hinge and LBD variants, as well as hinge region variants for *UpEcR* (Chung et al., 1998a; Durica et al., 2002). This is in contrast to the situation in insects, where A/B domain isoforms have been characterized, but no LBD isoforms have been observed (see Riddiford, 2001 for review). In this paper, we focus on the UpRXR variants. One class of UpRXR variant has a five-aa insertion/deletion at the "T" box in the hinge region, another class of UpRXR variant has a 33-aa insertion/deletion between helix one and helix three in the LBD domain. These isoforms of UpRXR present different HRE and receptor protein-protein binding properties, indicating they may have different functional roles in regulating gene expression in crustaceans.

We examined *UpRXR* transcript abundance in ecdysteroid responsive tissues at different stages during the molt cycle. RPA analysis showed all four forms of *UpRXR* transcripts *UpRXR(+5+33), UpRXR(-5+33), UpRXR(+5-33)* and *UpRXR(-5-33)* were expressed in regenerating limbs soon after autotomy and during the premolt, as well as in ovarian tissues during intermolt (data not shown). Preliminary data suggest that the isoform ratios of these variants change in both regenerating limb buds and ovaries, and experiments to quantify isoform abundance are in progress. The predominant isoform in all tissues examined was *UpRXR(-5+33)*. While we do not know if these variant forms of UpRXR co-exist

in the same cells, the presence of four forms of UpRXR presents the potential for some UpRXR variants to differentially interact with UpEcR, and/or to interact with each other. RXR and its insect homolog USP also dimerize with other NRs (Mangelsdorf and Evans, for review, 1995; Zhu et al., 2000; Hirai et al., 2002; Zhu et al., 2003; Baker et al., 2003). The heterogeneity of UpRXR also suggests the potential for differences in heterodimer interaction with other NRs and the possibility of involvement of UpRXR in other signaling pathways.

EMSA experiments were used to test the HRE binding characteristics of crab UpEcR /UpRXR heterocomplexes. UpEcR must form a heterodimer with UpRXR(±5+33) to bind to either synthetic canonical HREs with various half site orientations and spacer lengths or naturally occurring HREs (IRhsp-1, *eip28/29*). This observation is in agreement with *Drosophila* (Riddihough and Pelham, 1987; Cherbas et al., 1991; Horner et al., 1995; Antoniewski et al., 1996) and mosquito (Wang et al., 1998; Wang et al., 2000) receptor/HRE binding data. The UpEcR/UpRXR(-5+33) heterodimer complex has a K_d value for a DR-4 (2.18 nM) HRE similar to mosquito AaEcR/AaUSPb (Wang et al., 1998). Competition EMSA experiments also suggest that the UpEcR/UpRXR(-5+33) heterodimer binds most efficiently with IRper-1, IRhsp-1 and DR-4 elements, and increase in spacer length and deviation of sequence composition from a perfect consensus element (AGGTCA) decreases receptor affinity for the HRE.

This is the first report showing that LBD isoforms of a RXR can lead to distinct HRE binding characteristics. When UpRXR(±5-33) isoforms, which lacked the 33-aa insertion in the LBD domain, were used in EMSA experiments, we obtained markedly different results from that observed with UpRXR(-5+33). First, the UpRXR(±5-33) variants were not able to interact with UpEcR and bind effectively to an IRper-1 element. UpRXR(±5-33) also did not compete with UpRXR(-5+33) for UpEcR binding. Second, UpRXR(-5-33) bound independently of UpEcR to a DR-1G element, an HRE found to interact with vertebrate RXRs (Yang et al., 1995; Castelein et al., 1996). UpRXR(+5-33), however, did not interact with a DR-1G element under similar experimental conditions. Since UpRXR(-5-33) did not bind to single half site elements and migrates on EMSA similar to the UpEcR/UpRXR(±5+33) heterocomplexes, these observations suggest that the lack of the five-aa hinge region insertion confers upon UpRXR(-5-33) the ability to specifically interact with a DR-1G element as a homodimer or to interact with a partner from reticulocyte lysate.

In some EMSA experiments, rabbit reticulocyte lysate without expressed crab receptors resulted in retardation. The retarded band, however, migrated differently than the expressed crab receptor-DNA complexes, which suggests that the retardation may be caused by unknown factors (such as a mammalian DNA-binding protein) present in the lysates. The presence of these lysate factors appeared to be lot-dependent and variable (compare Figure 4 and Figure 10, lane

2). Nevertheless, we can not exclude the possibility that expressed *Uca* NRs may complex with lysate factors in these EMSA analyses.

Variability between UpRXR isoforms in the "T" box region leads to differences in the ability to bind to a DR-1G element independently of UpEcR and the relative affinity of the UpRXR/UpEcR heterodimer for an IRper-1 element. Comparison of vertebrate RXR NMR structure data (Holmbeck et al., 1998a) with crystallography data on the DNA bound form of RXR homodimers or RXR/RAR heterodimers (Zhao et al., 2000; Rastinejad et al., 2000) suggests that the "T" box has a large degree of structural freedom. This property is important in conferring cooperative binding ability to form receptor-DNA complexes (Holmbeck et al., 1998b; Rastinejad et al., 2000). The zebrafish RXR-ε also carries an eight-aa addition in the "T" box region, along with a 14-aa addition corresponding to H7 of the LBD. In contrast, the 33-aa LBD insertion/deletion of UpRXR is between helices H1 and H3. The RXR-ε variant did not bind 9-cis retinoic acid and showed no activity on RXR response elements in transfection assays, presumably due to the insertion seen in its LBD (Jones et al., 1995). However, it can bind DNA as a heterodimer with RAR and TR, and since it was active in TR transfection assays, it may be involved *in vivo* in mediating a balance in homodimer/heterodimer concentrations for selective response elements (Jones et al., 1995).

The function of the LBD in nuclear receptor ligand binding, dimerization, and transactivation is well documented through physical binding studies and crystallographic analysis (Forman and Samuels, 1990 for review; Danielson et al., 1992; Maksymowysch et al., 1993; Durand et al., 1994; Perlmann et al., 1996; Schulman et al., 1996; Riddiford et al., 2001 for review; Aranda and Pascual., 2001 for review). Dimerization interfaces have been identified in both the LBD and DBD. Like type II vertebrate nuclear receptors, insect USP/RXR binds to HREs as a heterodimer with EcR. The crystal structure data on the USP/EcR heterodimer is not yet available. Recently, however, the crystal structure of USP LBDs from the lepidopteran *Heiliothis virescens* and the dipteran *Drosophila melanogaster* have been reported (Billas et al., 2001; Clayton et al., 2001), and computer modeling studies have been performed (Sasorith et al., 2002). The resolved structures show a long connecting loop (L1-3) between helices H1 and H3, which prevent the transactivation domain in H12 from adopting an agonist conformation, a situation very distinct from the vertebrate class II nuclear receptors. In other known nuclear receptors, human vitamin D receptor (VDR) (Miyamoto et al., 1997) and cockroach *Periplaneta* USP (Bonneton et al., 2003) also have a long L1-3 region between H1 and H3. The deletion of the loop region made no difference in VDR functional assays, as it retained similar characteristics in ligand binding, dimerization, and transactivation with the wild type VDR (Rochel et al., 2000; Rochel et al., 2001). Notably, the LBD variants isolated for the crab UpRXR ortholog fell within the L1-3 region, and were correlated with their ability to dimerize with UpEcR and bind to distinct HREs. RXR variants

similar to those of *Uca* have also been recently discovered in another brachyuran, the red land crab *Gecarcinus lateralis* (H. W. Kim and D. L. Mykles, personal communication). How splicing variants in this region may affect UpRXR dimerization properties is unclear, as well as how variants in this region may govern potential ligand or coactivator/corepressor binding. The crustacean receptor may present molecular interfaces quite different from both insect USP/EcR and mammalian RXR/RAR.

GST-pull down experiments using bacterially synthesized GST-UpRXR isoforms and reticulocyte lysate expressed [^{35}S]-UpEcR generally supported the results of the EMSA experiments. While the GST-UpRXR(±5+33) fusion proteins bound [^{35}S]-UpEcR, the GST-UpRXR(±5-33) fusion proteins were not able to interact with UpEcR, suggesting that differences in this region of the LBD promote conformational changes in the heterodimerization interface between these receptors. GST-pull down experiments also indicated that the five-aa insertion in the hinge region has no direct effect on the heterodimerization of UpEcR and UpRXR, because both UpRXR(-5+33) and UpRXR(+5+33) isoforms bound to UpEcR with similar affinity (normalized amount of protein trapped same amount of bait protein, data not shown). We also saw weak interactions between the [^{35}S]-UpRXR(±5-33)/GST-UpRXR(-5+33) isoforms, but not the [^{35}S]-UpRXR(±5+33)/GST-UpRXR(-5+33) isoforms, which suggests that UpRXR(-33) and UpRXR(+33) can form a homodimer interface. The observation that GST-UpRXR(-5-33) was not able to pull down

[^{35}S]-UpRXR(-5-33), even in the presence of the DR-1G element, suggests that in EMSA experiments, either UpRXR(-5-33) requires a lysate factor to interact with the DR-1G element, or the bacterially expressed GST-UpRXR(-5-33) had a different conformation than the UpRXR synthesized in the reticulocyte lysate.

Transfection assay experiments also indicate that UpRXR(+33) isoforms are required for a functionally complete ecdysteroid receptor complex. The different transactivation abilities of UpRXR(-33) and UpRXR(+33) isoforms suggest that UpRXR(+33) is capable of mediating transactivation via UpEcR ligand binding, indicating that the LBD variants could have potential functional differences *in vivo*.

This paper reports for the first time the presence of crustacean UpRXR isoforms in ecdysteroid responsive tissues. Unlike EcR and USP isoforms in insects, the crustacean RXR isoforms are variant in both the LBD and hinge region. These isoforms show distinctive DNA and protein-protein binding properties. In a mammalian cell culture expression system, *in vivo* transfection experiments demonstrate that the LBD isoforms lead to significant reporter gene transactivation differences in response to ecdysteroid signaling. Questions relating to the tissue-specific and/or temporal-specific expression of these receptor isoforms need further study, particularly in relation to their abilities to interact with physiologically relevant ligands.

Acknowledgements

We thank Andria Parker for her help in RNA quantification and ribonuclease protection assays. We also thank Dr. D. L Mykles, and H. W. Kim, for providing unpublished information on the land crab RXR sequences. This research was supported by NSF grant IBN-9816709 to David S. Durica and Penny M. Hopkins.

Figure Legends

Figure 1.

Illustration of domain structures relative to the five-aa insertion and 33-aa insertion sites of clones *UpRXR13b (+5-33)* and *UpRXR(-5+33)*. These clones were used to generate the four UpRXR expression constructs as described in the Materials and Methods section: *UpRXR(+5+33)*, *UpRXR(-5+33)*, *UpRXR(+5-33)* and *UpRXR(-5-33)*. Vertical arrows show the restriction sites for relevant enzymes. Horizontal arrows indicate T7 RNA polymerase promoter of plasmid.

Figure 2.

Representative RPA quantifying *UpRXR* RNAs from regenerating limb bud tissues. Ten micrograms of total RNA for each indicated experimental stage (A+8, D_0) were hybridized to the D/E *UpRXR* region RPA probe (see Materials and Methods). The protected fragments are indicated by arrows. Control sense strand *UpRXR(-5+33)* and *UpRXR(+5-33)* mRNAs were synthesized and loaded in the indicated amounts. The smallest protected fragment (*) is apparently derived from *UpRXR(-5+33)* since a similar fragment is seen in the control *UpRXR(-5+33)* control lane.

Figure 3.

EMSA experiment with DR-4 HRE and UpEcR/UpRXR(-5+33). The nucleotide sequence of one strand of the HRE is indicated at the top of the figure.

The HRE oligonucleotides were radiolabeled, annealed, and used in EMSAs with reticulocyte lysate-synthesized UpEcR and UpRXR(-5+33). 20E (750 nM) was added to the reactions to test its effect on HRE binding activity in indicated lanes. Free probe is indicated by an open arrow; retarded probe is indicated by a bold arrow; supershifted probe is indicated by a thin arrow.

Figure 4.

EMSA experiment with IRper-1 HRE and UpEcR/UpRXR(-5+33). The experimental protocol is the same as in Figure 3. Lane 9 used a higher Mg^{2+} (2 mM) concentration than standard (TNM) buffer. 20E (500 nM) was added in lane 10 as indicated in the figure. Free probe is indicated by an open arrow; retarded probe is indicated by a bold arrow; supershifted probe is indicated by a thin arrow; non-specific binding is indicated by an arrowhead. Competitor HRE is unlabeled IRper-1 element.

Figure 5.

EMSA experiment with IRhsp-1 HRE and UpEcR/UpRXR(-5+33). The experimental protocol is the same as in Figure 3. Free probe is indicated by an open arrow; retarded probe is indicated by a bold arrow; supershifted probe is indicated by a thin arrow.

Figure 6.

EMSA experiment with *eip28/29* gene HRE and UpEcR/UpRXR(-5+33). The experimental protocol is the same as in Figure 3. Free probe is indicated by an open arrow; retarded probe is indicated by a bold arrow; supershifted probe is indicated by a thin arrow.

Figure 7.

Quantification of competition EMSA experiments examining the relative binding affinities of UpEcR/UpRXR(-5+33) for various HREs. Competitive oligonucleotides were annealed and used in excess in EMSAs with radiolabeled IRper-1 and DR-4/3C as described in Materials and Methods. Competitive oligonucleotide sequences were: IRper-0, agagacaagAGGTCATGACCTtgtccaa; IRper-1, agagacaagAGGTCAa-TGACCTtgtccaat; IRper-2, agagacaagAGG-TCAatTGACCTtgtccaa; IRper-3, agagacaagAGGTCAaatTGACCTtgtccaa; IRper-5, agagacaagAGGTCAaataaTGACCTtgtccaa; IRhsp-0, agagacaagGGT-TCATGCACTtgtccaa; IRhsp-1, agagacaagGGTTCAaTGCACTtgtccaat; IRhsp-3, agagacaagGGTTCAaatTGCACTtgtccaa; DR-1G, gatccgtggGGGTCAgAGG-TCActcgagatc; DR-4/HS, ttggacaAGGTCAcaggAGGTCActtgtct; DR-4/3C, aagcgaaAGGTCAaggaAGGTCAggaaaat.

Figure 8.

Measurement of equilibrium dissociation constant of UpEcR/UpRXR(-5+33) to a DR-4 HRE. A determination of the equilibrium dissociation constant (K_d) of UpEcR/UpRXR(-5+33) and DR-4/3C was assessed in EMSA experiments as

described in Materials and Methods. Radioactivity associated with free probe and with crab receptor-probe complexes were quantified by electronic autoradiography, allowing the construction of a saturation curve (A) and a Scatchard plot (B).

Figure 9.

EMSA experiment with IRper-1 HRE and UpEcR/UpRXR isoforms. The experimental protocol is the same as in Figure 3. Free probe is indicated by an open arrow; retarded probe is indicated by a bold arrow; non-specific band is indicated by an arrowhead. Binding reactions were repeated in two different EMSA buffers (see Materials and Methods). Lanes 1-7, TNM buffer; Lanes 8-11, HKN buffer.

Figure 10.

EMSA experiment with IRper-1 HRE and UpEcR/UpRXR isoform combinations. The experimental protocol is the same as in Figure 3. Free probe is indicated by an open arrow; retarded probe is indicated by a bold arrow.

Figure 11.

Measurement of equilibration dissociation constant of UpEcR/UpRXR(-5+33) and UpEcR/UpRXR(+5+33) to IRper-1 element. The experimental protocol measuring bound verses free probe and the calculating of K_d is the same as described in Figure 8. A. Saturation curve (left) and Scatchard plot (right) for

UpEcR/UpRXR(-5+33) complex. B. Saturation curve (left) and Scatchard plot (right) for UpEcR/UpRXR(+5+33) complex.

Figure 12.

EMSA experiment with DR-1G HRE and UpRXR isoforms. The experimental protocol is the same as in Figure 3. Free probe is indicated by an open arrow; retarded probe is indicated by a bold arrow; supershift is indicated by a thin arrow; non-specific band is indicated by an arrowhead.

Figure 13.

Quantification of competition EMSA experiments examining the relative binding affinities of UpRXR(-5-33) for various HREs. Competitive oligonucleotides were annealed and used in excess in EMSA with radiolabeld DR-1G as described in Materials and Methods. See Figure 7 legend for list of competitor oligonuleotide sequences; DR-4, ttggacaAGGTCAcaggAGGTCA-cttgtctt.

Figure 14.

GST-pull down experiments using *in vitro* synthesized UpEcR and UpRXR variant proteins. Reticulocyte lysate containing radiolabeled UpEcR (predicted 57.5 KDa protein) and UpRXR (predicted 51 KDa protein) were incubated with glutathione-sepharose bound GST-UpRXR (predicted 77 KDa protein, open arrow) or GST alone (predicted 26 KDa protein, bold arrow) as indicated in

Materials and Methods section. Panels A and C represent Coomassie blue stained SDS-PAGE gels. Panels B and D represent autoradiographs of the respective stained gel above, displaying the labeled proteins that bound to the GST-UpRXR fusion proteins. Arrows show the trapped full-length protein relative to the migration of the molecular weight markers; radiolabeled proteins running below full-length UpEcR are synthesized only if UpEcR plasmid is added to lysate and presumably result from internal initiation on this template. Tick marks are the molecular size markers (KDa). Panel E represents about one fifth of the input [^{35}S] labeled receptor protein used in above experiments.

Figure 15.

GST-pull down experiment using *in vitro* synthesized UpRXR variant proteins. Experimental protocol is the same as in Figure 14. Panels A and C represent Coomassie blue stained SDS-PAGE gels (Open arrows indicate the predicted full length UpRXR isoforms). Panels B and D represent autoradiographs of the respective stained gel above, displaying the labeled proteins. Arrow in panel D shows the trapped protein that bound to the GST-UpRXR fusion proteins. Tick marks are the molecular size markers (KDa).

Figure 16.

Transfection experiments. DNA samples of GAL4:UpEcR(DEF)[G:UpE(DEF)], VP16:UpRXR(EF)[V:UpR(EF) (+/- the 33-aa insert) and reporter vector pFRLUC regulated by 5X GAL4 response elements

were transfected into 3T3 cells. A second reporter, pRLTK, under a thymidine kinase constitutive promoter, was co-transfected and was used for normalization. Maximum fold activation observed for each treatment is shown on top of bars. Each data point represents three replicates of experiment. Pon A: Ponasterone A ; RG-102240: GS™-E [N-(1,1-dimethylethyl)-N'-(2-ethyl-3-methoxybenzoyl)-3,5-dimethylbenzohydrazide].

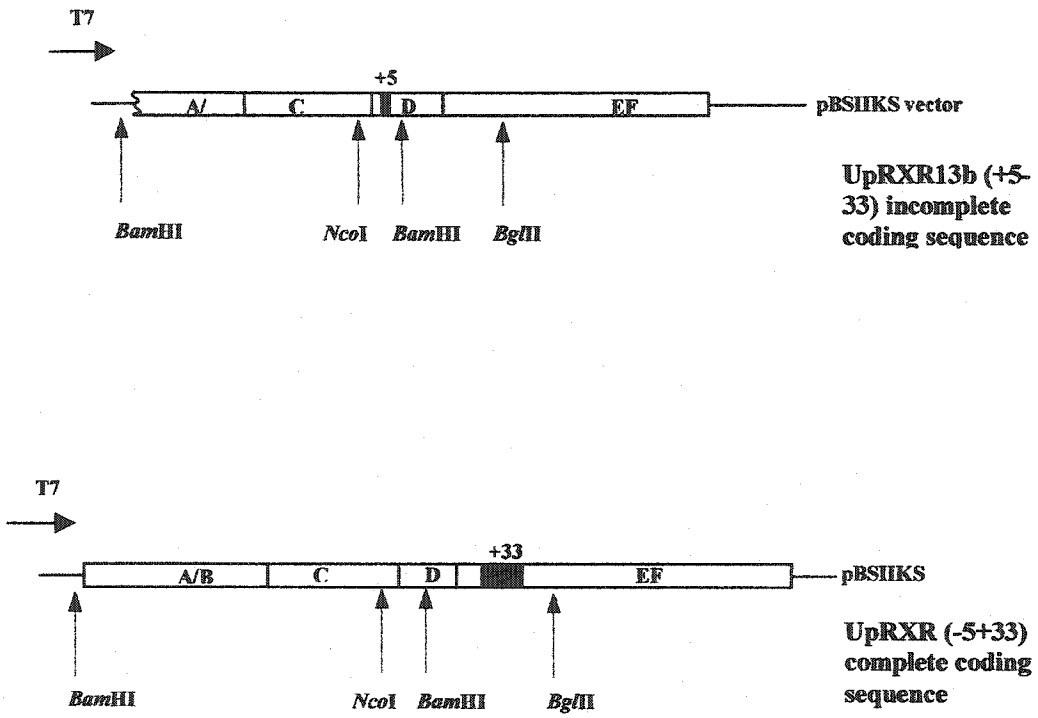
T7
+5
A/
C
D
EF
pBSIIKS vector
UpRXR13b (+5-33) incomplete coding sequence
BamHI
NcoI
BamHI
BglII
T7
+33
A/B
C
D
EF
pBSIIKS
UpRXR (-5+33) complete coding sequence
BamHI
NcoI
BamHI
BglII

Figure 1

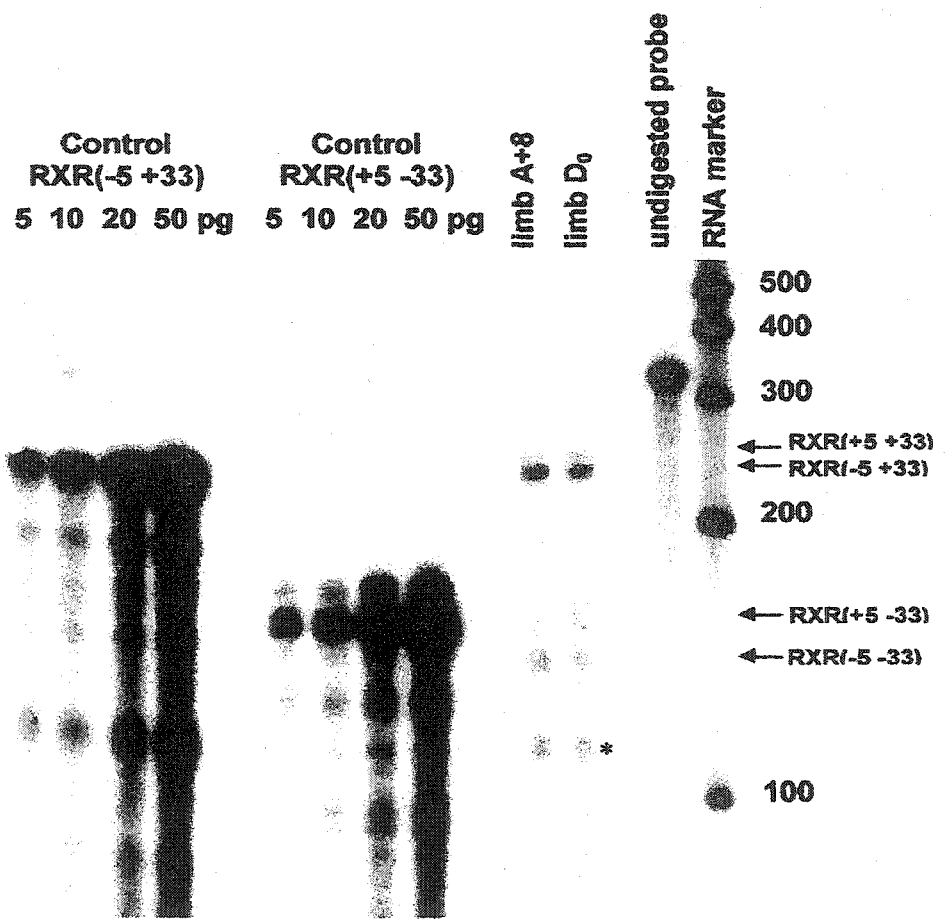
Control
RXR(-5 +33)
5 10 20 50 pg
Control
RXR(+5 -33)
5 10 20 50 pg
limb A+8
limb D0
undigested probe
RNA marker
500
400
300
RXR(+5 +33)
RXR(-5 +33)
200
RXR(+5 -33)
RXR(-5 -33)
100
*

Figure 2

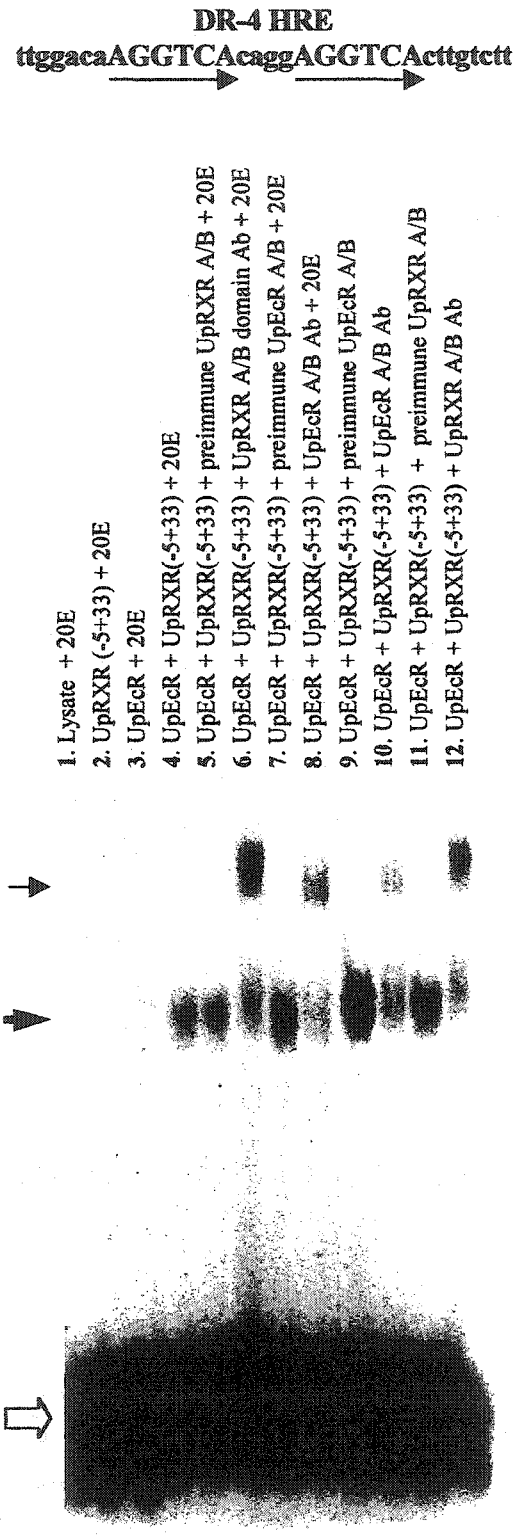
DR-4 HRE
ttggacaAGGTCAcaggAGGTCActtgtctt
1. Lysate + 20E
2. UpRXR (-5+33) + 20E
3. UpEcR + 20E
4. UpEcR + UpRXR(-5+33) + 20E
5. UpEcR + UpRXR(-5+33) + preimmune UpRXR A/B + 20E
6. UpEcR + UpRXR(-5+33) + UpRXR A/B domain Ab + 20E
7. UpEcR + UpRXR(-5+33) + preimmune UpEcR A/B + 20E
8. UpEcR + UpRXR(-5+33) + UpEcR A/B Ab + 20E
9. UpEcR + UpRXR(-5+33) + preimmune UpEcR A/B
10. UpEcR + UpRXR(-5+33) + UpEcR A/B Ab
11. UpEcR + UpRXR(-5+33) + preimmune UpRXR A/B
12. UpEcR + UpRXR(-5+33) + UpRXR A/B Ab

Figure 3

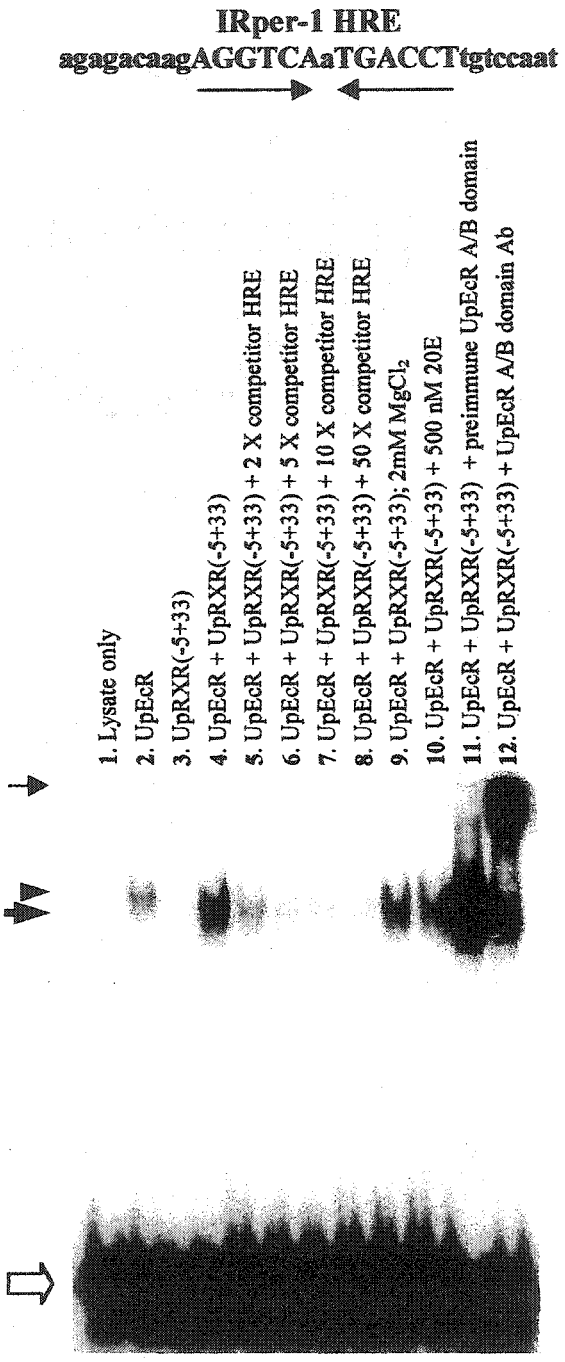
IRper-1 HRE
agagacaagAGGTCAaTGACCTtgtccaat
1. Lysate only
2. UpEcR
3. UpRXR(-5+33)
4. UpEcR + UpRXR(-5+33)
5. UpEcR + UpRXR(-5+33) + 2 X competitor HRE
6. UpEcR + UpRXR(-5+33) + 5 X competitor HRE
7. UpEcR + UpRXR(-5+33) + 10 X competitor HRE
8. UpEcR + UpRXR(-5+33) + 50 X competitor HRE
9. UpEcR + UpRXR(-5+33); 2mM $MgCl_2$
10. UpEcR + UpRXR(-5+33) + 500 nM 20E
11. UpEcR + UpRXR(-5+33) + preimmune UpEcR A/B domain
12. UpEcR + UpRXR(-5+33) + UpEcR A/B domain Ab

Figure 4

1. Lysate only
2. UpRXR (-5+33)
3. UpEcR
4. UpEcR + UpRXR(-5+33)
5. UpEcR + UpRXR(-5+33) + preimmune UpRXR common
6. UpEcR + UpRXR(-5+33) + UpRXR-common domain Ab
7. UpEcR + UpRXR(-5+33) + preimmune UpRXR-A/B
8. UpEcR + UpRXR(-5+33) + UpRXR-A/B Ab
9. UpEcR + UpRXR(-5+33) + preimmune UpEcR-A/B
10. UpEcR + UpRXR(-5+33) + UpEcR-A/B Ab
11. UpEcR + UpRXR(-5+33)
12. UpEcR + UpRXR(-5+33) + 2 X competitor HRE
13. UpEcR + UpRXR(-5+33) + 5 X competitor HRE
14. UpEcR + UpRXR(-5+33) + 10 X competitor HRE
15. UpEcR + UpRXR(-5+33) + 50 X competitor HRE
IRhsp-1 HRE
agagacaagGGTTCAaTGCACTtgtccaat

Figure 5

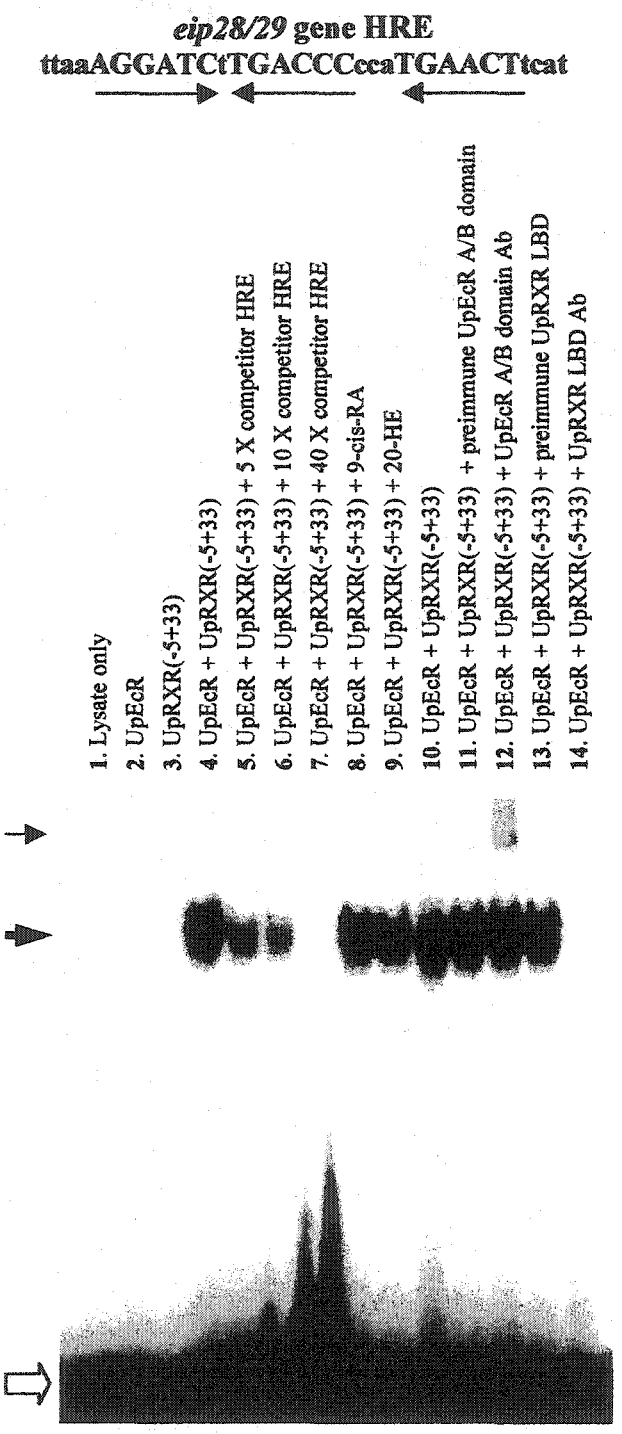
eip28/29 gene HRE
ttaaAGGATCtTGACCCccaTGAACTtcat
1. Lysate only
2. UpEcR
3. UpRXR(-5+33)
4. UpEcR + UpRXR(-5+33)
5. UpEcR + UpRXR(-5+33) + 5 X competitor HRE
6. UpEcR + UpRXR(-5+33) + 10 X competitor HRE
7. UpEcR + UpRXR(-5+33) + 40 X competitor HRE
8. UpEcR + UpRXR(-5+33) + 9-cis-RA
9. UpEcR + UpRXR(-5+33) + 20-HE
10. UpEcR + UpRXR(-5+33)
11. UpEcR + UpRXR(-5+33) + preimmune UpEcR A/B domain
12. UpEcR + UpRXR(-5+33) + UpEcR A/B domain Ab
13. UpEcR + UpRXR(-5+33) + preimmune UpRXR LBD
14. UpEcR + UpRXR(-5+33) + UpRXR LBD Ab

Figure 6

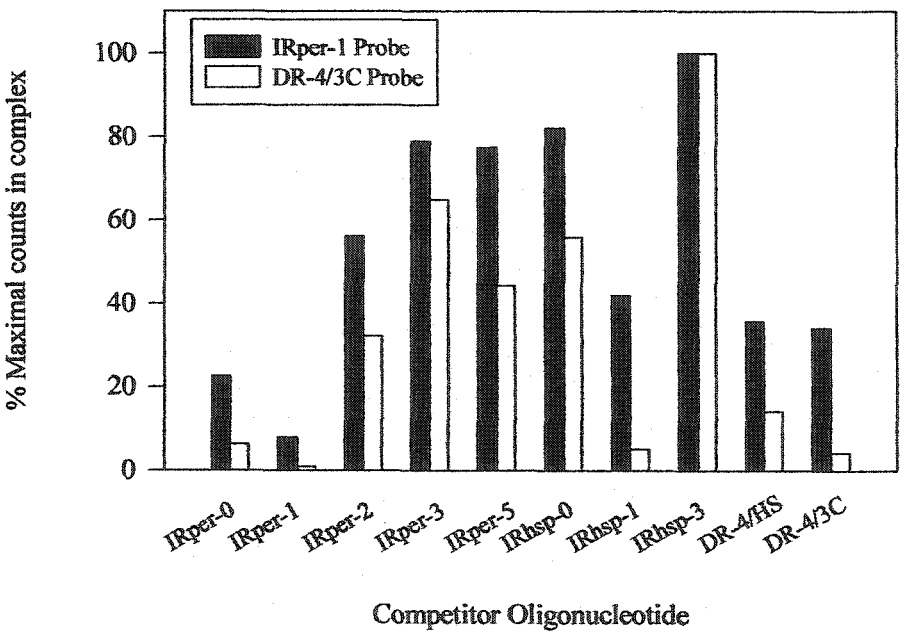
IRper-1 Probe
DR-4/3C Probe
% Maximal counts in complex
100
80
60
40
20
0
IRper-0
IRper-1
IRper-2
IRper-3
IRper-5
IRhsp-0
IRhsp-1
IRhsp-3
DR-4/HS
DR-4/3C
Competitor Oligonucleotide

Figure 7

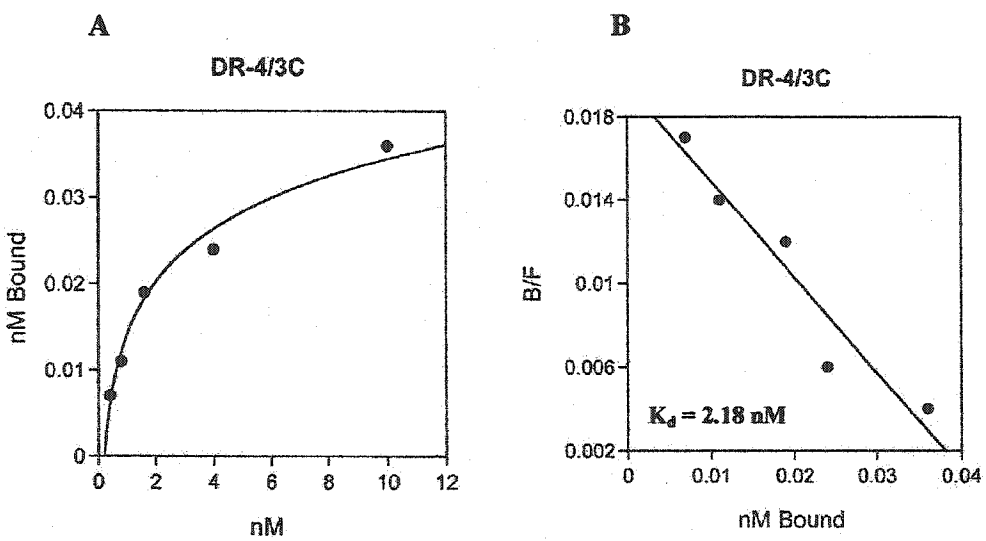
A
DR-4/3C
nM Bound
0.04
0.03
0.02
0.01
0
0
2
4
6
8
10
12
nM
B
DR-4/3C
B/F
0.018
0.014
0.01
0.006
0.002
K_d = 2.18 nM
0
0.01
0.02
0.03
0.04
nM Bound

Figure 8

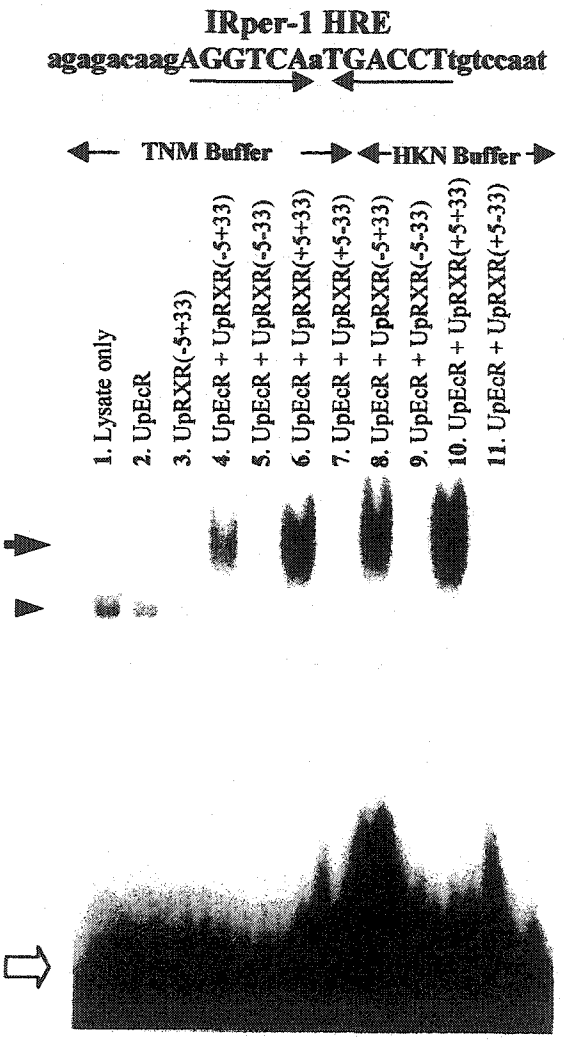
IRper-1 HRE
agagacaagAGGTCAaTGACCTtgtccaat
TNM Buffer
HKN Buffer
1. Lysate only
2. UpEcR
3. UpRXR(-5+33)
4. UpEcR + UpRXR(-5+33)
5. UpEcR + UpRXR(-5-33)
6. UpEcR + UpRXR(+5+33)
7. UpEcR + UpRXR(+5-33)
8. UpEcR + UpRXR(-5+33)
9. UpEcR + UpRXR(-5-33)
10. UpEcR + UpRXR(+5+33)
11. UpEcR + UpRXR(+5-33)

Figure 9

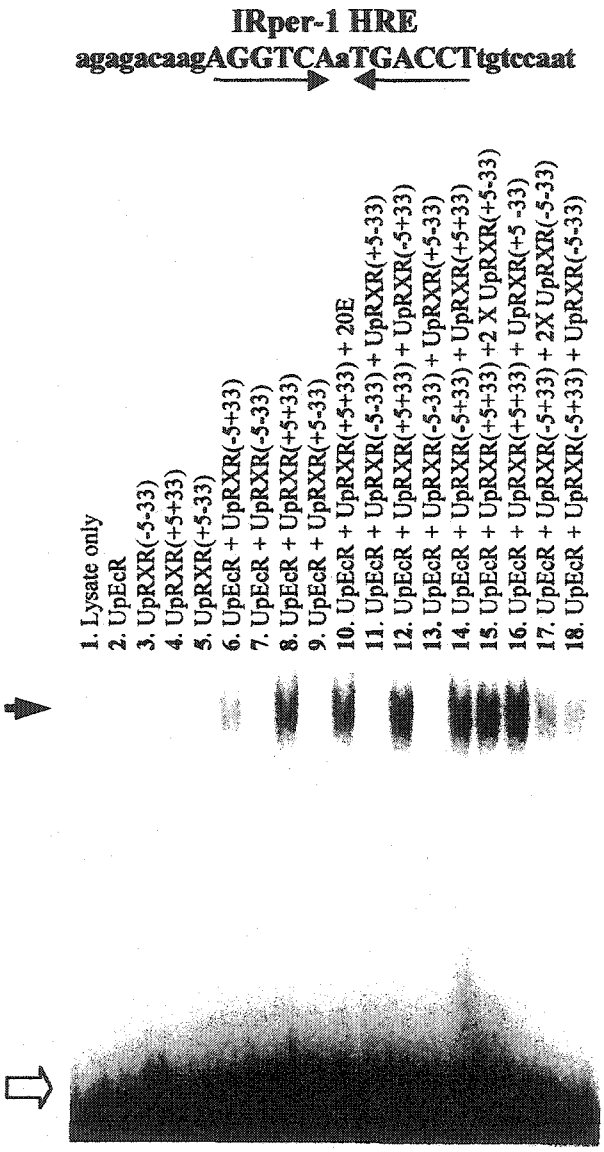
IRper-1 HRE
agagacaagAGGTCAaTGACCTtgtccaat
1. Lysate only
2. UpEcR
3. UpRXR(-5-33)
4. UpRXR(+5+33)
5. UpRXR(+5-33)
6. UpEcR + UpRXR(-5+33)
7. UpEcR + UpRXR(-5-33)
8. UpEcR + UpRXR(+5+33)
9. UpEcR + UpRXR(+5-33)
10. UpEcR + UpRXR(+5+33) + 20E
11. UpEcR + UpRXR(-5-33) + UpRXR(+5-33)
12. UpEcR + UpRXR(+5+33) + UpRXR(-5+33)
13. UpEcR + UpRXR(-5-33) + UpRXR(+5-33)
14. UpEcR + UpRXR(-5+33) + UpRXR(+5+33)
15. UpEcR + UpRXR(+5+33) +2 X UpRXR(+5-33)
16. UpEcR + UpRXR(+5+33) + UpRXR(+5 -33)
17. UpEcR + UpRXR(-5+33) + 2X UpRXR(-5-33)
18. UpEcR + UpRXR(-5+33) + UpRXR(-5-33)

Figure 10

A

IRper-1 Element: UpEcR + UpRXR(-5+33)

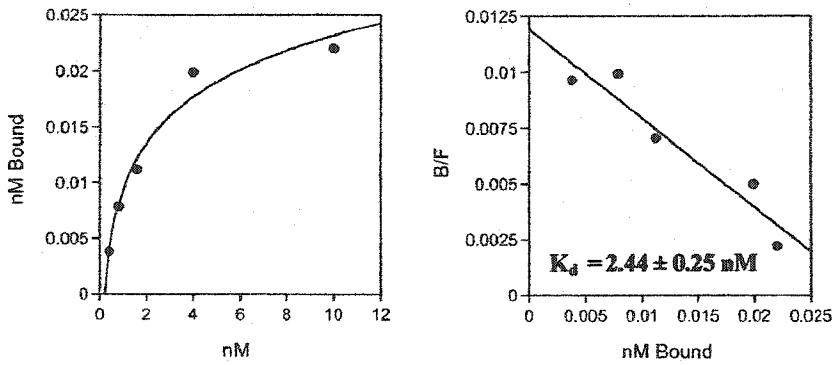

B

IRper-1 Element: UpEcR + UpRXR(+5+33)

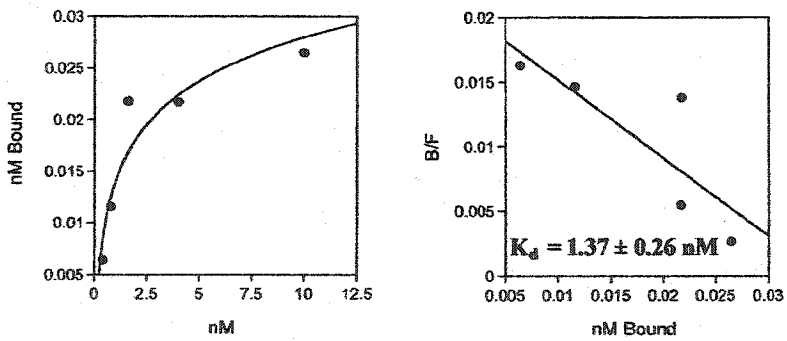

Figure 11

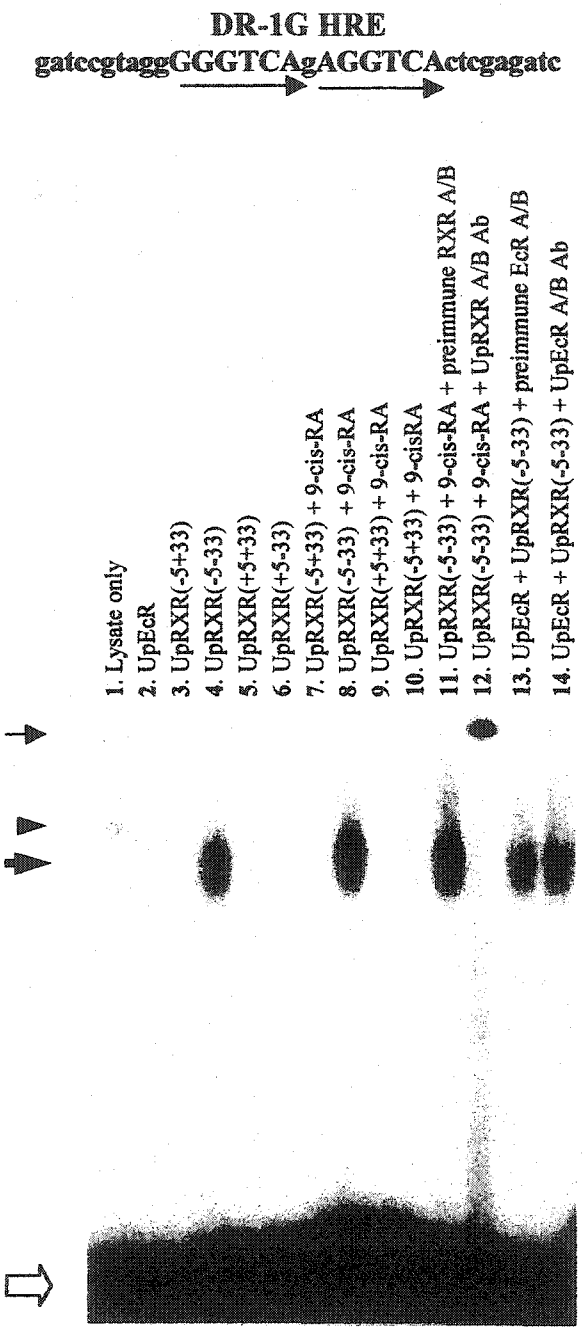
DR-1G HRE
gatccgtaggGGGTCAgAGGTCActcgagatc
1. Lysate only
2. UpEcR
3. UpRXR(-5+33)
4. UpRXR(-5-33)
5. UpRXR(+5+33)
6. UpRXR(+5-33)
7. UpRXR(-5+33) + 9-cis-RA
8. UpRXR(-5-33) + 9-cis-RA
9. UpRXR(+5+33) + 9-cis-RA
10. UpRXR(-5+33) + 9-cisRA
11. UpRXR(-5-33) + 9-cis-RA + preimmune RXR A/B
12. UpRXR(-5-33) + 9-cis-RA + UpRXR A/B Ab
13. UpEcR + UpRXR(-5-33) + preimmune EcR A/B
14. UpEcR + UpRXR(-5-33) + UpEcR A/B Ab

Figure 12

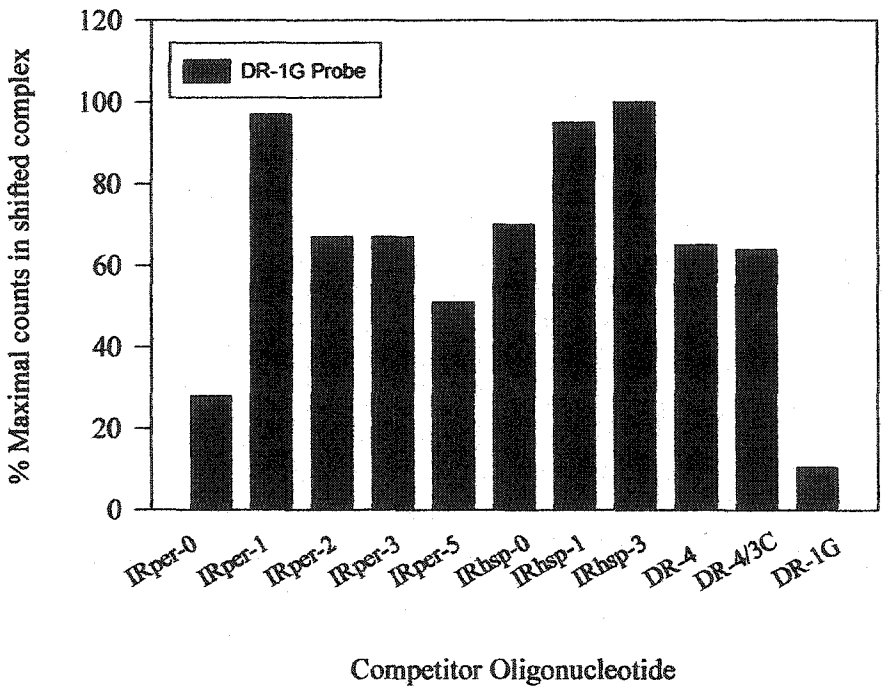
120
100
80
60
40
20
0
% Maximal counts in shifted complex
DR-1G Probe
IRper-0
IRper-1
IRper-2
IRper-3
IRper-5
IRhsp-0
IRhsp-1
IRhsp-3
DR-4
DR-4/3C
DR-1G
Competitor Oligonucleotide

Figure 13

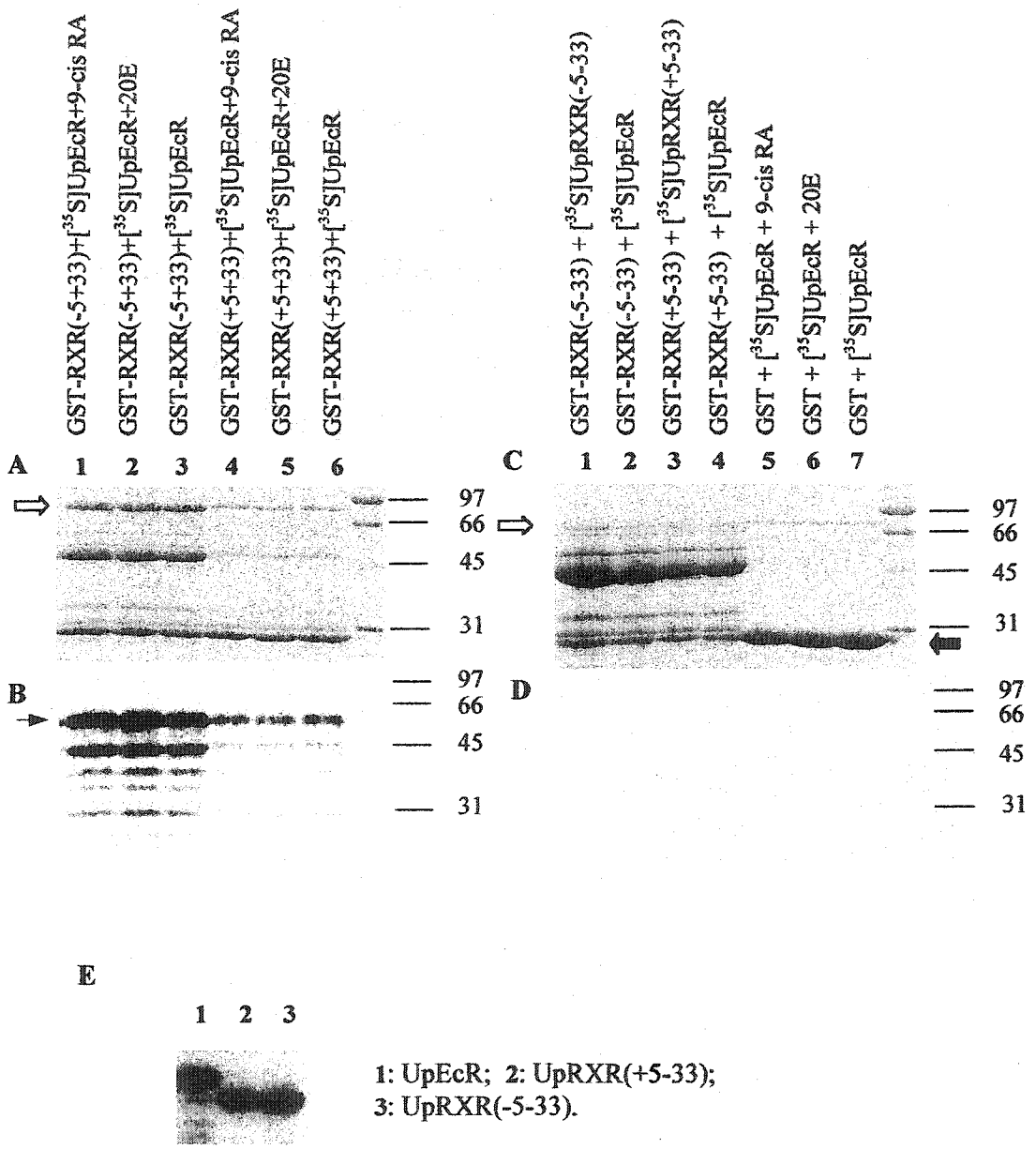
A
1 2 3 4 5 6
GST-RXR(-5+33)+[35S]UpEcR+9-cis RA
GST-RXR(-5+33)+[35S]UpEcR+20E
GST-RXR(-5+33)+[35S]UpEcR
GST-RXR(+5+33)+[35S]UpEcR+9-cis RA
GST-RXR(+5+33)+[35S]UpEcR+20E
GST-RXR(+5+33)+[35S]UpEcR
97
66
45
31
B
97
66
45
31
C
1 2 3 4 5 6 7
GST-RXR(-5-33) + [35S]UpRXR(-5-33)
GST-RXR(-5-33) + [35S]UpEcR
GST-RXR(+5-33) + [35S]UpRXR(+5-33)
GST-RXR(+5-33) + [35S]UpEcR
GST + [35S]UpEcR + 9-cis RA
GST + [35S]UpEcR + 20E
GST + [35S]UpEcR
97
66
45
31
D
97
66
45
31
E
1 2 3
1: UpEcR; 2: UpRXR(+5-33);
3: UpRXR(-5-33).

Figure 14

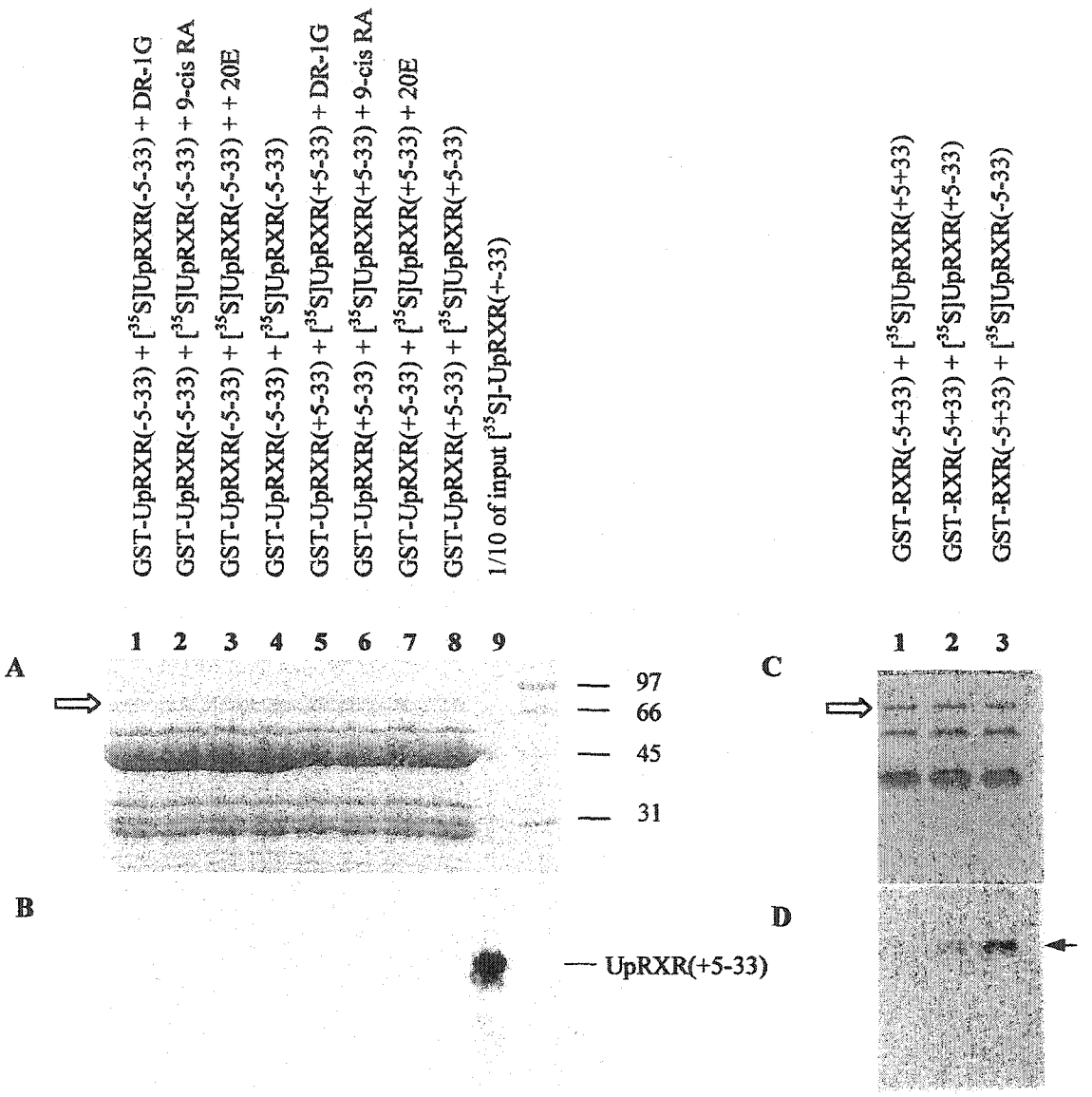
A
B
C
D
1 2 3 4 5 6 7 8 9
GST-UpRXR(-5-33) + [35S]UpRXR(-5-33) + DR-1G
GST-UpRXR(-5-33) + [35S]UpRXR(-5-33) + 9-cis RA
GST-UpRXR(-5-33) + [35S]UpRXR(-5-33) + + 20E
GST-UpRXR(-5-33) + [35S]UpRXR(-5-33)
GST-UpRXR(+5-33) + [35S]UpRXR(+5-33) + DR-1G
GST-UpRXR(+5-33) + [35S]UpRXR(+5-33) + 9-cis RA
GST-UpRXR(+5-33) + [35S]UpRXR(+5-33) + 20E
GST-UpRXR(+5-33) + [35S]UpRXR(+5-33)
1/10 of input [35S]-UpRXR(+-33)
97
66
45
31
UpRXR(+5-33)
1 2 3
GST-RXR(-5+33) + [35S]UpRXR(+5+33)
GST-RXR(-5+33) + [35S]UpRXR(+5-33)
GST-RXR(-5+33) + [35S]UpRXR(-5-33)

Figure 15

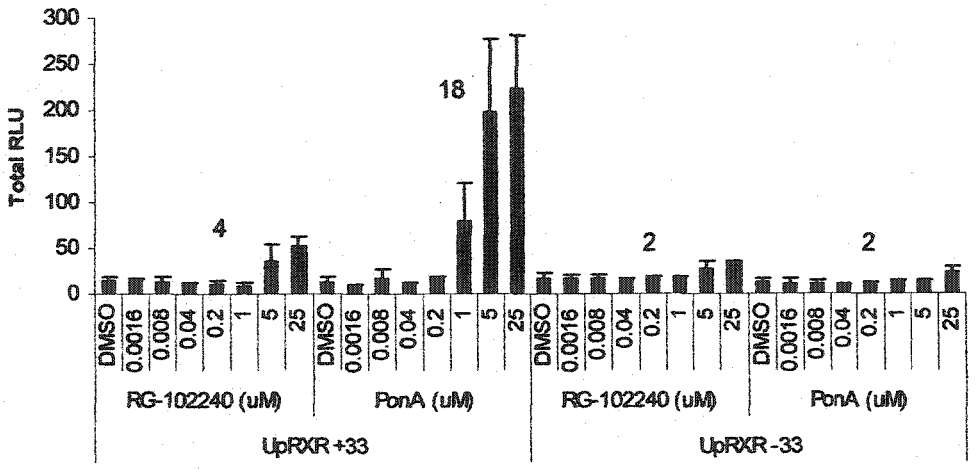
Total RLU
300
250
200
150
100
50
0
4
18
2
2
DMSO
0.0016
0.008
0.04
0.2
1
5
25
RG-102240 (uM)
PonA (uM)
UpRXR +33
UpRXR -33

Figure 16

Chapter IV

Examination of the temporal and spatial expression patterns of UpEcR and UpRXR during limb regeneration and the relationship of receptor expression to changing titers of circulating ecdysteroids

Abstract

Expression vectors were constructed to express A/B domain and common domain proteins of UpEcR and UpRXR in *E. coli*. These *E. coli* expressed proteins were used as antigen to immunize naïve rabbits. The commercially recovered polyclonal antibodies were used to localize cells expressing receptors in fiddler crab (*Uca pugilator*) limb bud tissues during the limb regeneration cycle. The ecdysteroid titers in the circulating hemolymph of these animals were also quantified by radioimmunoassay (RIA). The immunohistochemical staining results show that throughout the regeneration process, UpEcR and UpRXR are often found in the same tissues and cell types. Epidermal cell nuclei are immunoreactive to UpRXR antibody. In most stages tested using adjacent or near adjacent tissue sections, those epidermal cells also are immunoreactive to UpEcR antibody. At an early premolt stage, muscle nuclei are also immunoreactive to both UpEcR and UpRXR antibodies in a similar pattern. Cases where UpEcR has a different distribution pattern than that of UpRXR are also observed. At five days after autotomy, more connective tissue cells are shown to be immunoreactive to UpRXR than to UpEcR antibody. In an early premolt stage, some epidermal cells are shown to be UpRXR immunoreactive but not UpEcR immunoreactive. These immunoreactive patterns suggest that UpEcR and UpRXR are often expressed in the same tissues and cells, and as suggested also by biochemical analysis, they may function as heterodimer partners. The occasional discrepancy from an equivalent staining pattern suggests that UpRXR or UpEcR may have

other dimerization partners. When the immunoreactive patterns were compared to the circulating ecdysteroid titers, receptors were observed regardless of the level of ecdysteroid. Expression of UpEcR and UpRXR were observed when either low or high titers of ecdysteroid were present in the circulating hemolymph, indicating that any change in distribution pattern could not be explained by a simple change of circulating ecdysteroid titer alone.

1. Introduction

In the fiddler crab, *Uca pugilator*, the regeneration of a lost limb begins with closure of the autotomy membrane and scab formation shortly after autotomy. This process involves two growth stages, basal growth and proecdysial growth (Bliss, 1960). Basal growth results in the formation of a segmented miniature limb bud, and proecdysial growth is the hypertrophic limb bud growth including such physiological events as protein synthesis and water uptake (Hopkins 1993). The regeneration process can be further defined by the changes in the circulating ecdysteroid hormone titers and ratios (Hopkins 1992). Basal growth occurs after autotomy. It involves cell migration, cell differentiation, and cell multiplication. These events happen when ecdysteroid titers are low. The transition from basal growth to proecdysial growth is associated with an obligatory small peak of ecdysteroids (Hopkins 1989). After the small peak, there is a drop in ecdysteroid titer, and proecdysial growth begins when the ecdysteroid titer is still low. Near the end of proecdysial growth, ecdysteroid titer rapidly peaks (Hopkins 1986). A drop from this peak precedes the end of limb bud growth, after which the animal is in the final stage of preparation for molt. Other ecdysteroid peaks during this time are correlated with the ecdysis of the exoskeleton. The newly regenerated bud becomes free from its cuticular sac at ecdysis, fills with blood, unfolds, and stretches into a complete limb (Hopkins 1993).

In the fiddler crab, and other crustaceans, several major ecdysteroids circulate

in the hemolymph (Hopkins 1983; Lachaise and Lafont 1984; Snyder and Chang 1991). The levels and ratios of circulating ecdysteroids change in a molt cycle-related pattern (Hopkins 1983, 1986, 1989, 1992). These fluctuations, in addition to controlling regeneration, may be responsible for regulating many other physiological and biochemical processes related to the molting event such as proliferation of epidermal cells, secretion of layers of new cuticles, withdrawal and storage of calcium salt from the old cuticle and construction of new exoskeleton underneath the old one (Chang 1989, for review).

In arthropods, the ecdysteroid hormones regulate growth, differentiation, and reproduction by influencing gene expression (Segraves 1994; Thummel 1996). The most active ecdysteroid in insects, 20-hydroxyecdysone, (20E; Riddiford 1993; Riddiford et al., 2001, for review), functions by binding to a cognate receptor, the ecdysteroid receptor (EcR). In insects, EcR binds with the ultraspiracle protein (USP, a homolog of the vertebrate retinoid X receptor, RXR), forming a functional heterodimer (Koelle et al., 1991; Yao et al., 1992; Koelle at al., 1992; Thomas et al., 1993; Yao et al., 1993; Swevers et al., 1996; Hall and Thummel, 1998). This EcR/USP heterodimer triggers gene expression by binding to an array of specific regulatory DNA sequences, the ecdysone responsive elements (EcREs). This binding activates or inactivates an array of down-stream genes, a cascade of events well characterized in *Drosophila melanogaster* (Segraves and Hogness 1990; Karim and Thummel 1992; Thummel 1995, review; Fisk and Thummel 1998).

In *D. melanogaster*, three EcR A/B domain isoforms (EcR-A, EcR-B1, and EcR-B2) have been characterized (Talbot et al., 1993), which share common DNA and hormone-binding domains but have different N-terminal A/B regions. Immunohistochemical studies using monoclonal antibodies against EcR-A or EcR-B1 isoforms showed that EcR is widely expressed in imaginal discs, the imaginal rings, and various larval tissues at the onset of metamorphosis (Talbot et al., 1993). The expression patterns are EcR isoform-specific in that tissues in the same metamorphic class often exhibit the same expression pattern. For example, the imaginal discs form an obvious metamorphic class, and the different discs uniformly exhibit a high anti-A to anti-B staining ratio. Similarly, the imaginal cells of the midgut islands and histoblast nests also form a clear metamorphic class, characterized by massive cell multiplication and migration distinct from disc response (Roseland and Schneiderman, 1979). Their staining pattern exhibits the highest anti-B to anti-A ratio. These observations support the hypothesis that particular metamorphic responses require particular EcR isoforms (Talbot et al., 1993). Interestingly, while EcR shows differential expression patterns in different tissues, USP appears to be ubiquitous at this developmental stage (Talbot et al., 1993). Hence, it is possible that variation in active receptor complexes (EcR/USP) is due to variation in the respective EcR component.

The expression profiles of EcR in the central nervous system of *Drosophila* and *Manduca* during metamorphosis have also been studied by

immunohistochemistry using isoform-specific monoclonal and polyclonal antibodies, and their expression patterns were compared to circulating ecdysteroid titer changes (Truman et al., 1994; Riddiford et al., 2001, for review). In brief, EcR is broadly expressed at the onset of metamorphosis, but specific patterns of EcR expression correlate with distinct patterns of ecdysteroid response. In early stages of larval neuronal development, the expression level of EcR is very low (*Manduca*) or undetectable (*Drosophila*), and these cells show no response to ecdysteroid surges between molts. At the onset of metamorphosis, however, these same cells show high levels of EcR-B1 expression, and in response to a surge of circulating ecdysteroid titer, they begin to lose their larval characteristics. At the transition from pupal to adult stage, these cells switch to EcR-A expression and transform to adult form (Truman et al., 1994). Overall, two EcR isoforms correlate with different types of ecdysteroid responses: EcR-A predominates when cells are undergoing maturational response whereas EcR-B1 predominates during proliferative activity or regressive response (Truman et al., 1994).

Immunohistochemical studies of *Manduca* dorsal external oblique muscles during metamorphosis also show that expression of specific EcR isoforms is correlated to specific physiological events and in response to changing ecdysteroid titers (Hegstrom et al., 1998). Muscle degeneration and apoptosis of myonuclei are correlated with the expression of EcR-A before pupal ecdysis and then with the expression of low levels of both EcR-A and EcR-B1 shortly after pupation. The only muscle fiber that participates in the adult muscle regrowth

shows an increase in EcR-B1 expression, which is evident at three days after pupal ecdysis (Hegstrom et al., 1998).

EcR expression was also shown to be involved in butterfly *Precis coenia* wing color pattern formation during metamorphosis (Koch et al., 2003). Immunohistochemical studies using heterologous monoclonal antibodies against *Manduca sexta* EcR-B1 show that EcR expression correlate with all major events of wing development and color pattern formation. EcR is expressed in cell nuclei corresponding to wing lacunae and prospective veins. EcR is also expressed early in pupal wing development in "focal" cells which are thought to release determining signals in a process leading to eyespot formation. EcR expression patterns in prospective eyespots show that these special pattern elements are specified in concert with other factors of color pattern formation such as the transcription factor Distal-less. In eyespot foci, Distal-less is expressed simultaneously with EcR, but Distal-less precedes EcR expression in eyespot-forming cells (Koch et al., 2003).

The ecdysteroid receptor (*UpEcR*) and retinoid X receptor (*UpRXR*) gene homologs from *Uca pugilator*, have been cloned (Durica and Hopkins, 1996; Chung et al., 1998a; Durica et al., 2002). Using probes derived from common regions of *UpEcR* and *UpRXR*, their temporal and spatial expression patterns have been studied at the mRNA level. Northern blot and ribonuclease protection assays (RPA) show both *UpEcR* and *UpRXR* transcripts are present together in

multiple tissues throughout the molt cycle (Chung et al., 1998b; Durica et al., 2002). Changes in the steady-state concentrations of these receptor transcripts imply molt cycle-related differences in the potential of these tissues to respond to changing titers of ecdysteroids in the hemolymph (Chung et al., 1998b). Using polyclonal antibodies against UpEcR and UpRXR, I studied here the expression pattern of UpEcR and UpRXR proteins during the process of limb regeneration by immunohistochemistry. These studies indicate that a large group of tissues and cell populations are immunoreactive to UpEcR and UpRXR antibodies. The immunoreactive staining profiles suggest that UpEcR and UpRXR are often expressed in the same tissues and cell types. When the immunoreactive patterns were compared to the circulating ecdysteroid titers, expressions of UpEcR and UpRXR receptors were observed regardless of the level of ecdysteroid present in the circulating hemolymph, indicating that the distribution of nuclear receptor can not be explained by a simple change of circulating ecdysteroid titer alone.

2. Materials and Methods

2.1. Animals and staging

Animals were obtained and maintained as described in previous chapters. Staging of regenerating limb buds was also as described in previous chapters. The limb growth stages are also correlated with molting stages using the level of the circulating ecdysteroid titer (Hopkins, 1986).

2.2. Subcloning for antibody production

The construction of expression vectors for UpEcR A/B domain and UpRXR A/B domain proteins has been described in Chapter I. UpEcR A/B domain and UpRXR A/B domain proteins were expressed in *E. coli* using the QIAexpressionist™ (Qiagen, Valencia, CA) expression system using optimized inducible promoter-operator (T5-*lac*) elements. Figure 1 and Figure 2 show the expressed amino acid sequences of UpEcR A/B and UpRXR A/B domain fusion proteins produced for antibody production. These fusion proteins have estimated molecular weights of 14.8 KDa and 11.7 KDa, respectively (from Expasy program at http://www.expasy.ch/).

To express and isolate the expressed UpEcR A/B and UpRXR A/B domain proteins as antigens, one ml of a three ml overnight culture from a single colony was transferred to 500 ml pre-warmed LB medium (NaCl 0.5%, bactotryptone 1%, yeast extract 0.5%) containing ampicillin (100 μg/ml) and kanamycin (25

μg/ml). The culture was incubated at 37°C with vigorous shaking (~250 rpm) until an OD_{550} of 0.7 was reached. IPTG was then added to the culture to a final concentration of 1 mM. Culture was continued for another 2 to 3 hours. Cells were harvested by centrifugation at 4000 rpm for 30 min in 50 ml Falcon tubes at 4°C. The cell pellet was frozen quickly in liquid nitrogen, and stored at -80°C for batch protein isolation. Cell pellets were thawed on ice for 15 min and resuspended in 2 ml lysis buffer (50 mM NaH_2PO_4, pH 8.0, 300 mM NaCl, 10 mM imidazole) containing freshly prepared sarcosyl (0.05 g of sarcosyl was dissolved in 10 ml lysis buffer, protease inhibitors [0.1 mM PMSF, 0.1 mM $Na_2S_2O_5$, 1 μg/ml pepstatin and leupeptin, 2 μg/ml aprotinin] were also included). Lysozyme was added to 1 mg/ml. The mixture was then incubated on ice for 30 min. The cells were briefly sonicated on ice and cell debris removed by centrifugation at 11,000X g for 30 min. One ml of Ni-NTA resin was applied to the supernatant and the mixture was rotated on a roller drum at 4°C for 1 hour. This lysate-Ni-NTA mixture was then loaded into a column and washed with twice with 4 ml wash buffer (50 mM NaH_2PO_4, pH 8.0, 300 mM NaCl, 20 mM imidazole). The 6xHis tagged fusion UpEcR or UpRXR was finally eluted out with 4 times of 0.5 ml elution buffer (50 mM NaH_2PO_4, pH 8.0, 300 mM NaCl, 250mM imidazole). Fractions from each step were collected for SDS-PAGE gel analysis (see below). UpEcR and UpRXR were excised from preparative gels following visualization of the band by precipitating the protein in situ with 0.1 M KCl. Polyclonal rabbit antisera against the recombinant proteins were then generated by a commercial supplier (Cocalico Biologicals, Philadelphia, PA)

2.3. SDS-PAGE and Western blots

Standard 10% or 12.5% SDS-PAGE (sodium dodecyl sulfate-polyacrylamide gel electrophoresis) were used to separate *E. coli* and *in vitro* synthesized proteins. For small molecular weight proteins such as UpEcR A/B domain and UpRXR A/B domain proteins, Tris-Tricine SDS-PAGE gels were used (Schägger and Jagow, 1987). Proteins were transferred to Protran™ pure nitrocellulose membrane BA85 (Schleicher & Schuell, Keene, NH). Western blots followed the standard procedure according to the manufacturer's instructions (Bio-Rad laboratory Inc., Hercules, CA). Briefly, blots were soaked in TBS buffer for 10 min and then placed in blocking buffer (10 % non-fat dry milk, 3% BSA, 0.2% Tween-20 in TBS buffer) for one hour at room temperature. Either immune sera (hereafter referred to as antibody) or preimmune sera (1:3000-1:5000 dilution) were added to the blocking solution and incubation continued for another hour. The blots were then rinsed in wash buffer and washed two times, 10 min each. The blots were then incubated in blocking buffer with secondary antibodies (1:2000-1:5000 HRP conjugated anti-rabbit or anti-mouse IgG, Bio-Rad Laboratory Inc.) for one hour. The blots were washed in TBS buffer and ECL reagent (Amersham Biosciences, Piscataway, NJ) was applied according to manufacturer's instructions.

2.4. Immunoprecipitation

TNT® reticulocyte lysate (Promega, Madison, WI) was used to synthesize

[^{35}S]-labeled UpRXR variant proteins and UpEcR protein. Lysate containing labeled receptor protein (10 µl) was added to thawed *E. coli* (DH5α) extract (10 mg/ml, 100 µl). Five µl of antibodies against UpEcR A/B or UpRXR A/B domain or their respective preimmune sera control were added to separate reactions. Immunoprecipitation buffer (50 mM Tris-Cl, pH 7.6, 5 mM $MgCl_2$, 100 mM NaCl, 0.1% Triton X-100, with protease inhibitors [0.1 mM PMSF, 0.1 mM $Na_2S_2O_5$, 1 µg/ml pepstatin and leupeptin, 2 µg/ml aprotinin] and 1 mM DTT included just before use) was added to final a volume of 500 µl. NaCl (4 M) was used to adjust the final salt concentration to 100 mM NaCl. The reactions were mixed on a roller drum for an hour at 4°C at gentle speed. Non-specific aggregates were spun down for 10 minat maximum speed at 4°C in a microcentrifuge. Supernatants were transferred to new tubes, and 50 µl of protein A slurry (Amersham Biosciences, Piscataway, NJ) containing 25 µl of protein A beads were added to the reactions and mixing was continued for one hour at 4°C. The protein A matrixes were pelleted by a brief spin (20 sec) at maximum speed in a microcentrifuge at 4°C. The pellet matrixes were washed five times by disruption of pellet and repelleting in immunoprecipitation buffer and the bound proteins were dissolved in one volume of 2X sample buffer by boiling for 5 min. The proteins were resolved by a SDS-PAGE gel, the gel was dried and subjected to electronic autoradiography on an InstantImager™ (Packard Bioscience).

2.5. Immunohistochemistry

Staged crabs were cooled by immersion in crushed ice for 10 min. Tissues

from regenerating limb buds were quickly dissected out and rinsed in PBS, and immediately fixed in a 20 volume excess of Lillie decalcification fixative (Presenell et al., 1997; 71 ml of saturated picric acid, 24 ml of 37-40% formaldehyde, 5 ml of concentrated formic acid) overnight. Tissues were also fixed in 4% paraformaldehyde solution overnight for comparison. Hemolymph samples were collected at the same time, and were quick frozen in liquid nitrogen and stored in –80C° until use. The hemolymph samples were subjected to radioimmunoassay (RIA) to determine the amount of circulating ecdysteroids (see below).

Fixed tissues underwent a standard dehydration series with ethanol and penetration with xylene (Presenell et al., 1997). Tissues were embedded in paraffin. Adjacent or near adjacent 5-8 μm sections were mounted (mounting solution: 1 g of gelatin, 500 ml distilled H_2O heated to 55°C, 500 ml of 80% ethanol, stored in refrigerator) on subbed slides (Gatenby subbing solution: 144 ml distilled H_2O, 3 g gelatin, 0.2 g chromium potassium sulfate premixed in 5 ml H_2O, 60 ml ethanol) for later immunohistochemical or hematoxylin/eosin (H/E) staining.

For immunohistochemical staining, tissues underwent standard serial deparaffinization and rehydration. Some rehydrated samples underwent antigen retrieval (Shi et al., 1993) by microwave treatment at 88°C for 3 min in a 6 M urea solution before being put into blocking solutions. Rehydrated tissues were

incubated in blocking solution TBS-T-Blotto (Tris-buffered saline, pH 7.4, 0.2% Tween-20, 3% BSA, 10% non-fat dry milk) for one hour at room temperature or overnight at 4°C. Slides were rinsed in TBS-T and primary antibodies were applied (1:250-1:500 for anti-UpEcR A/B domain antibody, 1:500-1:1000 for anti-UpRXR A/B domain antibody, the same concentration of preimmune serum were applied as controls) for 1-2 hours in a humid and sealed environment at room temperature or overnight at 4°C. Slides were then washed in TBS-T five times, each time for 10 min. After the wash, secondary antibodies (1:500-1:800 HRP conjugated anti-rabbit antibody, Bio-Rad) were applied for 1-2 hours in a humid and sealed environment at room temperature or overnight at 4°C. DAB (3,3'-Diaminobenzidine tetrahydrochloride, Sigma-Aldrich, St. Louis, MO) was used as the substrate for the peroxidase reaction. The enzymatic reaction was stopped by rinsing the slides in TBS. Slides then underwent a series of dehydration steps and were mounted under a number one coverslip with Permount (Sigma-Aldrich).

For hematoxylin/eosin staining, the slides were dewaxed in a series of xylene/ethanol washes and then hydrated in distilled water. Tissues were stained with Harris hematoxylin (Fisher Scientific International Inc, Hampton, NH) for 2 min. The slides were rinsed in water. After the wash, the slides were dipped in 1% ammonium hydroxide and were immediately taken out and washed well with distilled water. The slides were then counterstained with eosin (10 ml of 0.1% eosin in ethanol, 90 ml of 95% ethanol, 700 µl of glacial acetic acid) for 15 to 20

sec. The slides were dehydrated in 95% ethanol (3X) then 100% ethanol (3X), with each change for three minutes. Slides were cleared in xylene and mounted with Permount. Stained slides were examined under a microscope (Olympus AH-2) using bright field or DIC optics. Images were captured by a coolSNAP digital camera or 35-mm film and processed by the MetaMorph imaging system (Universal Imaging Corporation, Downingtown, PA) and Adobe photoshop5.0 (Adobe Systems Incorporated, San Jose, CA).

2.6. Quantification of circulating ecdysteroid hormones by radioimmunoassay (RIA)

Hemolymph samples were thawed on ice. Samples (20-50 µl) were extracted with three volumes of methanol. The extractions were spun for 10 min at 4°C at the maximum speed at 16,000 g on a bench top microcentrifuge. The supernatants were transferred to clean tubes and evaporated under N_2 at room temperature. Samples were stored at -20°C for batch processing. 20-Hydroxyecdysone (20E, Sigma-Aldrich) and Ponasterone A (Pon A, Sigma-Aldrich) standards were aliquoted in a serial dilution from 8000 pg/tube to 10 pg/tube. To set up RIA experiments, samples and standards were processed at the same time with each assay. Samples were dissolved in 5 µl of dimethylsulfoxide (DMSO). ^{3}H-Pon A (0.005 µCi or 6000-7000 CPM [counts per minute], diluted with borate buffer from a 120.3 Ci/mmol source, PerkinElmer Life Science, Inc., Boston, MA) was added to the sample. Then either preimmune sera (from the same animal that produced the antibody) or antibody (raised against

thyroglobulin-conjugated ecdysteroids), and rabbit naïve sera (from other non-immunized animals) in borate buffer were added (0.1 M boric acid, 0.025 M sodium tetraborate, 0.075 M sodium chloride, adjust to pH 8.4 with boric acid). After two hours incubation at room temperature, saturated ammonium sulfate [$(NH_4)_2SO_4$] were added to the reactions to 50/50 (V/V) and incubated on ice for 15 minutes to precipitate the antibody and ecdysteroid complex. The reactions were then spun in a microcentrifuge for 10 min at 4°C. The pellets were washed with 100 µl 1:1 [borate buffer/$(NH_4)_2SO_4$] mixture and spun another 10 min. The pellets were then dissolved in 100 µl ddH_2O, and 1 ml of hi-ionic fluor (Packard Bioscience) was added to the mixture. The samples were then counted on scintillation counter (Tri-Carb® 2100 TR, Packard Bioscience). A standard curve was obtained when the precipitated CPM was plotted against the logarithm value of the amount of standard ecdysteroid in each tube. The amounts of ecdysteroid in unknown crab hemolymph samples were derived from the standard curve.

3. Results

3.1. Expression of UpEcR A/B domain and UpRXR A/B domain proteins

Figure 3A represents a Coomassie blue stained SDS-PAGE gel of the Ni-NTA purification of the induced UpEcR A/B domain protein. When the flowthrough fraction and wash fractions (Figure 3A, lanes 2-5) were compared to the elution fractions (Figure 3A, lanes 6-8) of the purification process, this one-step purification process removed most of the non-specific bound proteins (eg. proteins that do not have the 6xHis affinity tag). Proteins that migrated at the expected position (arrow) in the elution fractions were evident (Figure 3A, lanes 6-7, arrow).

The time course of expression in induction experiments also showed that a protein band corresponding to UpEcR A/B protein is present only after IPTG induction. As shown in a western blot in Figure 3B, a monoclonal antibody against the 6xHis tag (Qiagen) specifically recognizes a single protein band (arrow) at the expected migration position in the induced *E. coli* cell culture lysate (lanes 2, 3), and the Ni-NTA affinity purified protein (lane 4), but not in the uninduced culture cell lysate on a SDS-PAGE (lane 1).

In Figure 4, panel A shows a Coomassie blue stained SDS-PAGE of the Ni-NTA purification of induced UpRXR A/B domain protein; panel B shows the

western blot of the exact same SDS-PAGE using a monoclonal antibody against the 6xHis tag (Qiagen). As shown by an arrow, the antibody also recognized a single specific protein band that migrated at the expected position in the induced culture cell lysate (panel B, lane 3) and several elution fractions 7-9 (panel B, lanes 7, 8, 9). In the uninduced *E. coli* cell culture lysate (panel B, lane 2), the flowthrough fraction (panel B, lane 4) and wash fractions (panel B, lanes 2-9), no protein band positive to the antibody was detected.

3.2. Determination of specificity of Anti-UpEcR A/B and Anti-UpRXR A/B domain antibodies

E.coli expressed UpEcR A/B and UpRXR A/B domain proteins were column purified. The protein bands identified by western analysis containing the UpEcR A/B and UpRXR A/B proteins were cut from gels and used for the production of polyclonal antibodies in rabbits. The obtained polyclonal antibodies against the UpEcR A/B domain and the UpRXR A/B domain were validated by western blot and immunoprecipitation experiments. Antibodies were first tested against *E. coli* expressed crab UpEcR A/B and UpRXR A/B domain protein. Western blots showed that these antibodies were highly reactive to these *E. coli* expressed crab proteins (data not shown). Since these antibodies were raised against these bacterially-expressed recombinant proteins, this validation alone is still not evidence that the antibodies could recognize full-length proteins in crab tissues. Immunoprecipitation experiments were then used to demonstrate that these

antibodies also specifically recognize reticulocyte lysate-expressed full-length crab receptor proteins.

In Figure 5, panel A represents an autoradiograph of an SDS-PAGE of TNT® (Promega) reticulocyte lysate synthesized full length UpEcR and UpRXR variant proteins (Wu et al., submitted; see Chapter II). The prominent bands represent the expressed full-length crab receptor proteins. These protein bands were present in the autoradiograph only when the cloned expression plasmids of UpEcR and UpRXR variants were added to the TNT® systems, representing the bona fide crab receptors. Panel B represents an autoradiograph of an SDS-PAGE of the immunoprecipitate of TNT® synthesized crab receptor proteins using the obtained UpRXR A/B domain-specific antibody. All four UpRXR isoforms were precipitated by the UpRXR A/B domain antibody, suggesting that the UpRXR A/B antibody indeed is able to specifically recognize all four UpRXR isoforms, which contain the same A/B domain. Panel C represents an autoradiograph of an SDS-PAGE of an immunoprecipitation experiment using the UpEcR A/B domain antibody against TNT® synthesized full length UpEcR protein. Only one protein band corresponding to UpEcR A/B was immunoprecipitated, indicating that the UpEcR A/B domain-specific antibody is effective also. Immunoprecipitation experiments using both preimmune sera of UpEcR A/B and UpRXR A/b antibodies did not result in precipitation (data not shown).

UpEcR and UpRXR are both members of nuclear receptor superfamily.

Family members share amino acid sequence similarity not only within each subfamily but also with each other. Although the A/B domain is not a conserved region, the construction of UpEcR and UpRXR both included cloning into a pQE vector that has the same 6xHis tag sequences, and that tag can be recognized by a monoclonal antibody RGS-His antibody (Qiagen). This could produce a potential problem if the obtained polyclonal antibodies are cross-reacting with each other due to this similarity. Because UpEcR and UpRXR can form heterodimers (see Chapter I and II), antibodies that recognize both UpEcR and UpRXR simultaneously are not suited for the studies concerning the cellular and tissue distribution of these receptors. Experiments were then conducted to test if these antibodies cross-react with each other. As shown in Figure 6, panel A represents a western blot using monoclonal RGS-His antibody (Qiagen) against the 6xHis tag that is present in both UpEcR A/B and UpRXR A/B domain proteins. Both proteins were detected by the antibody. From the intensity of the exposed film, the UpRXR A/B protein seems to have more protein loaded than UpEcR A/B protein. In panel B, Anti-UpEcR A/B domain antibody was used to probe both UpEcR A/B and UpRXR A/B proteins. On extended exposure, only UpEcR A/B was shown strongly reacting to the UpEcR A/B domain specific antibody, whereas UpRXR A/B was not able to react with UpEcR A/B antibody. In a reciprocal experiment, Anti-UpRXR A/B antibody was also not able to recognize UpEcR protein (data not shown).

3.3. Expression of UpEcR and UpRXR in regenerating limb buds

Antibodies against UpEcR and UpRXR A/B domain proteins were used for immunohistochemical studies at various stages of limb bud growth throughout the regeneration process. Five days after autotomy (A+5), when the limb bud is begining basal growth, epidermal cells underlining the cuticular sac show UpEcR A/B domain antibody nuclear staining (Figure 7A, arrow). A few connective tissue cells inside the coxa also show weak UpEcR staining (Figure 7A, arrow head). The control limb section stained with preimmune sera shows no staining (Figure 7C). Near adjacent sections of the same limb were also stained with antibody against UpRXR A/B domain protein. The staining pattern is very similar to that of UpEcR. Epidermal cells underlining the cuticular sac show strong nuclear staining with UpRXR A/B antibody (Figure 7B, arrow). The connective tissue cells inside the coxa, however, show more cells that are immunoreactive to UpRXR A/B antibody than to UpEcR A/B antibody (Figure 7B, arrow head). The preimmune UpRXR control also shows no staining (Figure 7D).

During early proecdysial growth, when the circulating ecdysteroid titers are low (8.5 pg/μl), regenerating limbs continues to show epidermal cell nuclear staining with UpEcR A/B antibody (Figure 8A, arrow), as well as strong epidermal nuclear staining with UpRXR A/B antibody (Figure 8B, arrow). Other cell types such as blood cells and other connective tissue cells inside the developing limb also show UpEcR and UpRXR staining. Their respective

preimmune sera controls show no staining at all (Figure 8C, D).

At a mid-proecdysial growth stage, when the crab's limb bud size is rapidly growing because of protein synthesis and water uptake (Hopkins, 1989), and the crab is at D_0 molting stage with the circulating ecdysteroid titer beginning to rise at 32.8 pg/μl, regenerating limbs show strong UpEcR A/B antibody staining with muscle cell nuclei (Figure 9A, arrow head), and connective tissue cell nuclear staining (Figure 9B, arrow). The adjacent or near adjacent limb sections stained with UpRXR A/B antibody show staining in connective tissue cells (Figure 9C, arrow) and muscle cell nuclei (Figure 9C, arrow head), but more epidermal cell nuclei show UpRXR staining (Figure 9D, arrow) than with UpEcR A/B antibody. Their respective preimmune control sera do not produce staining (data not shown).

At a later proecdysial stage, when the limb bud growth has slowed down, and the circulating ecdysteroid has decreased to 2.9 pg/μl, regenerating limbs again show wide spread UpEcR nuclear staining in epidermal cells (Figure 10A, arrow). The limb sections also show very similar epidermal nuclei staining pattern with UpRXR A/B antibody (Figure 10B, arrow). Other cells types such as blood cells, muscle cells, and other connective tissue cells also show UpEcR and UpRXR nuclear staining. Their respective preimmune sera do not show nuclei staining at all (Figure 10C, D). Interestingly, at proecdysial stage, cells usually do not undergo mitosis, the increase in the size of limb bud during this time is due to

increases in cell size (Adiyodi, 1972; Holland and Skinner, 1976). However, as shown in Figure 10E, mitotic figures are also observed at this stage. This same limb bud was also showed expression of UpEcR and UpRXR (Figure 10).

Initial immunostaining using paraformaldehyde fixation did not preserve the tissues well, and microwave antigen retrieval technique also changed the morphology of treated tissues (data not shown). These procedures were not used in later studies.

4. Discussion

The experiments described in this chapter examined the expression and distribution of UpEcR and UpRXR in regenerating limbs by immunohistochemistry studies, and their relation to circulating ecdysteroid levels monitored by RIA. 6xHis tagged UpEcR A/B and UpRXR A/B domain epitopes expressed in *E. coli* expression systems were developed to generate polyclonal antibodies. Previous experiments using *Drosophila*, *Manduca* and tick *Amblyomma americanum* antibodies raised against their respective receptor proteins were unsuccessful in obtaining nuclear staining in crab tissue sections, and/or in western blot and/or immunoprecipitation experiments; therefore, development of homologous antibody probes was required. The sensitivity and reliability of the antibodies were first analyzed. *E. coli* systems have been successfully used for eukaryotic protein expression for a variety of purposes including antibody production (Ausubel et al., 2001), but protein expression still is not a exact science. Foreign eukaryotic proteins are targets for proteolytic degradation inside host *E. coli* cells (Lee et al., 1984). To avoid such problems, inducible expression systems are usually used, taking advantage of a strong prokaryotic promotor-operator (T5-*lac*) which allows induction of foreign eukaryotic protein expression by IPTG. The purified recombinant fusion proteins also may not fold correctly, which may cause the protein to lose part or all of its biological activity (Lilie et al., 1998). To obtain UpEcR and UpRXR proteins for antibody production, I choose the QIAexpression™ expression system. This

expression system is an IPTG induceable expression system. It has a short leader peptide sequence including the 6xHis tag, which allows easy affinity chromatography purification of the fusion UpEcR and UpRXR A/B domain proteins.

As shown in the Results section, the 6xHis tagged UpEcR and UpRXR fusion proteins are only present after IPTG induction (Figure 3B; Figure 4, lanes 2, 3). They also have molecular weights as estimated and are specifically recognized by anti-6xHis tag antibody. These *E. coli* expressed proteins were then used to generate anti-UpEcR and anti-UpRXR anti-sera. The obtained anti-sera tested positive against the *E. coli* expressed UpEcR and UpRXR A/B domain proteins. These anti-sera also immunoprecipitated *in vitro* synthesized full length UpEcR and UpRXR variants made in reticulocyte lysates, showing that these antibodies were highly specific (Figure 5). Western blots also showed that anti-sera against UpEcR A/B did not crossreact with UpRXR, and *vice versa*.

Immunostaining of UpEcR and UpRXR was observed in epidermis throughout the limb regeneration process. The predominant tissue and cell types stained with UpEcR and UpRXR are the epidermal cells, which is in line with the cuticle secretion function of epidermal cells (Riddiford, 1994). Staining of muscle cell nuclei and other connective tissues nuclei suggest that UpEcR and UpRXR are also involved in other physiological events as well (Hegstrom et al., 1998).

Immunostaining patterns of UpEcR and UpRXR suggest that these nuclear receptor heterodimer partners are usually expressed at the same time and in the same tissue and cell types, which is expected given their hypothesized function as a heterodimer pair involved in gene regulation in response to hormone signaling. Overall, however, UpRXR seems to be more widely expressed than UpEcR. In some adjacent sections, UpEcR staining was shown to have a different tissue and cell staining pattern than UpRXR (connective tissue cells in Figure 7, arrowhead, and epidermal cells in Figure 9, circles). This observation suggests that UpRXR might have a dimerization partner other than UpEcR. In *Drosophila melanogaster*, the immunostaining patterns of EcR and RXR also do not always co-localize (Talbot et al., 1993). Recently, in *Drosophila*, an alternative ecdysteroid signaling pathway mediated by USP and DHR38 responsive to several ecdysteroids independent of EcR has been discovered (Baker et al., 2003). Whether UpRXR can function in an alternative pathway in *Uca* remains to be investigated.

When the immunostaining patterns of UpEcR and UpRXR in the regenerating limbs were compared to the circulating ecdysteroid titers, no apparent correlation between the changing titer of total ecdysteroids and the staining pattern was observed. There are several possible explanations for this lack of correlation. One possibility might be that the expression of UpEcR and UpRXR are not under the direct control of ecdysteroids. The signal transmission from ecdysteroids to target genes through the UpEcR and UpRXR receptors are

not directly dependent on the relative expression level of UpEcR and UpRXR. It also needs to be noted that in this study, RIA was only able to measure the total ecdysteroid titer in the circulating hemolymph. There are at least four ecdysteroids present in the hemolymph, which change in their ratios (Hopkins, 1992). It is possible that a specific ecdsyteroid might be more directly correlated to the expression level of UpEcR and UpRXR or to isoforms of the proteins not recognized by these polyclonal antibodies. In insects, the expression of EcR and USP also do not always show apparent quantitative correlation with the circulating ecdysteroid titers. Complex physiological activities are observed in response to a common ecdysteroid signaling through EcR receptor isoforms or alternative signaling pathway (see Chapter II for more details).

Overall, this chapter describes a pilot project to study the expression of UpEcR and UpRXR by immunohistochemistry. Initial results suggest that both UpEcR and UpRXR are widely expressed in the regenerating limbs throughout the regeneration process. The expression patterns suggest that UpEcR and UpRXR are often expressed in the same tissues and cells, and are not correlated to overall levels of circulating ecdysteroid. This corroborates earlier studies examing mRNA distributions (Chung et al., 1998b). If isoform-specific antibodies were available, future studies could focus on the UpRXR and UpEcR isoform expression and distribution and their relationship to each individual circulating ecdysteroid. RNA interference or antibody disruption experiments of UpEcR and UpRXR on regenerating limb buds could also be performed to study

the function of these receptors in regenerating limb buds, and how would they react to changes in circulating ecdysteroid titer.

Figure Legends

Figure 1.

Expressed UpEcR A/B sequence (121 amino acids). The coding sequence of UpEcR A/B domain was cloned into the pQE32 vector (Qiagen), directly down stream of the leader sequence including the 6xHis tag. The expected molecular weight of the expressed fusion protein is 14.8 KDa (from Expasy program at http://www.expasy.ch/).

Figure 2.

Expressed RXR-A/B sequence (96 amino acids). The coding sequence for UpRXR A/B domain was cloned into pQE31 vector (Qiagen), directly down stream of the the leader sequence including the 6xHis tag. The expected molecular weight of expressed fusion protein is 11.7 KDa (from Expasy program at http://www.expasy.ch/).

Figure 3.

Isolation of *E.coli* expressed UpEcR A/B domain protein and antibody specificity determination by western blot. Panel A: One µl broad range protein size markers (Bio-Rad) were dissolved in 9 µl 1X sample buffer, five µl of each isolation fraction was dissolved in 5 µl 2X sample buffer. Samples and markers were boiled for 5 min and separated by 12.5% Tris-Tricine SDS-PAGE. Gels were run about 40 min at 200 V constant voltage. Gels were stained in

Coomassie blue, mounted and dried on a filter paper. Panel B: Western blot using anti-6xHis antibody against 6xHis tagged UpEcR A/B fusion protein induction and purification experiment. Samples of uninduced or induced *E. coli* culture containing the expression vector for UpEcR A/B were extracted in SDS-sample buffer. Similar amount of total proteins from these extractions were loaded on a Tris-tricine SDS-PAGE gel. Purified UpEcR A/B domain protein was also loaded on the same gel. The proteins were transferred to a nitro-cellulose membrane, and the fusion proteins were detected by anti-6xHis monoclonal antibody as described in the Materials and Methods section.

Figure 4.

SDS-PAGE gel and western blot using anti-6xHis antibody against 6xHis tagged UpRXR A/B fusion protein induction and purification experiment. Panel A represents a Coomassie blue stained Tris-tricine SDS-PAGE of the Ni-NTA purification of over-expressed UpRXR A/B domain protein. The running conditions were the same as given in Figure 3. Panel B represents a western blot detection by anti-6xHis monoclonal antibody of a parallel gel. Western blot and antibody detection were the same as in Figure 3 and described in the Materials and Methods section.

Figure 5.

Immunoprecipitation of UpEcR and UpRXR by UpEcR A/B and UpRXR A/B polyclonal antibodies. Panel A represents an autoradiograph of a SDS-PAGE gel

of TNT *in vitro* synthesized [^{35}S]-labeled UpEcR and UpRXR variant proteins. Panel B represents an autoradiograph of a SDS-PAGE gel of the immunoprecipitation of UpRXR variant proteins by anti-UpRXR A/B domain polyclonal antibody. Panel C represents an autoradiograph of a SDS-PAGE gel of the immuno-precipitation of UpEcR protein by anti-UpEcR A/B domain polyclonal antibody.

Figure 6.

Western blot demonstrating UpEcR A/B domain polyclonal antibody specificity. Panel A represents a western blot using monoclonal anti-6xHis antibody against 6xhis tagged UpEcR A/B and UpRXR A/B fusion proteins. Both proteins are detected. Panel B represents a western blot using UpEcR A/B domain antibody with a parallel SDS-PAGE gel. SDS-PAGE and western blots were performed as described in the Materials and Methods section.

Figure 7.

Immunohistochemistry studies of the expression of UpEcR and UpRXR in regenerating limbs, five days after limb loss. The ecdysteroid titer was measured at 7.2 pg/μl. Bar = 20 μm. Panel A represents a section stained with anti-UpEcR A/B antibody. Arrow shows the epidermal cell nuclei stained with UpEcR A/B antibody. Arrowhead shows connective tissue cell nuclei also stained with UpEcR A/B antibody. Panel C represents a control section for A stained with preimmune sera. Panel B represents a section stained with anti-UpRXR A/B

antibody. Arrow shows the epidermal cell nuclei stained with UpRXR A/B antibody. Arrowhead shows connective tissue cell nuclei also stained with UpRXR A/B antibody. Panel D represents a control section for B stained with preimmune sera. CS, cuticular sac.

Figure 8.

Immunohistochemistry studies of the expression of UpEcR and UpRXR in regenerating limb buds, early proecdysial growth stage with R3 = 10.2, ER = 17.8. The ecdysteroid titer was at 8.5 pg/μl. Bar = 20 μm. Panel A represents a section stained with anti-UpEcR A/B antibody. Panel C represents a control section for A stained with preimmune sera. Panel B represents a section stained with anti-UpRXR A/B antibody. Panel D represents a control section for B stained with preimmune sera. Arrows pointed to stained epidermal cell nuclei.

Figure 9.

Immunohistochemistry studies of the expression of UpEcR and UpRXR in regenerating limb buds, at mid-proecdysial growth stage with R3 = 15.1, ER = 59.4. The ecdysteroid titer was 32.8 pg/μl. Bar = 20 μm. Panels A, B represent sections stained with anti-UpEcR A/B antibody. Panels C, D represent sections stained with anti-UpRXR A/B antibody. Large arrows show the connective tissue cell nuclei staining. Middle arrow shows the epidermal cell nuclei staining. Arrowhead shows the muscle nuclei staining. Circles show the difference of epidermal staining with UpEcR A/B antibody and UpRXR A/B antibody.

Figure 10.

Immunohistochemistry studies of the expression of UpEcR and UpRXR in regenerating limb buds, at a late proecdysial growth stage with R3 = 18.1, ER = 35. The ecdysteroid titer was 2.9 pg/μl. Bar = 20 μm. Panel A represents a section stained with anti-UpEcR A/B antibody. Panel C represents a control section for A stained with preimmune sera. Panel B represents a section stained with anti-UpRXR A/B antibody. Panel D represents a control section for B stained with preimmune sera. Panel E represents an H&E-stained section showing mitotic figures. Arrows point to stained epidermal cell nuclei. Arrowheads point to mitotic figures.

MRGSHHHHHHGIR	6xHis leader sequence
MAKVLATAVRDGMFVLGSGVATLNLSTMGDESCSEVS SSSPLTSPGALSPPALVSVGVSVGMSPPTSLASSDIG EVDLDFWDLDLNSPSPPHGMASVASTNALLLNPRAVA SPSDTSSLSG	EcR A/B domain
YPGVDLQPSLIS	Sequence on pQE32 vector prior to stop codon

Figure 1

MRGSHHHHHHTDP	6xHis leader sequence
MIMIKKEKPVMSVSSIIHGSQQRAWTPGLDIGMSGSLD RQSPLSVAPDTVSLLSPAPSFSTANGGPASPSISTPPF TIGSSNTTGLSTSPSQYPPS	Expressed RXR-A/B region
KLN	Sequence on pQE31 vector prior to stop codon

Figure 2

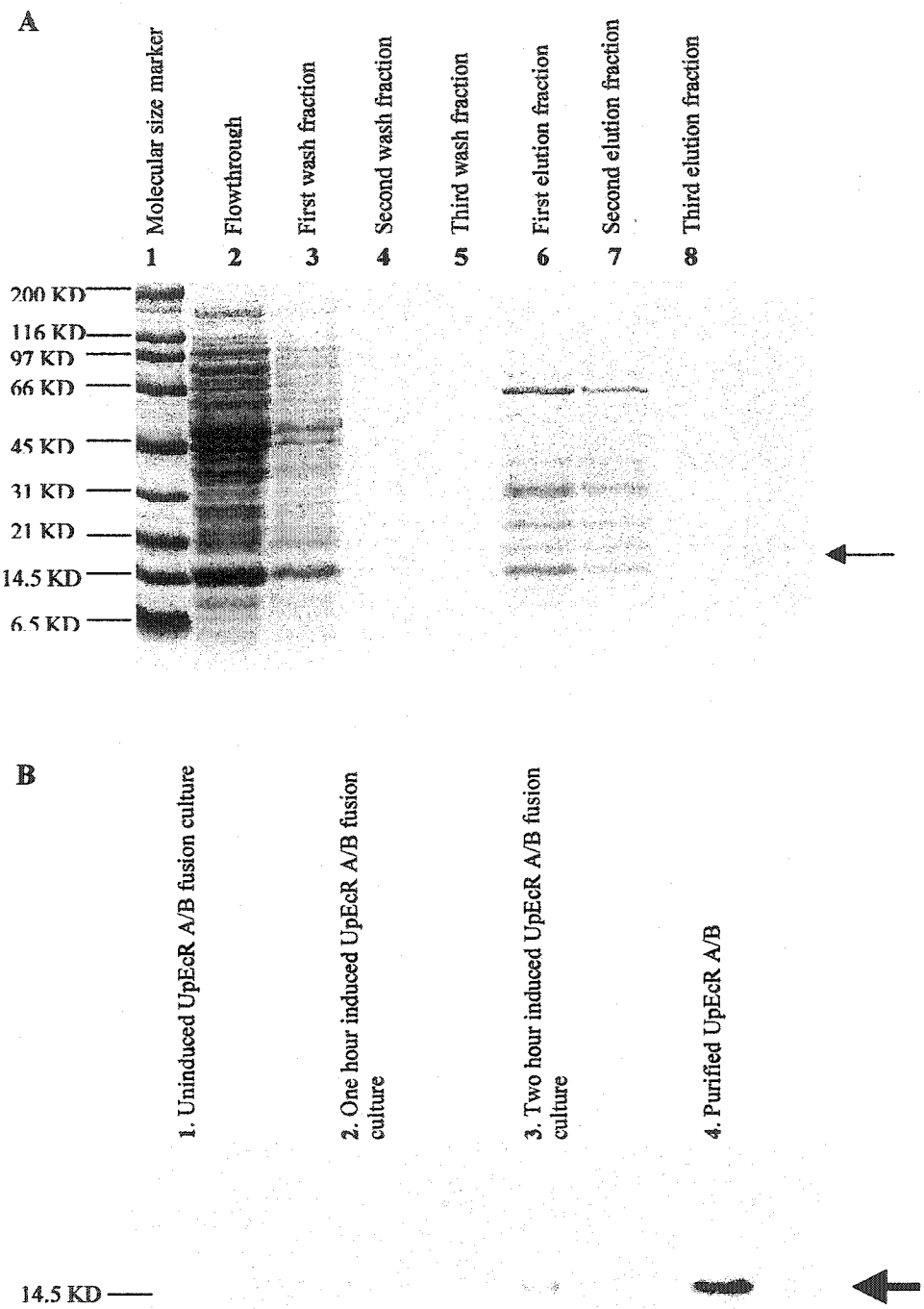
A
1 Molecular size marker
2 Flowthrough
3 First wash fraction
4 Second wash fraction
5 Third wash fraction
6 First elution fraction
7 Second elution fraction
8 Third elution fraction
200 KD
116 KD
97 KD
66 KD
45 KD
31 KD
21 KD
14.5 KD
6.5 KD
B
1. Uninduced UpEcR A/B fusion culture
2. One hour induced UpEcR A/B fusion culture
3. Two hour induced UpEcR A/B fusion culture
4. Purified UpEcR A/B
14.5 KD

Figure 3

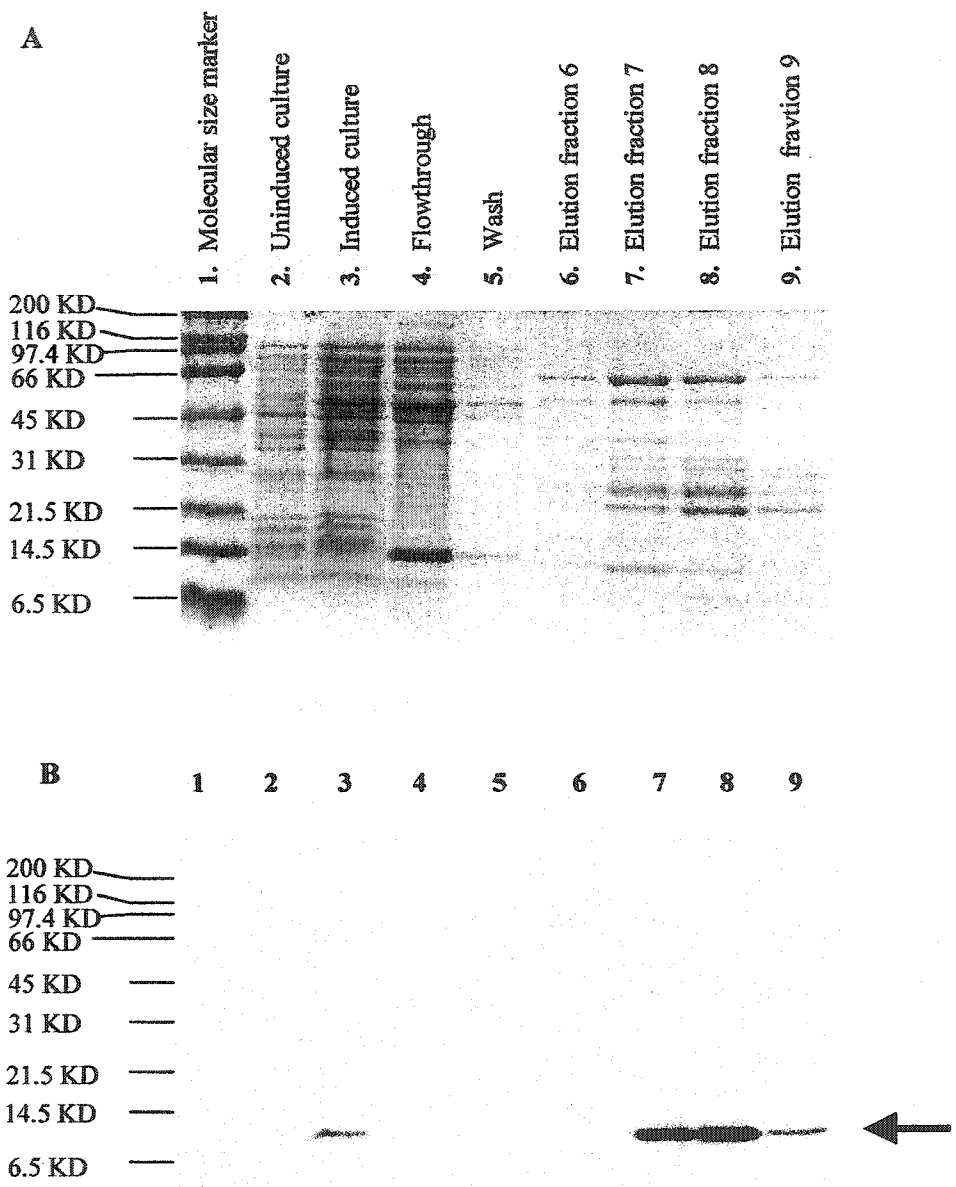
A
1. Molecular size marker
2. Uninduced culture
3. Induced culture
4. Flowthrough
5. Wash
6. Elution fraction 6
7. Elution fraction 7
8. Elution fraction 8
9. Elution fravtion 9
200 KD
116 KD
97.4 KD
66 KD
45 KD
31 KD
21.5 KD
14.5 KD
6.5 KD
B
1 2 3 4 5 6 7 8 9
200 KD
116 KD
97.4 KD
66 KD
45 KD
31 KD
21.5 KD
14.5 KD
6.5 KD

Figure 4

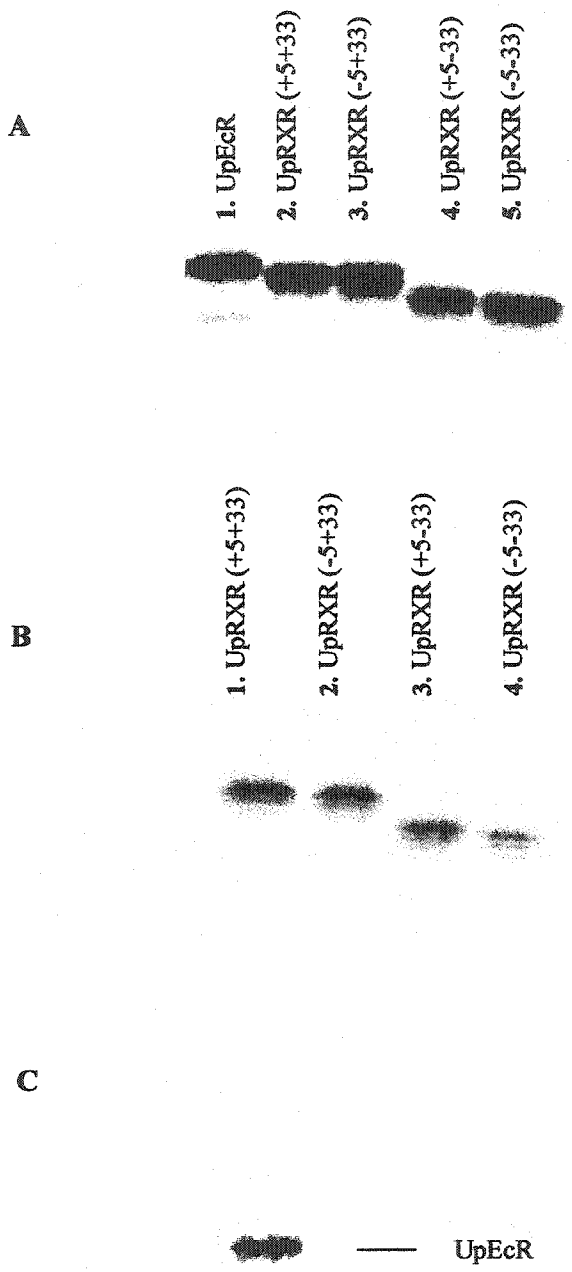
A
1. UpEcR
2. UpRXR (+5+33)
3. UpRXR (-5+33)
4. UpRXR (+5-33)
5. UpRXR (-5-33)
B
1. UpRXR (+5+33)
2. UpRXR (-5+33)
3. UpRXR (+5-33)
4. UpRXR (-5-33)
C
UpEcR

Figure 5

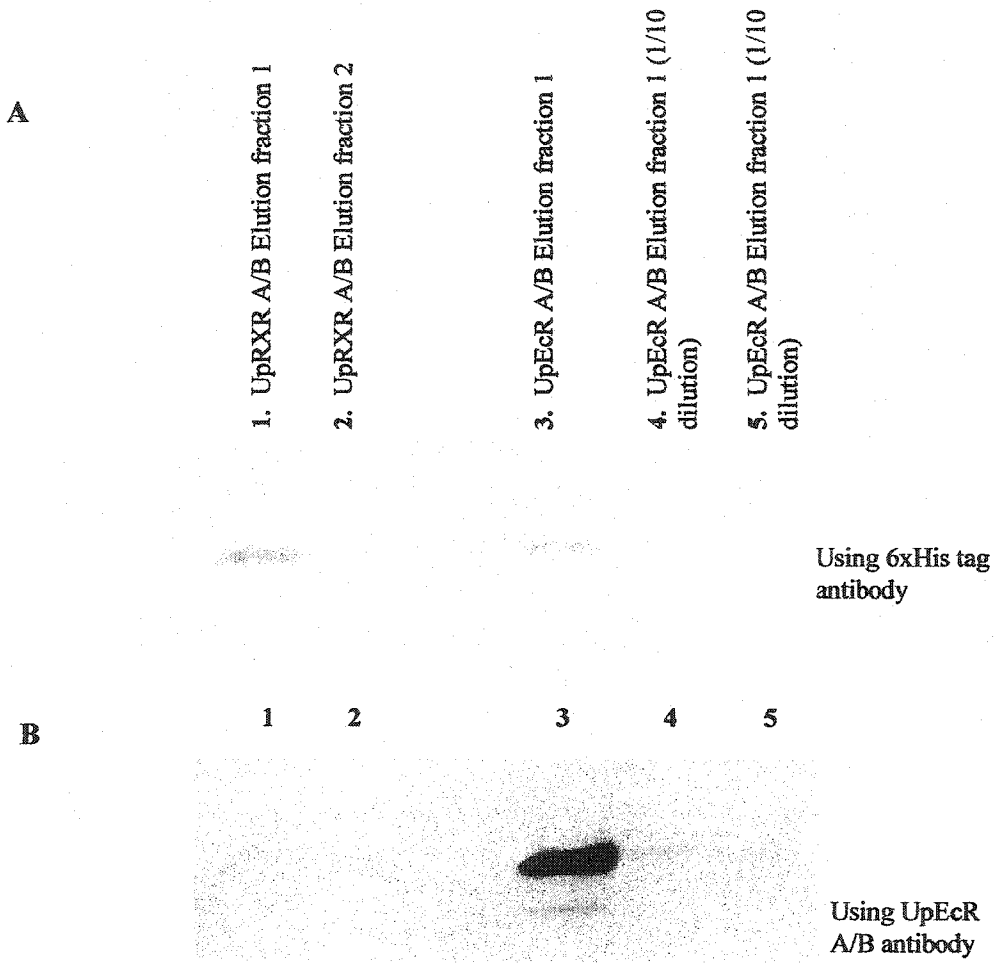
A
1. UpRXR A/B Elution fraction 1
2. UpRXR A/B Elution fraction 2
3. UpEcR A/B Elution fraction 1
4. UpEcR A/B Elution fraction 1 (1/10 dilution)
5. UpEcR A/B Elution fraction 1 (1/10 dilution)
Using 6xHis tag antibody
B
1
2
3
4
5
Using UpEcR A/B antibody

Figure 6

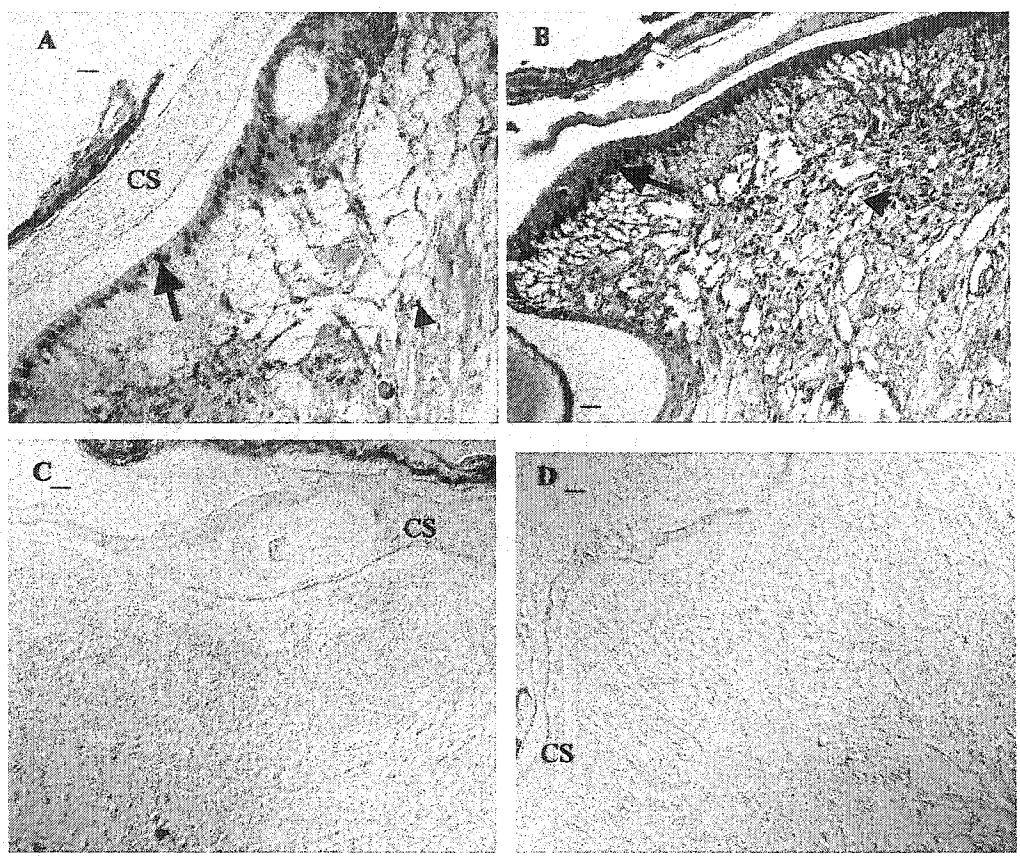

Figure 7

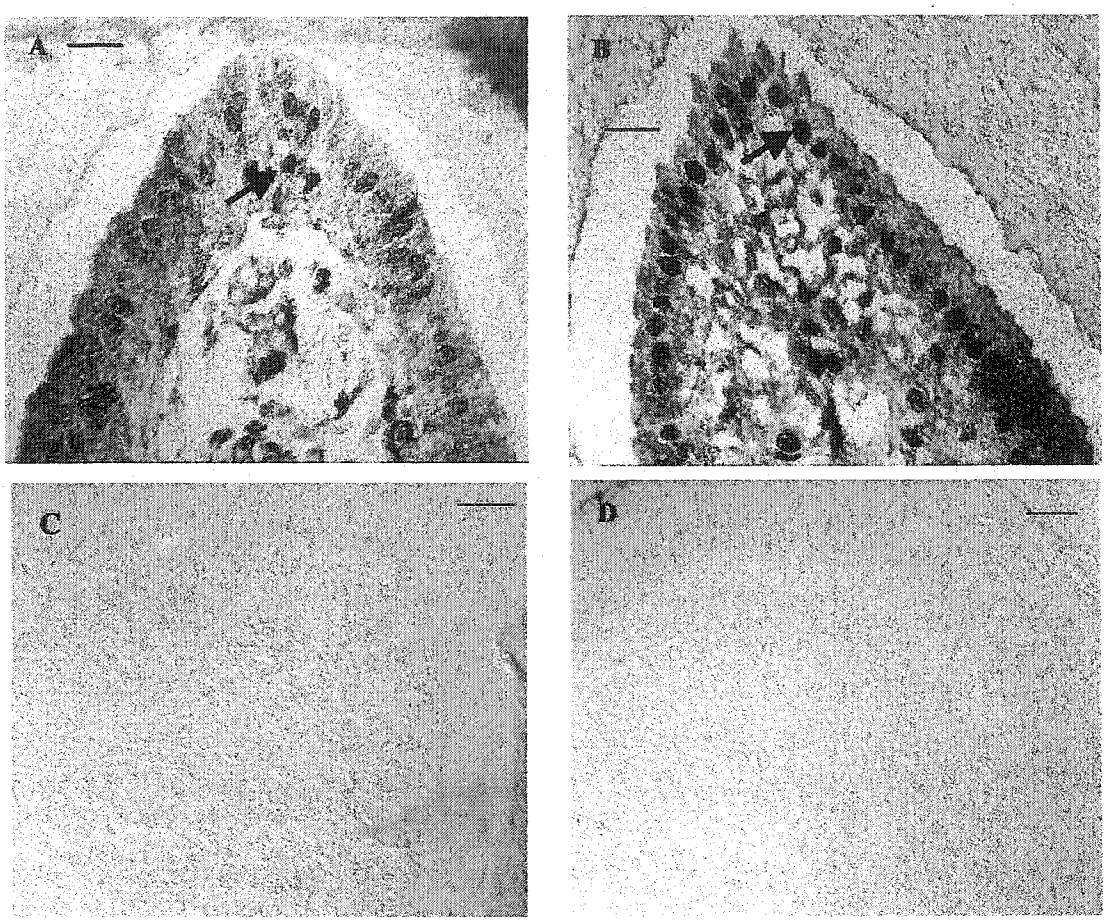

Figure 8

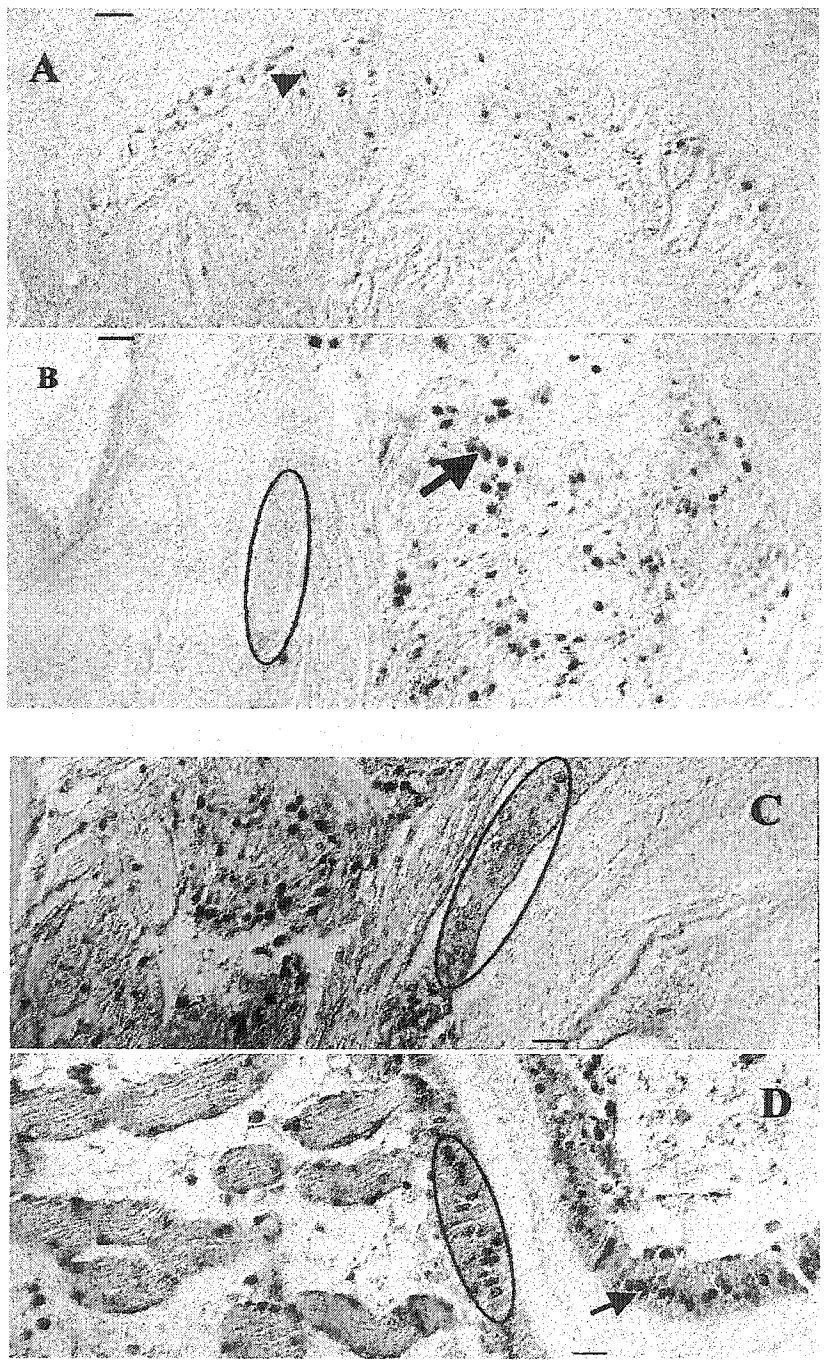

Figure 9

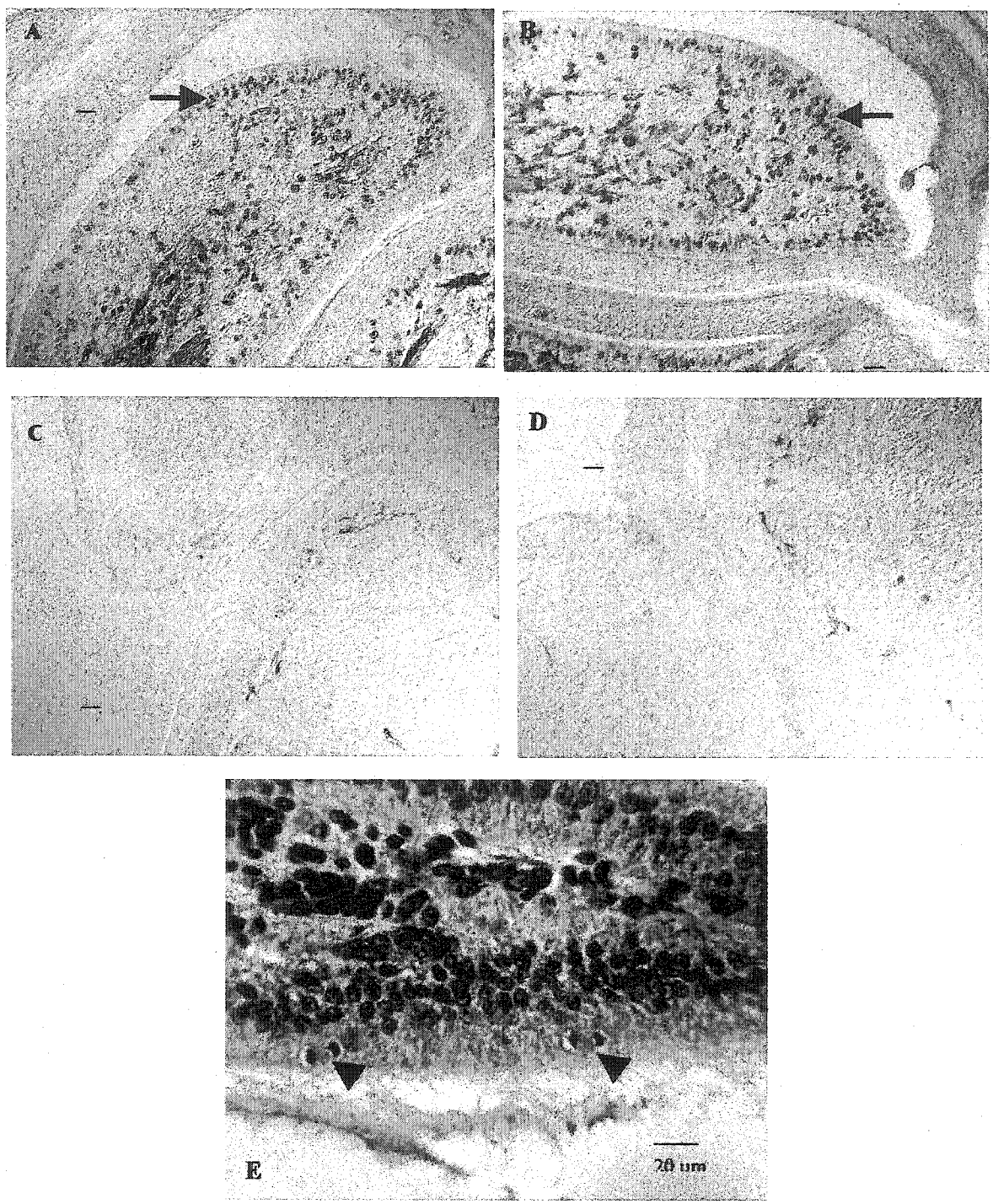

Figure 10

Literature cited:

Adiyodi, R. D. 1972. Wound healing and regeneration in the crab, *Paratelphusa hydrodromus*. Int. Rev. Cytol. 32, 257-289.

Andres, A.J., Thummel, C.S. 1992. Hormones, puffs and flies: the molecular control of metamorphosis by ecdysone. Trends Genet 8, 132-138.

Antoniewski, C., Laval, M., Lepesant, J. A. 1993. Structural features critical to the activity of an ecdysone receptor binding site. Insect Biochem Mol Biol. 23, 105-114.

Antoniewski, C., Mugat, B., Delbac, F., Lepesant, J. A. 1996. Direct repeats bind the EcR/USP receptor and mediate ecdysteroid responses in *Drosophila melanogaster*. Mol Cell Biol. 16, 2977-2986.

Antoniewski, C., O'Grady, M. S., Edmondson, R. G., Lassieur, S. M., Benes, H. 1995. Characterization of an EcR/USP heterodimer target site that mediates ecdysone responsiveness of the *Drosophila* Lsp-2 gene. Mol Gen Genet 249, 545-556.

Aranda, A., Pascual., A. 2001. Nuclear hormone receptors and gene expression. Physiol Rev. 81, 1269-1304.

Ashburner, M., Chihara, C., Meltzer, P., Richards, G. 1974. On the temporal control of puffing activity in polytene chromosomes. Cold Spring Harb Symp Quant Biol. 38, 655-662.

Auerbach, S. S., Ramsden, R., Stoner, M. A., Verlinde, C., Hassett, C., Omiecinski, C. J. 2003. Alternatively spliced isoforms of the human constitutive androstane receptor. Nucleic Acids Res. 15, 3194-3207.

Ausubel, F. M., Brent, R., Kingston, R. E., Moore, D. D., Seidman, J. G., Smith, J. A., Struhl, K. 2001. Current Protocols in Molecular Biology. Vol 3. Chapter 16. "Protein expression". John Wiley& Sons, Inc.

Bai, J., Uehara, Y., Montell, D.J. 2000. Regulation of invasive cell behavior by Taiman, a *Drosophila* protein related to AIB1, a steroid receptor coactivator amplified in breast cancer. Cell 103, 1047–1058.

Baker, K. D., Shewchuk, L. M., Kozlova, T., Makishima, M., Hassell, A., Wisely, B., Caravella, J. A., Lambert, M. H., Reinking, J. L., Krause, H., Thummel, C. S., Willson, T. M., Mangelsdorf, D. J. 2003. The Drosophila orphan nuclear receptor DHR38 mediates an atypical ecdysteroid signaling pathway. Cell. 13, 731-742.

Beato, M., Chalepakis, G., Schauer, M., Slater, E.P. 1989. DNA regulatory elements for steroid hormones. J Steroid Biochem. 32, 737-747.

Beato, M., Klug, J. 2000. Steroid hormone receptors: an update. Hum Reprod Update. 6, 225-236.

Beckett, B.R., Petkovich, M. 1999. Evolutionary conservation in retinoid signalling and metabolism. Am. Zool. 39, 783–795.

Beckstead, R., Ortiz, J.A., Sanchez, C., Prokopenko, S.N., Chambon, P., Losson, R., Bellen, H.J. 2001. Bonus, a *Drosophila* homolog of TIF1 proteins, interacts with nuclear receptors and can inhibit betaFTZ-F1-dependent transcription. Mol. Cell. 7, 753–765.

Bender, M., Imam, F.B., Talbot, W.S., Ganetzky, B., Hogness, D.S. 1997. *Drosophila* ecdysone receptor mutations reveal functional differences among receptor isoforms. Cell 91, 777–788.

Bevan, C.L., Hoare, S., Claessens, F., Heery, D.M., Parker, M.G. 1999. The AF1 and AF2 domains of the androgen receptor interact with distinct regions of SRC1. Mol Cell Biol. 19, 8383-8392.

Billas, I.M., Moulinier, L., Rochel, N., Moras, D. 2001. Crystal structure of the ligand binding domain of the ultraspiracle protein USP, the ortholog of RXRs in insects. J. Biol. Chem. 276, 7465–7474.

Bliss, D.E. 1956. Neurosecretion and the control of growth in a decapod crustacean. In: Wingstrand, K.G. (Ed.), Bertil Hanstrom. Zoological Papers in Honour of His Sixty-Fifth Birthday. Zoological Institute, Lund, pp. 56–75.

Bliss, D. E. 1960. Autotomy and regeneration. Waterman, T. H. (ed): "The Physiology of Crustacea." New York: Academic Press. Vol 1, pp 561-589.

Bliss, D.E., Hopkins, P.M. 1974. Bioassay and characterization of crustacean limb growth-controlling factors. In: Neurosecretion—The Final Neuroendocrine Pathway, VI International Symposium Neurosecretion, 1973. Springer, New York, pp. 104–114.

Bonneton, F., Zelus, D., Iwema, T., Robinson-Rechavi, M., Laudet, V. 2003. Rapid Divergence of the Ecdysone Receptor in Diptera and Lepidoptera Suggests Coevolution Between ECR and USP-RXR. Mol Biol Evol. 20, 541-553.

Borst, D.W., Laufer, H., Landau, M., Chang, E.S., Hertz, W.A., Baker, F.C., Schooley, D.A. 1987. Methyl farnesoate and its role in crustacean reproduction and development. Insect Biochem. 17, 1123–1127.

Brodu, V., Mugat, B., Roignant, J.Y., Lepesant, J.A., Antoniewski, C. (1999). Dual requirement for the EcR/USP nuclear receptor and the dGATAb factor in an ecdysone response in *Drosophila melanogaster*. Mol Cell Biol. 19, 5732-5742.

Burtis, K.C., Thummel, C.S., Jones, C.W., Karim, F.D., Hogness, D.S. 1990. The *Drosophila* 74EF early puff contains E74, a complex ecdysone-inducible gene that encodes two ets-related proteins. Cell 61, 85-99.

Carney, G.E., Bender, M. 2000. The *Drosophila* ecdysone receptor (EcR) gene is required maternally for normal oogenesis. Genetics 154, 1203–1211.

Castelein, H., Janssen, A., Declercq, P. E., Baes, M. 1996. Sequence requirements for high affinity retinoid X receptor-alpha homodimer binding. Mol Cell Endocrinol. 119, 11-20.

Champlin, D.T., Truman, J.W. 1998. Ecdysteroids govern two phases of eye development during metamorphosis of the moth, *Manduca sexta*. Development 125, 2653–2664.

Chang, E.S., Sage, B.A., O'Connor, J.D. 1976. The qualitative and quantitative determinations of ecdysones in tissues of the crab, *Pachygrapsus crassipes*, following molt induction. Gen Comp Endocrinol. 30, 21-33.

Chang, E. S. 1989. Endocrine regulation of molting in Crustacea. Rev. Aquat. Sci. 1, 131–157.

Chen, D. G., Ma, H., Hong, H., Koh, S.S., Huang, S.M., Schurter, B.T., Aswad, D.W., and Stallup, M.R. 1999. Regulation of transcription by a protein methyltransferase. Science 284, 2174-2177.

Cherbas, L., Lee, K., Cherbas, P. 1991. Identification of ecdysone response elements by analysis of the *Drosophila* Eip28/29 gene. Genes Dev 5, 120-131.

Cherbas, L., Hu, X., Zhimulev, I., Belyaeva, E., Cherbas, P. 2003. EcR isoforms in Drosophila: testing tissue-specific requirements by targeted blockade and rescue. Development. 130, 271-284.

Chung, A.C.-K., Durica, D.S., Clifton, S.W., Roe, B.A., Hopkins, P.M. 1998a. Cloning of crustacean EcR and RXR gene homologs and elevation of RXR mRNA by retinoic acid. Mol. Cell Endocrinol. 139, 209–227.

Chung, A.C.-K., Durica, D.S., Hopkins, P.M. 1998b. Tissue-specific patterns and steady-state concentrations of ecdysteroid receptor and retinoid-X receptor mRNA during the molt cycle of the fiddler crab, *Uca pugilator*. Gen. Comp. Endocrinol. 109, 375–389.

Clayton, G.M., Peak-Chew, S.Y., Evans, R.M., Schwabe, J.W.R. 2001. The structure of the ultraspiracle ligand-binding domain reveals a nuclear receptor locked in an inactive conformation. Proc. Natl. Acad. Sci. USA 98, 1549–1554.

Clever, U. 1964. Actinomycin and puromycin: Effects on sequential gene activation by ecdysone. Science 146, 794-795.

Crispi, S., Giordano, E., D'Avino, P. P., Furia, M. 1998. Cross-talking among Drosophila nuclear receptors at the promiscuous response element of the ng-1 and ng-2 intermolt genes. J Mol Biol. 275, 561-574.

Danielson, P. S., White, R., Lees, J. A., Parker, M. G. 1992. Identification of a conserved region reguired for hormon dependent transcriptional activation by steroid hormone receptors. EMBO J. 11, 1025-1033.

Darimont, B.D., Wagner, R.L., Apriletti, J.W., Stallcup, M.R., Kushner, P.J., Baxter, J.D., Fletterick, R.J., Yamamoto, K.R 1998. Structure and specificity of nuclear receptor-coactivator interactions. Genes Dev. 2, 3343-3356.

D'Avino, P. P., Crispi, S., Cherbas, L., Cherbas, P., Furia, M. 1995. The moulting hormone ecdysone is able to recognize target elements composed of direct repeats. Mol Cell Endocrinol. 113, 1-9.

D'Avino, P. P., Thummel, C. S. 2000. The ecdysone regulatory pathway controls wing morphogenesis and integrin expression during Drosophila metamorphosis. Dev Biol. 220, 211-224.

Dobens, L., Rudolph, K., Berger, E. M. 1991. Ecdysterone regulatory elements function as both transcriptional activators and repressors. Mol Cell Biol. 11, 1846-1853.

Drach, P. 1939. Mue et cycle d'intermue chez les Crustace´s De´capodes. Ann. Inst. Oceanogr. Monaco. 19, 103–391.

Durand, B., Saunders, M., Gaudon, C., Roy, B., Losson, R., Chambon, P. 1994. Activation function 2 (AF-2) of retinoic acid receptor and 9-cis retinoic acid receptor: presence of a conserved autonomous constitutive activating domain and influence of the nature of the response element on AF-2 activity. EMBO J. 13, 5370-5382.

Durica, D.S., Chung, A.C.-K., Hopkins, P.M. 1999. Evolution of the steroid/thyroid/retinoic acid receptors—characterization of EcR and RXR gene homologs and receptor expression during the molt cycle in the crab, *Uca pugilator*. Am. Zool. 39, 758–774.

Durica, D. S., Hopkins, P. M. 1996. Expression of the genes encoding the

ecdysteroid and retinoid receptors in regenerating limb tissues from the fiddler crab, *Uca pugilator*. Gene.171, 237-241.

Durica, D. S., Wu, X., Anilkumar, G., Hopkins, P. M., Chung, A. C. 2002. Characterization of crab EcR and RXR homologs and expression during limb regeneration and oocyte maturation. Mol Cell Endocrinol. 189, 59-76.

Egea, P.F., Klaholz, B.P., Moras, D. 2000. Ligand-protein interactions in nuclear receptors of hormones. FEBS Lett. 476, 62–67.

Elke, C., Rauch, P., Spindler-Barth, M., Spindler, K. D. 1999. DNA-binding properties of the ecdysteroid receptor-complex (EcR/USP) of the epithelial cell line from Chironomus tentans. Arch Insect Biochem Physiol. 1999, 124-133.

Evans, R.M. 1988. The steroid and thyroid hormone receptor superfamily. Science. 240, 889-895.

Fisk, G. J., Thummel, C. S. 1998. The DHR78 nuclear receptor is required for ecdysteroid signaling during the onset of Drosophila metamorphosis. Cell. 93, 543-555.

Forman, B. M., Samuels, H. H. 1990. Dimerization among nuclear hormone receptors. New Biol. 2, 587-594.

Fujiwara, H., Jindra, M., Newitt, R., Palli, S.R., Hiruma, K., Riddiford, L.M. 1995. Cloning of an ecdysone receptor homolog from *Manduca sexta* and the developmental profile of its mRNA in wings. Insect Biochem. Mol. Biol. 25, 845–856.

Gervois, P., Torra, I. P., Chinetti, G., Grotzinger, T., Dubois, G., Fruchart, J. C., Fruchart-Najib, J., Leitersdorf, E., Staels, B. 1999. A truncated human peroxisome proliferator-activated receptor alpha splice variant with dominant negative activity. Mol Endocrinol. 1999 13, 1535-1549.

Giguere, V., McBroom, L. D., Flock, G. 1995. Determinants of target gene specificity for ROR alpha 1: monomeric DNA binding by an orphan nuclear receptor. Mol Cell Biol. 15, 2517-2526.

Grad, I., Kochman, M., Ozyhar, A. 2002. Functionality versus strength - has functional selection taken place in the case of the ecdysteroid receptor response element? Acta Biochim Pol. 49, 747-756.

Grad, I., Niedziela-Majka, A., Kochman, M., Ozyhar, A. 2001. Analysis of Usp DNA binding domain targeting reveals critical determinants of the ecdysone receptor complex interaction with the response element. Eur J Biochem. 268, 3751-3758.

Guo, X., Harmon, M.A., Laudet, V., Mangelsdorf, D.J., Palmer, M.J. 1997. Isolation of a functional ecdysteroid receptor homologue from the ixodid tick *Amblyomma americanum* (L.). Insect Biochem. Mol. Biol. 27, 945–962.

Guo, X., Xu, Q., Harmon, M., Jin, X., Laudet, V., Mangelsdorf, D.J., Palmer, M.J. 1998. Isolation of two functional retinoid X receptor subtypes from the ixodid tick, *Amblyomma americanum* (L.). Mol. Cell Endocrinol. 139, 45–60.

Hall, B.L., Thummel, C.S. 1998. The RXR homolog ultraspiracle is an essential component of the *Drosophila* ecdysone receptor. Development 125, 4709–4717.

Hannan, G.N., Hill, R.J. 1997. Cloning and characterization of LcEcR, a functional ecdysone receptor from the sheep blowfly, *Lucilia cuprina*. Insect Biochem. Mol. Biol. 27, 479–488.

Harmon, M.A., Boehm, M.F., Heyman, R.A., Mangelsdorf, D.J. 1995. Activation of mammalian retinoid X receptors by the insect growth regulator methoprene. Proc. Natl. Acad. Sci. USA 92, 6157–6160.

Hayward, D.C., Bastiani, M.J., Trueman, J.W.H., Truman, J.W., Riddiford, L.M., Ball, E.E. 1999. The sequence of *Locusta* RXR, homologous to Drosophila Ultraspiracle, and its evolutionary implications. Dev. Genes Evol. 209, 564–571.

Hegstrom, C.D., Riddiford, L.M., Truman, J.W. 1998. Steroid and neuronal regulation of ecdysone receptor expression during metamorphosis of muscle in the moth, *Manduca sexta*. J. Neurosci. 18, 1786–1794.

Henrich, V.C., Sliter, T.J., Lubahn, D.B., MacIntyre, A., Gilbert, L.I. 1990. A steroid/thyroid hormone receptor superfamily member in *Drosophila melanogaster* that shares extensive sequence similarity with a mammalian homologue. Nucleic Acids Res. 18, 4143–4148.

Hirai, M., Shinoda, T., Kamimura, M., Tomita, S., Shiotsuki, T. 2002. Bombyx mori orphan receptor, BmHR78: cDNA cloning, testis abundant expression and putative dimerization partner for Bombyx ultraspiracle. Mol Cell Endocrinol. 189, 201-211.

Hiruma, K., Bocking, D., Lafont, R., Riddiford, L.M. 1997. Action of different ecdysteroids on the regulation of mRNAs for the ecdysone receptor, MHR3, dopa decarboxylase, and a larval cuticle protein in the larval epidermis of the tobacco hornworm, *Manduca sexta*. Gen. Comp. Endocrinol. 107, 84–97.

Hiruma, K., Shinoda, T., Malone, F., Riddiford, L.M. 1999. Juvenile hormone modulates 20-hydroxyecdysone-inducible ecdysone receptor and ultraspiracle

gene expression in the tobacco hornworm, *Manduca sexta*. Dev. Genes Evol. 209, 18–30.

Holland, C. A., Skinner, D. M. 1976. Interaction between molting and regenerating in the land crab. Biol Bull 150, 222-240.

Holmbeck, S. M., Dyson, H. J., Wright, P. E. 1998b. DNA-induced conformational changes are the basis for cooperative dimerization by the DNA binding domain of the retinoid X receptor. J Mol Biol. 284, 533-539.

Holmbeck, S. M., Foster, M. P., Casimiro, D. R., Sem, D. S., Dyson, H. J., Wright, P. E. 1998a. High-resolution solution structure of the retinoid X receptor DNA-binding domain. J Mol Biol. 281, 271-284.

Hopkins, P.M. 1982. Growth and regeneration patterns in the fiddler crab, *Uca pugilator*. Biol. Bull. 163, 301–319.

Hopkins, P. M. 1983. Patterns of serum ecdysteroids during induced and uninduced proecdysis in the fiddler crab, *Uca pugilator*. Gen Comp Endocrinol. 52, 350-356.

Hopkins, P. M. 1986. Ecdysteroid titers and Y-organ activity during induced and uninduced proecdysis in fiddler crab, *Uca pugilator*. Gen. Comp. Endocrinol. 63, 362-373.

Hopkins, P.M. 1988. Control of regeneration in crustaceans. In "Endocrinology of selected Invertebrate Types" (R. Downer and H. Laufer, Eds.), Vol.2, pp.327-340, A.R.Liss, New York.

Hopkins, P.M. 1989. Ecdysteroids and regeneration in the fiddler crab, *Uca pugilator*. J. Exp. Zool. 252, 293–299.

Hopkins, P.M. 1992. Hormonal control of the molt cycle in the fiddler crab, *Uca pugilator*. Am. Zool. 32, 450–458.

Hopkins, P.M. 1993. Regeneration of walking legs in the fiddler crab, *Uca pugilator*. Am. Zool. 33, 348–356.

Hopkins, P. M. 2001. Limb regeneration in the fiddler crab, *Uca pugilator*: hormonal and growth factor control. Am. Zool., 41, 389-398.

Hopkins, P.M., Chung, A.C.-K., Durica, D.S. 1999. Limb regeneration in the fiddler crab, *Uca pugilator*: histological, physiological and molecular considerations. Am. Zool. 39, 513–526.

Hopkins, P.M., Durica, D.S. 1995. Effects of all trans retinoic acid on regenerating limbs of the fiddler crab, *Uca pugilator*. J. Exp. Zool. 272, 455–463.

Horner, M. A., Chen, T., Thummel, C. S. 1995. Ecdysteroid regulation and DNA binding properties of Drosophila nuclear hormone receptor superfamily members. Dev Biol. 68, 490-502.

Hu, X. 1998. The Mechanism of activating the functional ecdysone receptor complex. Ph.D. thesis, Indiana University, Bloomington.

Jayachandran, G., Fallon, A. M. 2001. Antisense expression of the 20-hydroxyecdysone receptor (EcR) in transfected mosquito cells uncovers a new EcR isoform that varies at the C-terminal end. In Vitro Cell Dev Biol Anim. 37, 522-529.

Jindra, M., Malone, F., Hiruma, K., Riddiford, L.M. 1996. Developmental profiles and ecdysteroid regulation of the mRNAs for two ecdysone receptor isoforms in the epidermis and wings of the tobacco hornworm, *Manduca sexta*. Dev. Biol. 180, 258–272.

Jindra, M., Huang, J.-Y., Malone, F., Asahina, M., Riddiford, L.M. 1997. Identification and mRNA developmental profiles of two ultraspiracle isoforms in the epidermis and wings of *Manduca sexta*. Insect Mol. Biol. 6, 41–53.

Jo, Q.-T., Laufer, H., Biggers, W.J., Kang, H.S. 1999. Methyl farnesoate induced ovarian maturation in the spider crab, *Libinia emarginata*. Invert. Reprod. Dev. 36, 79–85.

Jones, B.B., Ohno, C.K., Allenby, G., Boffa, M.B., Levin, A.A., Grippo, J.F., Petkovich, M. 1995. New retinoid X receptor subtypes in zebra fish (*Danio rerio*) differentially modulate transcription and do not bind 9-cis retinoic acid. Mol. Cell. Biol. 15, 5226–5234.

Jones, G., Sharp, P.A. 1997. Ultraspiracle: an invertebrate nuclear receptor for juvenile hormones. Proc. Natl. Acad. Sci. USA 94, 13499–13503.

Kamimura, M., Tomita, S., Fujiwara, H. 1996. Molecular cloning of an ecdysone receptor (B1 isoform) homologue from the silkworm, Bombyx mori, and its mRNA expression during wing disc development. Comp Biochem Physiol B Biochem Mol Biol. 113, 341-347.

Kamimura, M., Tomita, S., Kiuchi, M., Fujiwara, H. 1997. Tissue-specific and stage-specific expression of two silkworm ecdysone receptor isoforms—ecdysteroid-dependent transcription in cultured anterior silk glands. Eur. J. Biochem. 15, 786–793.

Kapitskaya, M., Wang, S., Cress, D.E., Dhadialla, T.S., Raikhel, A.S. 1996. The mosquito *ultraspiracle* homologue, a partner of ecdysteroid receptor heterodimer: cloning and characterization of isoforms expressed during vitellogenesis. Mol. Cell Endocrinol. 121, 119–132.

Karim, F. D., Thummel C. S. 1992. Temporal coordination of regulatory gene expression by the steroid hormone ecdysone. EMBO J. 11, 4083-4093.

Karlson, P. 1996. On the hormonal control of insect metamorphosis. A historical review. Int. J. Dev. Biol. 40, 93–96.

Kastner, P., Mark, M., Leid, M., Gransmuller, A., Chin, W., Grondona, J.M., De´cimo, D., Krezel, W., Dierich, A., Chambon, P. 1996. Abnormal spermatogenesis in RXR mutant mice. Genes Dev. 10, 80–92.

Koch, P. B., Merk, R., Reinhardt, R., Weber, P. 2003. Localization of ecdysone receptor protein during colour pattern formation in wings of the butterfly *Precis coenia* (Lepidoptera: Nymphalidae) and co-expression with Distal-less protein. Dev Genes Evol. 212, 571-584.

Koelle, M. R., Segraves, W. A., Hogness, D. S. 1992. DHR3: a Drosophila steroid receptor homolog. Proc. Natl. Acad. Sci. USA. 89, 6167-6171.

Koelle, M.R., Talbot, W.S., Segraves, W.A., Bender, M.T., Cherbas, P., Hogness, D.S. 1991. The *Drosophila EcR* gene encodes an ecdysone receptor, a new member of the steroid receptor superfamily. Cell 67, 59–77.

Kontrogianni-Konstantopoulos, A., Flytzanis, C. N. 2001. Differential cellular compartmentalization of the nuclear receptor SpSHR2 splicing variants in early sea urchin embryos. Mol Reprod Dev. 60, 147-157.

Koslova, T., Thummel, C.S. 2000. Steroid regulation of postembryonic development and reproduction in *Drosophila*. Trends Endocrinol. Metab. 11, 276–280.

Kothapalli, R., Palli, S.R., Ladd, T.R., Sohi, S.S., Cress, D., Dhadialla, T.S., Tzertzinis, G., Retnakaran, A. 1995. Cloning and developmental expression of the ecdysone receptor gene from the spruce budworm, *Choristoneura fumiferana*. Dev. Genet. 17, 319–330.

Kurokawa, R., DiRenzo, J., Boehm, M., Sugarman, J., Gloss, B., Rosenfeld, M. G., Heyman, R. A., Glass, C. K. 1994. Regulation of retinoid signalling by receptor polarity and allosteric control of ligand binding. Nature. 371, 528-531.

Lachaise, F., Lafont, R. 1984. Ecdysteroid metabolism in a crab: *Carcinus maenas* L. Steroids 43, 243–259.

Lan, Q., Hiruma, K., Hu, X., Jindra, M., Riddiford, L.M. 1999. Activation of a delayed-early gene encoding MHR3 by the ecdysone receptor heterodimer EcR-B1/USP-1 but not by EcR-B1/USP-2. Mol. Cell Biol. 7, 4897–4906.

Laufer, H., Jonna, J.S.B., Sagi, A. 1993. The role of juvenile hormones in crustacean reproduction. Am. Zool. 33, 365–374.

Laufer, H., Biggers, W.J., Ahl, J.S. 1998. Stimulation of ovarian maturation in the crayfish *Procambarus clarkii* by methyl farnesoate. Gen. Comp. Endocrinol. 111, 113–118.

Lee, N., Cozzikorto, J., Wainwright, N., and Testa, D. 1984. Cloning with tandem gene systems for high level gene expression. Nucl. Acids Res. 12, 6797-6812.

Lee, T., Marticke, S., Sung, C., Robinow, S., Luo, L. 2000. Cell-autonomous requirement of the USP/EcR-B ecdysone receptor for mushroom body neuronal remodeling in *Drosophila*. Neuron 28, 807–818.

Lehmann, M., Korge, G. 1995. Ecdysone regulation of the Drosophila Sgs-4 gene is mediated by the synergistic action of ecdysone receptor and SEBP 3. EMBO J. 14, 716-726.

Lehmann, M., Wattler, F., Korge, G. 1997. Two new regulatory elements controlling the Drosophila Sgs-3 gene are potential ecdysone receptor and fork head binding sites. Mech Dev. 62, 15-27.

Lilie H, Schwarz E, Rudolph R. 1998. Advances in refolding of proteins produced in *E. coli*. Curr Opin Biotechnol. 9, 497-501.

Livera, G., Rouiller-Fabre, V., Valia, J., Habert, R. 2000. Effects of retinoids on the meiosis in the fetal rat ovary in culture. Mol. Cell Endocrinol. 165, 225–231.

Madden, T.L., Tatusov, R.L., Zhang, J. 1996. Applications of the network BLAST server. Methods Enzymol. 266, 131–141.

Maksymowysch, A. B., Hsu, T.-C., Litwack, G. 1993. A novel, highly conserved structure motif is present in all members of the steroid receptor superfamily. Receptor 2, 225-240.

Mangelsdorf, D.J., Borgmeyer, U., Heyman, R.A., Zhou, J.Y., Ong, E.S., Oro, A.E., Kakizuka, A., Evans, R.M. 1992. Characterization of three RXR genes that mediate the action of 9-cis retinoic acid. Genes Dev. 6, 329–344.

Mangelsdorf, D. J., Evans, R. M. 1995. The RXR heterodimers and orphan receptors. Cell 83, 841-850.

Mangelsdorf, D.J., Thummel, C., Beato, M., Herrlich, P., Schutz, G., Umesono, K., Blumberg, B., Kastner, P., Mark, M., Chambon, P. 1995. The nuclear receptor superfamily: the second decade. Cell 83, 835–839.

Martin, D., Wang, S.F., Raikhel, A.S. 2001. The vitellogenin gene of the mosquito *Aedes aegypti* is a direct target of ecdysteroid receptor. Mol. Cell Endocrinol. 173, 75–86.

Melcher, K., Johnson, S.A. 1995. Gal4 interacts with TATA-binding protein and co-activators. Mol. Cell Biol. 15, 2839–2848.

Minakuchi, C., Nakagawa, Y., Kiuchi, M., Tomita, S., Kamimura, M. 2002. Molecular cloning, expression analysis and functional confirmation of two ecdysone receptor isoforms from the rice stem borer *Chilo suppressalis*. Insect Biochem Mol Biol. 32, 999-1008.

Minegishi, T., Hirakawa, T., Kishi, H., Abe, K., Tano, M., Abe, Y., Miyamoto, K. 2000. The mechanisms of retinoic acid-induced regulation on the follicle-stimulating hormone receptor in rat granulose cells. Biochim. Biophys. Acta 1495, 203–211.

Miura, K., Wang, S.F., Raikhel, A.S. 1999. Two distinct subpopulations of ecdysone receptor complex in the femal mosquito during vitellogenesis. Mol. Cell Endocrinol. 156, 111–120.

Miyamoto, K., Kesterson, R. A., Yamamoto, H., Taketani, Y., Nishiwaki, E., Tatsumi, S., Inoue, Y., Morita, K., Takeda, E., Pike, J. W. 1997. Structural organization of the human vitamin D receptor chromosomal gene and its promoter. Mol Endocrinol. 11, 1165-1179.

Morita, Y., Tilly, J.L. 1999. Segregation of retinoic acid effects on fetal ovarian germ cell mitosis versus apoptosis by requirement for new macromolecular synthesis. Endrocrinology 140, 2696–2703.

Mouillet, J.F., Delbecque, J.P., Quennedey, B., Delachambre, J. 1997. Cloning of two putative ecdysteroid receptor isoforms from *Tenebrio molitor* and their developmental expression in the epidermis during metamorphosis. Eur. J. Biochem. 248, 856–860.

Nicolai, M., Bouhin, H., Quennedey, B., Delachambre, J. 2000. Molecular cloning and expression of *Tenebrio molitor ultraspiracle* during metamorphosis and in vivo induction of its phosphorylation by 20-hydroxyecdysone. Insect Mol. Biol. 9, 241–249.

Oro, A.E., McKeown, M., Evans, R.M. 1990. Relationship between the product of the *Drosophila ultraspiracle* locus and the vertebrate retinoid X receptor. Nature 347, 298–301.

Ozyhar, A., Pongs, O. 1993. Mutational analysis of the interaction between ecdysteroid receptor and its response element. J Steroid Biochem Mol Biol. 46, 135-145.

Palli, S. R., Kapitskaya, M. Z., Kumar, M. B., Cress, D.E. 2003. Improved ecdysone receptor-based inducible gene regulation system. Eur J Biochem. 270,1308-1315.

Perera, S. C, Ladd, T. R., Dhadialla, T. S., Krell, P. J., Sohi, S. S., Retnakaran, A., Palli, S. R. 1999. Studies on two ecdysone receptor isoforms of the spruce budworm, *Horistoneura fumiferana.* Mol Cell Endocrinol. 152, 73-84.

Perera, S.C., Palli, S.R., Ladd, T.R., Krell, P.J., Retnakaran, A. 1998. The ultraspiracle gene of the spruce budworm, *Choristoneura fumiferana*, cloning of cDNA and developmental expression of mRNA. Dev. Genet. 22, 169–179.

Perlmann, T., Umesono, K., Rangarajan, P. N., Forman, B. M., Evans, R. M. 1996. Two distinct dimerization interfaces differentially modulate target gene specificity of nuclear hormone receptors. Mol Endocrinol. 10, 958-966.

Pierceall, W.E., Li, C., Biran, A., Miura, K., Raikhel, A.S., Segraves, W.A. 1999. E75 expression in mosquito ovary and fat body suggests reiterative use of ecdysone-regulated hierarchies in development and reproduction. Mol. Cell Endocrinol. 150, 73–89.

Presenell, J. K., Schreibman, M. P. (ed) 1997. Humason's Animal tissue techniques. 5th ed. Baltimore, Md. Johns Hopkins University Press.

Raikhel, A.S., Miura, K., Segraves, W.A. 1999. Nuclear receptors in mosquito vitellogenesis. Am. Zool. 722–735.

Rastinejad, F., Wagner, T., Zhao, Q., Khorasanizadeh, S. 2000. Structure of the RXR–RAR DNA-binding complex on the retinoic acid response element DR1. EMBO J. 19, 1045–1054.

Renaud, J.P., Moras, D. 2000. Structural studies on nuclear receptors. Cell. Mol. Life Sci. 57, 1748–1769.

Riddihough, G., and Pelham, H. R. B. 1986. Activation of the *Drosophila hsp27* promoter by heat shock and by ecdysone involves independent and remote regulatory sequences. EMBO J. 5, 1653-1658.

Riddibough, G., and Pelham, H. R. B. 1987. Activation of the *Drosophila* hsp27 promoter by heat shock and by ecdysone involves independent and remote regulatory sequences. EMBO J. 6, 3729–3734.

Riddiford, L.M. 1993. Hormone receptors and the regulation of insect metamorphosis. Receptor 3, 203–209.

Riddiford, L. M. 1994. Cellular and molecular actions of Juvenile hormone. I. General considerations and premetamorphic actions. Adv. Insect Physiol. 24, 213-274.

Riddiford, L.M., Hiruma, K., Lan, Q., Zhou, B. 1999. Regulation and role of nuclear receptors during larval molting and metamorphosis of *Lepidoptera*. Am. Zool. 39, 736–746.

Riddiford, L.M., Cherbas, P., Truman, J.W. 2001. Ecdysone receptors and their biological actions. Vit. Horm. 60, 1–73.

Robinow, S., Talbot, W.S., Hogness, D.S., Truman, J.W. 1993. Programmed cell death in the *Drosophila* CNS is ecdysone-regulated and coupled with a specific ecdysone receptor isoform. Development 119, 1251–1259.

Rochel, N., Tocchini-Valentini, G., Egea, P. F., Juntunen, K., Garnier, J. M., Vihko, P., Moras, D. 2001. Functional and structural characterization of the insertion region in the ligand-binding domain of the vitamin D nuclear receptor. Eur J Biochem. 268, 971-979.

Rochel, N., Wurtz, J.M., Mitschler, A., Klaholz, B., Moras, D. 2000. The crystal structure of the nuclear receptor for vitamin D bound to its natural ligand. Mol Cell. 5, 173-179.

Rost, B., 1996. PHD: predicting one-dimensional protein structure by profile based neural networks. Methods Enzymol. 266, 525–539.

Ruse, M. D. Jr., Privalsky, M. L., Sladek, F. M. 2002. Competitive cofactor recruitment by orphan receptor hepatocyte nuclear factor 4alpha1: modulation by the F domain. Mol Cell Biol. 22, 1626-1638.

Saleh, D.S., Zhang, J., Wyatt, G.R., Walker, V.K. 1998. Cloning and characterization of an ecdysone receptor cDNA from *Locusta migratoria*. Mol. Cell. Endocrinol. 143, 91–99.

Sasorith, S., Billas, I. M. L., Iwema, T., Moras, D., Wurtz, J. M. 2002. Structure-based analysis of the ultraspiracle protein and docking studies of putative ligands. Journal of Insect Science. 2(25), 1-11.

Scatchard, G. 1949. The attractions of proteins for small molecules and ions. Ann. N. Y. Acad. Sci. 51, 660-672.

Schägger, H. and G. von Jagow. 1987. Tricine-sodium dodecyl sulfate-polyacrylamide gel electrophoresis for the separation of proteins in the range from 1 to 100 kDa. Analytical Biochemistry 166, 368-379.

Schubiger, M., Wade, A.A., Carney, G.E., Truman, J.W., Bender, M. 1998. *Drosophila* EcR-B ecdysone receptor isoforms are required for larval molting and for neuron remodeling during metamorphosis. Development 125, 2053–2062.

Schubiger, M., Truman, J.W. 2000. The RXR ortholog USP suppresses early metamorphic processes in *Drosophila* in the absence of ecdysteroids. Development 127, 1151–1159.

Schulman, I. G., Juguilon, H., Evans, R. M. 1996. Activation and repression by nuclear hormone receptors: hormone modulates an equilibrium between active and repressive states. Mol Cell Biol. 16, 3807-3813.

Schwartz, J. A., Zhong, L., Deighton-Collins, S., Zhao, C., Skafar, D. F. 2002. Mutations targeted to a predicted helix in the extreme carboxyl-terminal region of the human estrogen receptor-alpha alter its response to estradiol and 4-hydroxytamoxifen. J Biol Chem. 277, 13202-13209.

Segraves, W. A. 1994. Steroid receptors and other transcription factors in ecdysone response. Recent Prog Horm Res. 49,167-95.

Segraves, W. A., Hogness, D. S. 1990. The E75 ecdysone-inducible gene responsible for the 75B early puff in *Drosophila* encodes two new members of the steroid receptor superfamily. Genes Dev. 4, 204-219.

Seo, Y. W., Sanyal., S., Kim, H. J., Won, D. H., An, J. Y., Amano, T., Zavacki, A. M., Kwon, H. B., Shi, Y. B., Kim, W. S., Kang, H., Moore, D. D., Choi, H. S. 2002. FOR, a novel orphan nuclear receptor related to farnesoid X receptor. J Biol Chem. 277, 17836-17844.

Shea, M.J., King, D.L., Conboy, M.J., Mariani, B.D., Kafatos, F.C. 1990. Proteins that bind to *Drosophila* chorion cis-regulatory elements: a new C2H2 zinc finger protein and a C2C2 steroid receptor-like component. Genes Dev. 4, 1128–1140.

Shi, S. R., Chaiwun, B., Young, L., Cote, R. J., Taylor, C. R. 1993. Antigen retrieval technique utilizing citrate buffer or urea solution for immunohistochemical demonstration of androgen receptor in formalin-fixed paraffin sections. J Histochem Cytochem. 41,1599-1604.

Skinner, D., 1985. Molting and regeneration. In: Bliss, D.E., Mantel, L.H. (Eds.), The Biology of Crustacea. Academic Press, New York, pp. 43–146.

Smith, D.B., Corcoran, L.M., 1994. Expression and purification of Glutathione-S-transferase fusion proteins. In: Ausubel, F.M. (Ed.), Current Protocols in Molecular Biology. John Wiley, New York, pp. 16.7.1–16.7.7.

Snyder, M.J., Chang, E.S. 1991. Ecdysteroids in relation to the molt cycle of the American lobster, *Homarus americanus*. I. Hemolymph titers and metabolites. Gen. Comp. Endocrinol. 83, 133–145.

Subramoniam, T. 2000. Crustacean ecdysteroids in reproduction and embryogenesis. Comp. Biochem. Physiol. 125, 135–156.

Sutherland, J.D., Kozlova, T., Tzertzinis, G., Kafatos, F.C. 1995. *Drosophila* hormone receptor 38: a second partner for *Drosophila* USP suggests an unexpected role for nuclear receptors of the nerve growth factor-induced protein B type. Proc. Natl. Acad. Sci. USA 92, 7966–7970.

Swevers, L., Cherbas, L., Cherbas, P., Iatrou, K. 1996. Bombyx EcR (BmEcR) and Bombyx USP (BmCF1) combine to form a functional ecdysone receptor. Insect Biochem Mol Biol 26, 217-221.

Swevers, L., Drevet, J.R., Lunke, M.D., Iatrou, K. 1995. The silkmoth homolog of the *Drosophila* ecdysone receptor (B1 isoform): cloning and analysis of expression during follicular cell differentiation. Insect Biochem. Mol. Biol. 25, 857–866.

Talbot, W.S., Swyryd, E.A., Hogness, D.S. 1993. *Drosophila* tissues with different metamorphic responses to ecdysone express different ecdysone receptor isoforms. Cell 73, 1323–1337.

Tamone, S.L., Chang, E.S. 1993. Methyl fanesoate stimulate ecdysteroid secretion from Y-organs in vitro. Gen. Comp. Endocrinol. 89, 425–432.

Thomas, H.E., Stunnenberg, H.G., Stewart, A.F. 1993. Heterodimerization of the *Drosophila* ecdysone receptor with retinoid X receptor and *ultraspiracle*. Nature 362, 471–475.

Thompson, J.D., Higgins, D.G., Gibson, T.J. 1994. CLUSTAL W: improving the sensitivity of progressive multiple sequence alignment through sequence weighting, positions-specific gap penalties and weight matrix choice. Nucleic Acids Res. 22, 4673–4680.

Thormeyer, D., Tenbaum, S. P., Renkawitz, R., Baniahmad, A. 1999. EcR interacts with corepressors and harbours an autonomous silencing domain

functional in both *Drosophila* and vertebrate cells. J Steroid Biochem Mol Biol. 68, 163-169.

Thummel, C.S. 1995. From embryogenesis to metamorphosis: the regulation and function of *Drosophila* nuclear receptor superfamily members. Cell 83, 871–877.

Thummel, C.S. 1996. Flies on steroids—*Drosophila* metamorphosis and the mechanisms of steroid hormone action. Trends Genet. 12, 306–310.

Thummel, C.S. 1997. Dueling orphans—interacting nuclear receptors coordinate *Drosophila* metamorphosis. BioEssays 19, 669–672.

Truman, J.W., Talbot, W.S., Fahrbach, S.E., Hogness, D.S. 1994. Ecdysone receptor expression in the CNS correlates with stage specific responses to ecdysteroids during *Drosophila* and *Manduca* development. Development 120, 219–234.

Tsai, C. C., Kao, H. Y., Yao, T. P., McKeown, M., Evans, R. M. 1999. SMRTER, a *Drosophila* nuclear receptor coregulator, reveals that EcR-mediated repression is critical for development. Mol Cell. 4, 175-186.

Tsai, M. J., O'Malley, B. W. 1994. Molecular mechanisms of action of steroid/thyroid receptor superfamily members. Annu Rev Biochem. 63, 451-486.

Urness, L. D., Thummel, C. S. 1990. Molecular interactions within the ecdysone regulatory hierarchy: DNA binding properties of the *Drosophila* ecdysone-inducible E74A protein. Cell 63, 47-61.

van Pelt, A.M., deRooij, D.G., 1991. Retinoic acid is able to reinitiate spermatogenesis in vitamin-A deficient rats and high replicate doses support the full development of spermatogenic cells. Endocrinology 128, 697–704.

Verras, M., Gourzi, P., Zacharopoulou, A., Mintzas, A. C. 2002. Developmental profiles and ecdysone regulation of the mRNAs for two ecdysone receptor isoforms in the Mediterranean fruit fly *Ceratitis capitata*. Insect Mol Biol. 11, 553-565.

Verras, M., Mavroidis, M., Kokolakis, G., Gourzi, P., Zacharopoulou, A., Mintzas, A.C. 1999. Cloning and characterization of CcEcR. An ecdysone receptor homolog from the Mediterranean fruit fly *Ceratitis capitata*. Eur. J. Biochem. 265, 798–808.

Vögtli, M., Elke, C., Imhof, M. O., Lezzi, M. 1998. High level transactivation by the ecdysone receptor complex at the core recognition motif. Nucleic Acids Res. 26, 2407-2414.

Vögtli, M., Imhof, M. O., Brown, N. E., Rauch, P., Spindler-Barth, M., Lezzi, M., Henrich, V. C. 1999. Functional characterization of two Ultraspiracle forms (CtUSP-1 and CtUSP-2) from *Chironomus tentans*. Insect Biochem Mol Biol. 29, 931-942.

Wang, S. F., Ayer, S., Segraves, W.A., Williams, D.R., Raikhel, A.S. 2000a. Molecular determinants of differential ligand sensitivities of insect ecdysteroid receptors. Mol. Cell. Biol. 20, 3870–3879.

Wang, S. F., Li, C., Zhu, J., Miura, K., Miksicek, R. J., Raikhel, A. S. 2000b. Differential expression and regulation by 20-hydroxyecdysone of mosquito ultraspiracle isoforms. Dev Biol. 218, 99-113.

Wang, S. F., Miura, K., Miksicek, R. J., Segraves, W. A., Raikhel, A. S. 1998. DNA binding and transactivation characteristics of the mosquito ecdysone receptor-Ultraspiracle complex. J Biol Chem. 273, 27531-27540.

White, K.P., Hurban, P., Watanabe, T., Hogness, D.S. 1997. Coordination of *Drosophila* metamorphosis by two ecdysone-induced nuclear receptors. Science 276, 114–117.

Xu, L., Glass, C. K., and Rosenfeld, M. G. 1999. Coactivator and corepressor complexes in nuclear receptor function. Curr. Opin. Genet. Dev. 9, 140-147.

Yang, Y. Z., Subauste, J. S., Koenig, R. J. 1995. Retinoid X receptor alpha binds with the highest affinity to an imperfect direct repeat response element. Endocrinology. 136, 2896-2903.

Yao, T.P., Forman, B.M., Jiang, Z., Cherbas, L., Chen, J.D., McKeown, M., Cherbas, P., Evans, R.M. 1993. Functional ecdysone receptor is the product of EcR and Ultraspiracle genes. Nature 366, 476–479.

Yao, T.P., Seagraves, W.A., Oro, A.E., McKeown, M., Evans, R.M. 1992. *Drosophila* ultraspiracle modulates ecdysone receptor function via heterodimer formation. Cell 71, 63–72.

Zennaro, M. C., Souque, A., Viengchareun, S., Poisson, E., Lombes, M. 2001. A new human MR splice variant is a ligand-independent transactivator modulating corticosteroid action. Mol Endocrinol. 15, 1586-1598.

Zhang, X.K., Lehmann, J., Hoffmann, B., Dawson, M.I., Cameron, J., Graupner, G., Hermann, T., Tran, P., Pfahl, M. 1992. Homodimer formation of retinoid X receptor induced by 9-cis retinoic acid. Nature 358, 587–591.

Zhang, Y., Kast-Woelbern, H. R., Edwards, P. A. 2002. Natural structural variants of the nuclear receptor farnesoid X receptor affect transcriptional activation. J Biol Chem. 278, 104-110.

Zhao, Q., Chasse, S.A., Devarakonda, S., Sierk, M.L., Ahvazi, B., Rastinejad, F. 2000. Structural basis of RXR–DNA interactions. J. Mol. Biol. 296, 509–520.

Zelhof, A.C., Yao, T.P., Chen, J.D., Evans, R.M., McKeown, M. 1995a. Seven-up inhibits ultraspiracle-based signaling pathways in vitro and in vivo. Mol. Cell Biol. 15, 6736–6745.

Zelhof, A.C., Yao, T.P., Evans, R.M., McKeown, M. 1995b. Identification and characterization of a *Drosophila* nuclear receptor with the ability to inhibit the ecdysone response. Proc. Natl. Acad. Sci. USA 92, 10477–10481.

Zhu, J., Miura, K., Chen, L., Raikhel, A.S. 2000. AHR38, a homolog or NGFI-B, inhibits formation of the functional ecdysteroid receptor in the mosquito *Aedes aegypti*. EMBO J. 19, 253–262.

Zhu, J., Miura, K., Chen, L., Raikhel, A. S. 2003. Cyclicity of mosquito vitellogenic ecdysteroid-mediated signaling is modulated by alternative dimerization of the RXR homologue Ultraspiracle. Proc Natl Acad Sci USA. 100, 544-549.

Zilliacus, J., Wright, A. P., Carlstedt-Duke, J., Gustafsson, J. A. 1995. Structural determinants of DNA-binding specificity by steroid receptors. Mol Endocrinol. 9, 389-400.

Appendix

Observation of autotomy-independent limb regeneration in the fiddler crab *Uca pugilator*

Appendix I

Observation Of Autotomy-Independent Limb Regeneration In The Fiddler Crab *Uca pugilator*

Key words: *Uca pugilator*, autotomy, limb regeneration,

Abstract

When injured, the fiddler crab *Uca pugilator* can reflexively cast off a damaged limb at a predetermined site proximal to the injury. This reflex severs the damaged limb adjacent to the body wall between the basiioschiopodite and coxa. Autotomy, therefore, normally leads to the loss of all limb segments. Normal regeneration of autotomized limbs accompanies the animal's molt cycle, and newly formed limbs emerge as the animal undergoes ecdysis. Under laboratory conditions, however, another kind of limb regeneration was observed that was not associated with autotomy. Newly molted crabs were found to regenerate amputated limbs without the loss of all segments distal to the coxa. Regeneration occurred normally at every amputation site tested, including cuts at the propus, carpus and merus. Only the missing structures were regenerated, with appropriate proximal-distal segmentation. Newly regenerated limbs grow from the amputation site and complete limbs emerge at ecdysis similar to normal autotomy-associated limb regeneration.

1. Introduction

Autotomy is a reflective physiological event that involves specialized autotomy muscles (McVean, 1984). The most crucial muscle to the autotomy reflex is a rotating levator muscle. When stimulated, it switches the tension exerted by the remaining levators so that a crucial cuticular connection which spans the fracture plane between the basiioischium and coxa is broken, allowing the preformed fracture plane to separate (Findley and McVean, 1977). Immediately proximal to the fracture plane is a connective septum which extends across the entire limb base in such a way that it divides the hemocoelic venous cavity (Emmel, 1910; Needham, 1965; Hopkins and Mislan, 1986). Following autotomy, blood pressure in the body quickly distends the septum so that the septum balloons into the open gap immediately closing the hole created by the loss of the limb (Needham, 1952; Hopkins et al., 1999). This quick response assures that there is very little blood loss and minimal bacterial invasion. In a sense, autotomy is also an effective escape mechanism which allows the crab to avoid the attack from predators in the wild and allows the animal a chance of survival. After autotomy, a complete new functional limb will regenerate from this defined site within the next molt cycle. The process of regeneration has been discussed in previous chapters (Durica et al., 2001).

In *Uca pugilator*, regeneration of a partially damaged limb without autotomy has not been reported. Here we report the observation of autotomy-independent

limb regeneration, where the limb is appropriately regenerated, regardless of the point of amputation. This indicates that, like in vertebrate regenerating limbs, a mechanism for interpreting a positional cue must exist, allowing for the normal specification of limb axis formation.

2. Materials and Methods

2.1. Animals

U. pugilator were purchased from Gulf Specimen, Panacea, FL. The animals were acclimated to the laboratory as previously described (Hopkins, 1982; Hopkins and Durica, 1995). Seven limbs including the large cheliped were induced to autotomy by pinching with a forceps distal to the coxa. Autotomized animals were individually maintained in plastic shoe boxes in about 100 ml artificial sea water. Animals passed through one molt cycle. At molting, 3 to 8 newly regenerated limbs were amputated by a pair of sterilized scissors. Animals were allowed to stay in a dry area for a few minutes to facilitate clotting. After five minutes, animals were put back into individual containers. Animals were then monitored regularly by either measuring the R-value (Bliss, 1956) (if autotomy occurred) or by counting the days after amputation.

2.2. Histology

Crabs were cooled by immersion in crushed ice for 10 min. Tissues from regenerating limb buds were quickly dissected out and rinsed in *Uca* saline (46 mM $MgCl_2$, 42 mM Na_2SO_4, 286 mM NaCl, 11 mM KCl, 16 mM $CaCl_2$, 76 mM Tris, pH 7.8) and immediately fixed in a 20 volume excess of Lillie decalcification fixative (Presenell et al., 1997) overnight.

Fixed tissues underwent a standard dehydration series with ethanol and penetration with xylene (Presenell et al., 1997). Tissues were embedded in

paraffin. Adjacent or near adjacent 5-8 μm sections were mounted on subbed slides for later hematoxylin/eosin (H/E) or immunohistochemical staining.

For hematoxylin/eosin staining, the slides were dewaxed in a series of xylene/ethanol washes and then hydrated in distilled water. Tissues were stained with Harris Hematoxylin (Fisher Scientific International Inc, Hampton, NH) for 2 min. The slides were rinsed in water. After the wash, the slides were dipped in 1% ammonium hydroxide and were immediately taken out and washed well with distilled water. The slides were then counterstained with eosin (10 ml of 0.1% eosin in ethanol, 90 ml of 95% ethanol, 700 μl of glacial acetic acid) for 15-20 seconds. The slides were dehydrated in 95% ethanol (3X) then 100% ethanol (3X), with each change for three minutes. Slides were cleared in xylene and mounted with Permount (Sigma-Aldrich, St Louis, MO).

2.3. Microscopy and image processing

Regenerating limbs were examined under a dissecting microscope (Olympus SZH, Olympus America, Melville, NY). Images were captured by a digital camera (Olympus C-211) and processed by Adobe Photoshop5.0 (Adobe Systems Incorporated, San Jose, CA).

Stained slides were examined under a microscope (Olympus AH-2) using bright field or DIC optics. Images were captured by a coolSNAP digital camera or 35 mm film and processed by the MetaMorph imaging system (Universal imaging corporation, Downingtown, PA) and Adobe Photoshop5.0 (Adobe Systems Incorporated).

3. Results

3.1. Observation of autotomy-independent limb regeneration.

In *Uca pugliator*, damage to a limb usually causes autotomy, a reflexive loss of the injured limb at the basi-ischiopodite. A new limb will develop at that position inside a cuticular sac (Figure 1). Our initial observation involved a newly molted crab that was found to be attacked by cohorts in the same tank. Two of its walking legs were amputated within the merus, but the proximal portions of the two limbs were still attached to the coxa. This crab survived and the damaged limbs were regenerated. In Figure 2A, one damaged limb formed an apparent mini-bud (arrow) at the distal portion of the appendage. The regenerating limb sections were folded inside a cuticular sac like normal autotomy-dependent regeneration. Figure 2B shows the complete functional new leg following ecdysis after one molt cycle. Only the missing structures were regenerated. The newly regenerated limb part was less pigmented and more transparent than the old remaining part (arrowhead, the joint of old part and regenerated part).

3.2. Experimental demonstration of the existence of autotomy-independent limb regeneration

We experimentally repeated this initial observation. Three to eight limbs of newly molted crabs were amputated by a pair of scissors at various sites distal to the coxa of these limbs. Although most of the limbs were autotomized shortly

after the surgery or the next day (~66%), some limbs remained attached to the coxa. Since these animals did not molt at the exact same time, some animals still had a soft body at the time of amputation, while others already had partially hardened exoskeletons. Of the remaining amputated limbs, most (12 out of 15 limbs of suriving animals, not counting those limbs that were prepared for histological examination) were fully regenerated during the next molt cycle regardless of the cutting site location. However, a few limbs (three) were not regenerated until after a second molt cycle.

The limb shown in Figure 3was amputated at the joint of carpus and propus with a pair of scissors. In this animal, unlike the situation described above, regeneration occurred within the exoskeleton beneath a scab. This was the situation for all experimentally amputated limbs. Figure 3A shows the newly molted crab was able to regenerate only the amputated part (large arrow shows the cut site). The regenerated part (the whole propus and dactylus) again shows the less intense pigmentation common for newly regenerated limbs. Figure 3B shows the exoskeleton of this leg after molting. The scab at the cutting plane is still intact, but no bud-like structure like in Figure 1 was observed (arrowhead).

Regeneration of autotomy-independent limbs was also examined by histological staining. Figure 4 shows H&E stained limb sections from regenerating amputated limbs. Figure 4A shows a limb from a crab who was at early proecdysial stage (predicted from the limb bud size of an autotomized leg). The segmentation is beginning to form inside the old cuticle (arrows), underneath the intact scab. Figure 4B shows a limb from a crab at late proecdysial stage

(predicted from the limb bud size of an autotomized leg). The regenerated limb sections were originally beneath the scab as in Figure 3A and emerged from the wound site during histological preparation (braces). Cross-sectioned areas of the merus, carpus, propus, and dactylus are visible. The cutting site is indicated by the arrows (at the middle of merus). Figure 4C shows a cross section of a regenerating amputated limb (50 days after amputation). Several layers of cuticle are surrounding the developing limb (arrows), and the folding of the regenerating limb is obvious.

Not all amputated limbs regenerated within one molt cycle. Some limbs were not regenerated until after another cycle. In Figure 5, an amputated limb (at the tip of merus) was not able to regenerate in one molt cycle. Figure 5A shows after one cycle the amputated limb was still not regenerated, although the scab at the cutting plane was replaced by a cuticular cap at the end of the merus (arrow). Figure 5B shows the exoskeleton of the molted crab limb. The scab is still intact (arrowhead). This crab was able to regenerate this limb in the next molt cycle (not shown) within the cuticle and without the formation of an external bud.

4. Discussion

In *Uca pugilator*, autotomy always occurs at the specific site between the basiioischium and coxa. An entire limb is regenerated from this position within the next molt cycle. This autotomy-dependent regeneration implies a pattern formation mechanism which allows regeneration of a complete proximal distal axis.

The observation of autotomy-independent limb regeneration expands our observation of limb regeneration in *Uca pugilator*, indicating that limb regeneration can occur in partially amputated limbs. Autotomy is a muscular response to neurological stimuli (Wood and Wood, 1932; McVean, 1982). When the animal is weak, or when the levator muscles are not strong enough, autotomy may not happen (McVean, 1982). This may be the situation in newly molted animals.

Amputated limbs from multiple cutting sites along the proximal-distal axis only regenerate the lost limb segments suggesting that there are positional cues only for regeneration of the lost portions of the limb. In vertebrates, epimorphic limb regeneration in salamanders involves retinoic acid signaling transduction. Retinoic acid is synthesized in the regenerating limb wound epidermis and forms a gradient along the proximal-distal axis of the blastema (Brockes, 1992; Scadding and Maden, 1994; Viviano et al., 1995). This gradient of retinoic acid is thought to activate genes differentially across the blastema, resulting in the specification of pattern in the regenerating limb. One set of candidate genes that may be activated by retinoic acid is the *Hox* genes. Though the mechanism is still not clear, activated *Hox* genes are hypothesized to signal cells there position in the limb and how much they need to grow. Through regulation of Hox transcription factor expression, animals only regenerate the amputated portion of a damaged limb. Whether or not there exists a similar mechanism in crustacean regeneration remains to be investigated. Initial studies using antibodies against retinoid X receptor (RXR), a receptor for 9-cis-retinoid acid, also a dimer partner to retinoic

acid receptor (RAR) in vertebrates suggest that RXR is expressed during amputated limb regeneration (data not shown). Exogenous retinoids are found to disrupt normal limb regeneration in *Uca pugilator* (Hopkins and Durica, 1995). Retinoid metabolites are also found in early regenerating limbs in *Uca* (Hopkins, 2001). Recently, CRABP (cytoplasmic retinoic acid binding protein) homolog was recovered from *Uca* blastemal EST libraries. CRABP are thought to mediate the effects of retinoic acid (RA) on morphogenesis, differentiation, and homeostasis (Morriss-Kay, 1992). All these suggest that retinoids may also be involved in limb regeneration in crustacea.

The observation that the regenerating limb was wrapped inside the cuticular sac (Figure 2), which is the extension of the old limb cuticle, suggests that the damaged epidermis together with the cuticle or exoskeleton of a newly molted crab was able to re-grow. Experimentally amputated limbs were not observed to have a cuticular sac structure; instead, a scab formed at the wound site. This observation suggests that regrowth of the old cuticle is probably dependent on the stage of the epidermis at amputation. The initial observation of autotomy-independent limb regeneration was found in a crab whose cuticle was still very soft. The proliferation of limb tissue surrounded by an elastic cuticle could push the epidermis out forming a bud-like structure. The experimental crabs used to repeat the observation were amputated at a later stage when cuticles were partially hardened. The formation of an expandable cuticle may have been restricted by a change in the state of the underlying epidermis; consequently, the experimented

regeneration only happened inside the old-rigid cuticle and no bud-like structures were observed in these experiments.

The source of the regenerative tissue remains to be investigated. In salamanders, limb regeneration involves dedifferentiation and respecification. After amputation, a plasma clot forms. Epidermal cells from the remaining stump migrate to cover the wound surface, forming a wound epidermis. This epidermis later forms a blastema of stem cells and is required for the regeneration of the limb (Stocum, 1979, 2004). This is different from mammals in that no scar forms at the wound site. In *Uca*, like in mammals, a scab is also formed after amputation or autotomy before the formation of a blastema (Hopkins, 1988). Epidermal cells underneath the scab are believed to migrate to the wound site from other places (Hopkins, 1988).

Acknowledgements

We thank Wade Dressler for his help in taking some of the pictures. I also thank Dr. James N. Thompson jr.for allowing me to use his dissecting microscope.

Literature cited:

Bliss, D.E. 1956. Neurosecretion and the control of growth in a decapod crustacean. In: Wingstrand, K.G. (Ed.), Bertil Hanstrom. Zoological Papers in Honour of His Sixty-Fifth Birthday. Zoological Institute, Lund, pp. 56–75.

Brockes, J. P. 1992. Introduction of a retinoid reporter gene into the urodele limb blastema. Proc Natl Acad Sci U S A. 89,11386-11390.

Durica, D. S., Wu, X., Anilkumar, G., Hopkins, P. M., Chung, A. C. 2002. Characterization of crab EcR and RXR homologs and expression during limb regeneration and oocyte maturation. Mol Cell Endocrinol. 189, 59-76.

Emmel, V. E. 1910. A study of the differentiation of tissues in the regenerating crustacean limb. Am J Anat 10, 109-156.

Findlay, I., and McVean, A. R. 1977. The nervous control of limb autotomy in the hermit crab *Pagurus bernhardus* (L.) and the role of cuticular stress detector, CSD1. J. Exp. Biol. 70, 93-104.

Hopkins, P. M. 2001. Limb regeneration in the fiddler crab, *Uca pugilator*: hormonal and growth factor control. Am. Zool., 41, 389-398.

Hopkins, P.M., Chung, A.C.-K., Durica, D.S. 1999. Limb regeneration in the fiddler crab, *Uca pugilator*: histological, physiological and molecular considerations. Am. Zool. 39, 513–526.

Hopkins , M. P and Durica, S. D. 1995. Effect of all-trans retinoic acid on regenerating limbs of the fiddler crab, *Uca pugilator*. J. Exp. Zool. 272, 455-463.

Hopkins, P. M., Mislan, T. 1986. Wound healing in an autotomized limb: An electron and light microscopic study of the regenerating limb of *Uca pugilator*. Am Zool. 26, 60A.

Hopkins, P.M. 1988. Control of regeneration in crustaceans. In "Endocrinology of selected Invertebrate Types" (R. Downer and H. Laufer, Eds.), Vol.2, pp.327-340, A.R.Liss, New York.

Morriss-Kay, G., ed. 1992. *Retinoids in Normal Development and Teratogenesis* (Oxford Univ. Press, Oxford).

Needham, A. E. 1965. Regeneration in the arthropoda and its endocrine control. Regeneration in animals and related problems. Int Symp. 1964, pp 283-323.

McVean, A. 1984. Autotomy. In Bliss DE (ed):" The Biology of Crustacea." New York, Academic Press. pp 107-132.

Scadding, S. R., Maden, M. 1994. Retinoic acid gradients during limb regeneration. Dev Biol. 162, 608-617.

Stocum, D. L. 1979. Stages of forelimb regeneration in Ambystoma maculatum. J Exp Zool. 209, 395-416.

Stocum, D. L. 2004. Amphibian regeneration and stem cells. Curr Top Microbiol Immunol. 280, 1-70. Review.

Viviano, C. M., Horton, C. E., Maden, M., Brockes, J. P. 1995. Synthesis and release of 9-cis-retinoid acid by the urodele wound epidermis. Development 121, 3753-3762.

Wood, F. D., and Wood, H. E. 1932. Autotomy in decapod crustacea. The Journal of Experimental Zoology. 62, 1-49.

Figure legends

Figure 1.

Figure 1A shows a drawing of a regenerating limb bud and a fully developed limbs (Hopkins, 1993). Figure 1B shows a picture of external view of proecdysial buds (From Hopkins and Durica, 1995). Co, coxae of limbs attached to body of crabs. Segmentation is evident within the folded bud (large arrow) as well as chromatophores (small arrows).

Figure 2.

Figure 2A shows the regenerating segments with a mini-bud (arrow). Regenerating sections were folded inside a cuticular sac like normal autotomy associated regeneration. Figure 2B shows the complete functional new leg following ecdysis after one molt cycle. Only the missing structure was regenerated. Note the newly regenerated part was less pigmented and is more transparent (less light reflected) than the old remaining part (arrowhead, the joint of old part and regenerated part).

Figure 3.

A limb was amputated at the joint of carpus and propus with a pair of scissors. Figure 3A shows the newly molted regenerated only the amputated part (arrow shows the cut site). Note the much less pigmented exoskeleton of the regenerated part (the whole propus and dactylus). Figure 3B shows the exoskeleton of this leg after molting. Note the scab at the cutting plane is still

intact, no bud-like structure like in Figure 1 was observed from outside (arrowhead).

Figure 4.

H&E staining of regenerating amputated limbs. Limbs were fixed in decalcifying Lillie's solution. Paraffin embedded tissues were sectioned at 5-8 μm. Figure 4A shows a limb of a crab that was at early proecdysial stage (predicted from the size of limb bud of the same crab that was autotomized). Note segmentation was beginning to form inside the old cuticle (arrows), while the scab was still intact. Bar = 1 mm. Figure 4B shows a limb of a crab that was in late proecdysial stage (predicted from the limb bud size of autotomized leg). Note that the regenerated limb sections were popped out during the histological processing (brace). The cutting site is indicated by the arrows (at the middle of merus). M: merus; C: carpus; P: propus; D: dactylus. Bar = 1 mm. Figure 4C shows a cross section of a regenerating amputated limb (50 days after amputation). Arrows point to cuticle layers. Bar = 1 mm.

Figure 5.

An amputated limb (at the tip of merus) was not able to regenerate in the next molt cycle. Figure 5A shows the newly molted limb; only the old merus structure is obvious. The arrow shows the tip of the limb encased in cutilce. Figure 5B shows the exoskeleton of the molted crab limb. The scab is still intact

(arrowhead). This crab was able to regenerate this limb in the next molt cycle (not shown).

A

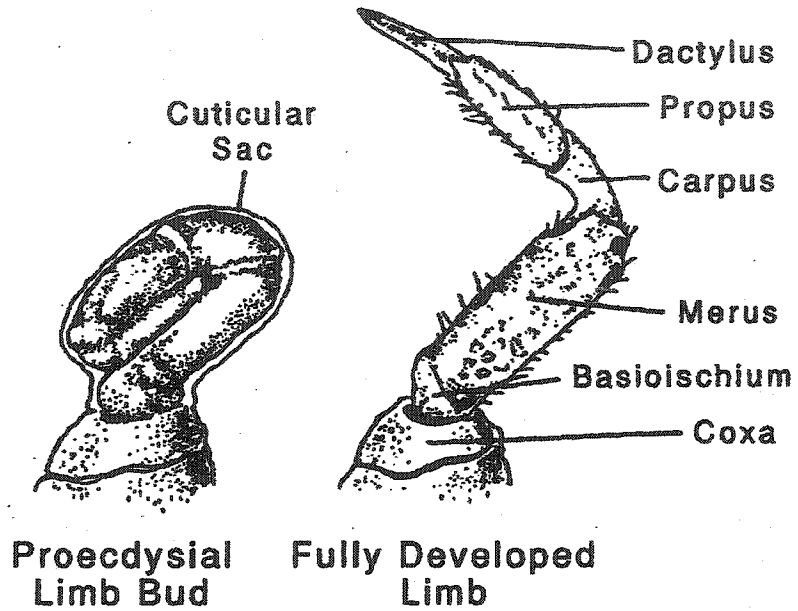
Cuticular Sac
Dactylus
Propus
Carpus
Merus
Basioischium
Coxa
Proecdysial Limb Bud
Fully Developed Limb

B

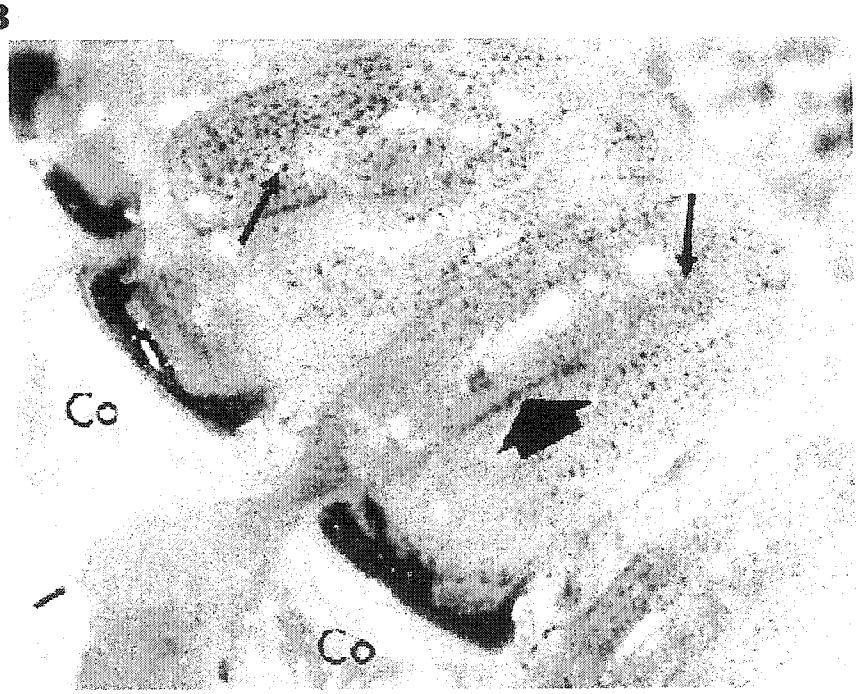
Co
Co

Figure 1

A

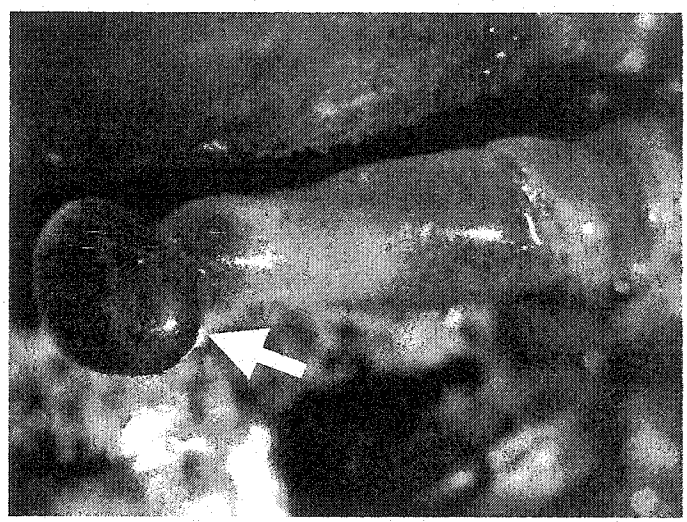

B

Figure 2

A

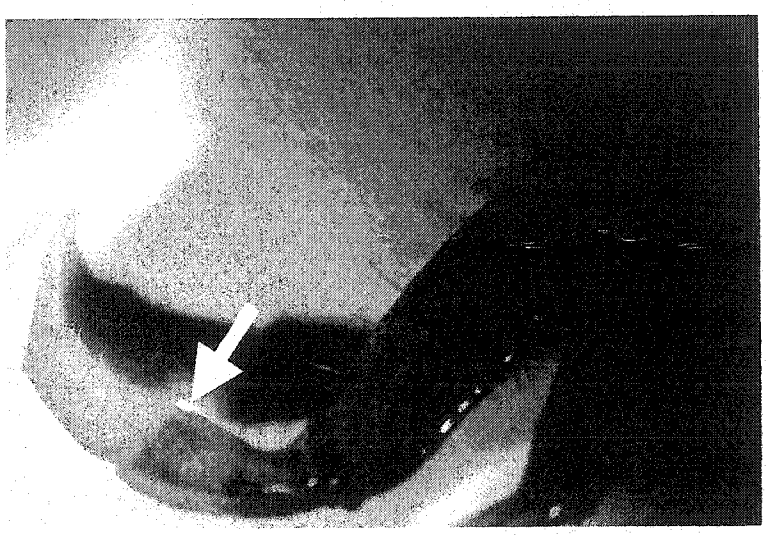

B

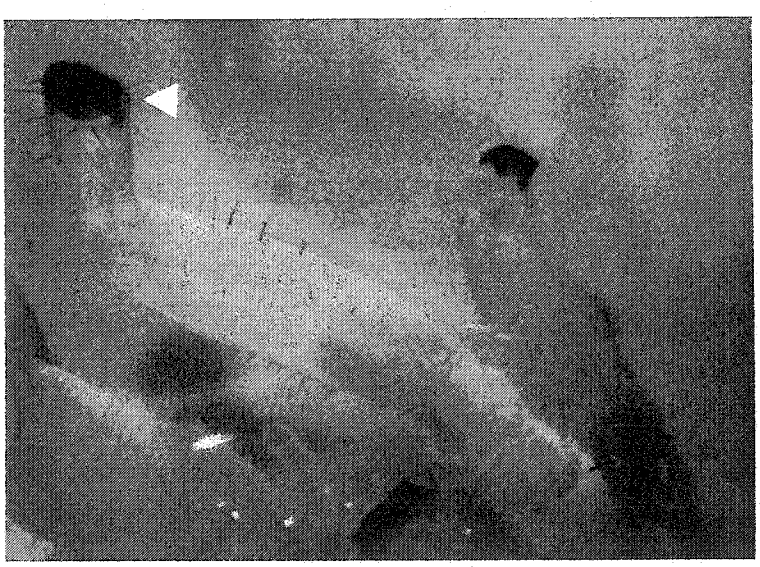

Figure 3

A

B

C

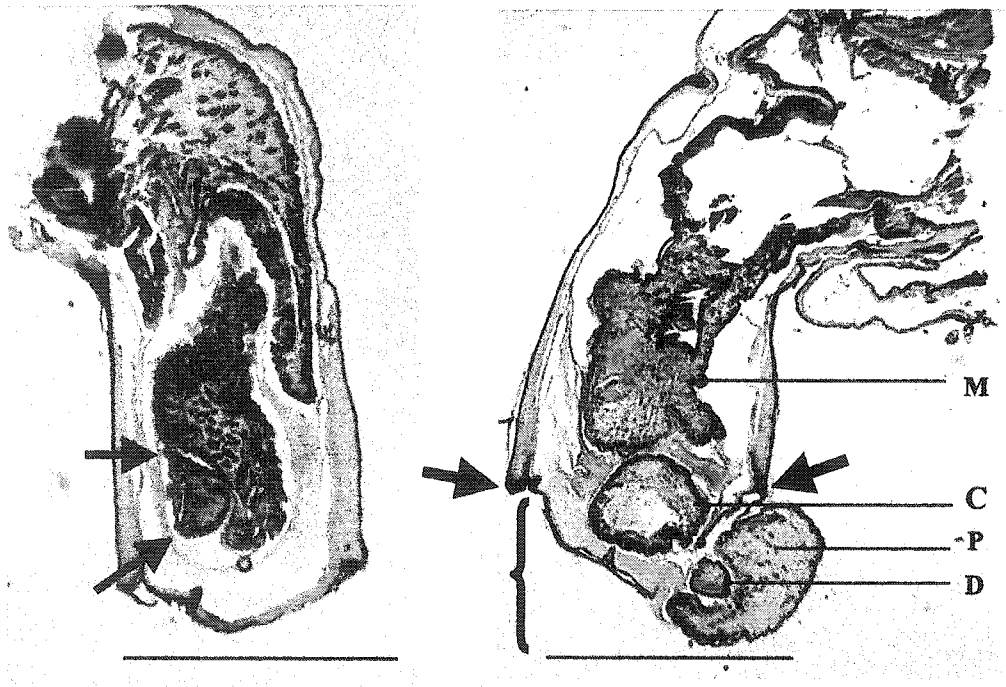

Figure 4

A

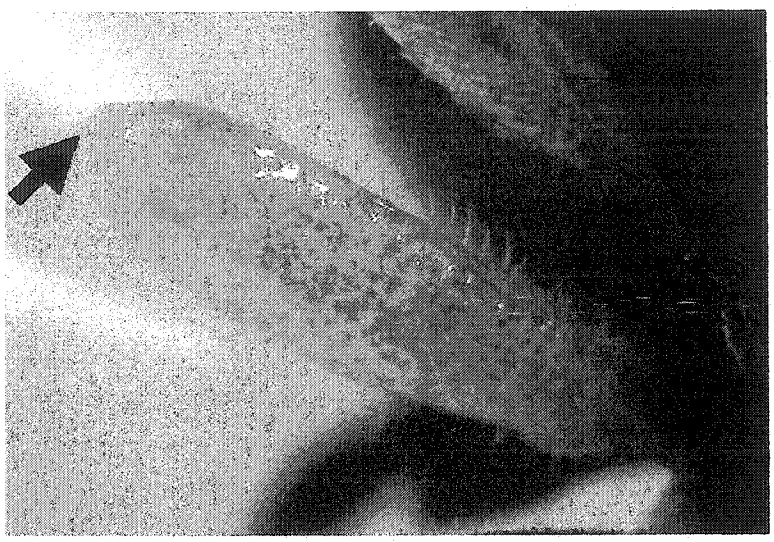

B

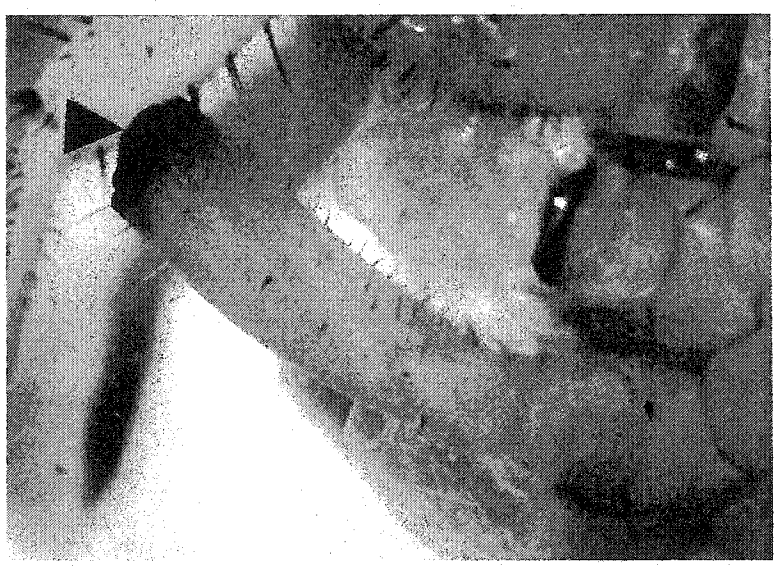

Figure 5